

Assessment controls on reservoir performance and the  
affects of granulation seam mechanics in the Bredasdorp  
Basin, South Africa

**MASTERS THESIS**

**BY**

**Hugh Je-Marco Schalkwyk**

SUPERVISOR: *Paul Carey PhD*

**Department of Earth Sciences,**

**University of the Western Cape**



*A thesis submitted in fulfilment of the requirements for the degree of Magister  
Scientiae in the Department of Earth Sciences, University of the Western Cape*

***November 2005***

# Assessment controls on reservoir performance and the affects of granulation seam mechanics in the Bredasdorp Basin, South Africa

Hugh Je-Marco Schalkwyk

## Key Words

South Africa

Block 9

Bredasdorp basin

Wells

Well data

Core analysis

Petrophysical analysis

Thin sections

Mini-Permeameter

Sandstone units

Hydrocarbon potential

Deep marine plays

Reservoirs



## Abstract

The Bredasdorp Basin is one of the largest hydrocarbon producing blocks within Southern Africa. The E-M field is situated approximate 50 km west from the FA platform and was brought into commission due to the potential hydrocarbons it may hold. If this field is brought up to full producing capability it will extend the lifespan of the refining station in Mosselbay, situated on the south coast of South Africa, by approximately 8 to 10 years.

An unexpected pressure drop within the E-M field caused the suite not to perform optimally and thus further analysis was imminent to assess and alleviate the predicament.

The first step within the project was to determine what might have cause the pressure drop and thus we had to go back to cores drilled by Soekor now known as Petroleum South Africa, in the early 1980's.

Analyses of the cores exposed a high presence of granulation seams. The granulation seams were mainly subjected within sand units within the cores. This was caused by rolling of sand grains over one another rearranging themselves due to pressure exerted through compaction and faulting, creating seal like fractures within the sand. These fractures caused these sand units to compartmentalize and prohibit flow from one on block to the next. With advance inquiry it was discovered that there was a shale unit situated within the reservoir dividing the reservoir into two main compartments. At this point it was determined to use Petrel which is windows based software for 3D visualization with a user interface based on the Windows Microsoft standards. This is easy as well as user friendly software thus the choice to go with it. The software uses shared earth modeling tool bringing about reservoir disciplines trough common data modelling. This is

one of the best modelling applications in the available and it was for this reason that it was chosen to apply within the given aspects of the project

A lack of data was available to model the granulation seams but with the data acquired during the core analyses it was possible to model the shale unit and factor in the influences of the granulation seams to assess the extent of compartmentalization.

The core revealed a thick shale layer dividing the reservoir within two sections which was not previously noted. This shale layer act as a buffer/barrier restricting flow from the bottom to the top half of the reservoir. This layer is thickest at the crest of the 10km<sup>2</sup> domal closure and thins toward the confines of the E-M suite. Small incisions, visible within the 3 dimensional models could serve as a guide for possible re-entry points for future drilling. These incisions which were formed through Lowstand and Highstand systems tracts with the rise and fall of the sea level.

The Bredasdorp Basin consists mainly of tilting half graben structures that formed through rifting with the break-up of Gondwanaland. The model also revealed that these faults segregate the reservoir further creating bigger compartments.

The reservoir is highly compartmentalized which will explain the pressure loss within the E-M suite. The production well was drilled within one of these compartments and when the confining pressure was relieved the pressure dropped and the production decrease.

As recommendation, additional wells are required to appraise the E-M structure and determine to what extent the granulation seams has affected fluid flow as well as the degree of sedimentation that could impede fluid flow. There are areas still containing untapped resources thus the recommendation for extra wells.

This work may well be reviewed with more data input from PetroSA (well, seismic and production data) for additional studies, predominantly with respect to reservoir modeling and flow simulation.

November 2005



## Declaration

I declare that, Assessment controls on reservoir performance and the affects of granulation seam mechanics in the Bredasdorp Basin, South Africa is my own work, that it has not been submitted for any degree or examination in any other university and that all the sources I have used or quoted have been indicated and acknowledge by complete references.



Full Name: Hugh Je-Marco Schalkwyk

Date:.....

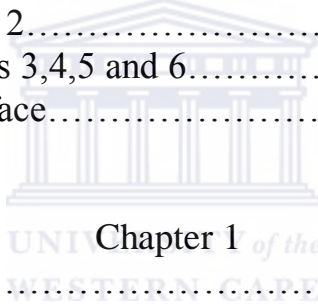
Signed:.....

## Acknowledgements

I would like to thank Ms. J. Du Toit and Mr. S. Davids at the Petroleum Agency of South Africa (PASA) for data supplied. Prof. P. Carey (supervisor), Mr. O. Olajide for their continued input and recommendations on the research. Furthermore thanks go out to Petroleum South Africa (PetroSA) for study material supplied and for the opportunity to work on one of the most productive hydrocarbon blocks with South Africa.

UNIVERSITY of the  
WESTERN CAPE

# Table of Contents

	Page Numbers
Title Page.....	i
Key Words.....	ii
Abstract.....	iii
Declaration.....	vi
Acknowledgements.....	vii
Table of Contents.....	viii
List of Figures.....	xi
List of Tables.....	xvi
Preface.....	xvii
Thesis Outline.....	xix
1.1 Chapter 1.....	xix
1.2 Chapter 2.....	xix
1.3 Chapters 3,4,5 and 6.....	xx
Impression of the subsurface.....	xxi
	
1 Introduction.....	24
1.1 Background.....	24
1.2 Research Problems.....	26
1.3 Research Design.....	27
Chapter 2	
2.1 Description of Study Area.....	28
2.2 Tectonic Setting.....	33
2.3 Tectonic History.....	36
2.4 Depositional Systems.....	37
2.5 Source Rock Maturity.....	38
2.6 Tectonic Elements in the Bredasdorp Basin.....	39
2.7 Paleogeography.....	40
2.8 Sequence Stratigraphy.....	41
2.8.1 Cycle Frequencies, Sequence and Parasequence.....	41
2.9 Lowstand Systems Tracts (LTS).....	45
2.10 Transgressive Systems Tracts (TST).....	46
2.11 Highstand systems Tracts (HST).....	46



## Chapter 3

3.1 Delineation of the E-M Suite.....	48
---------------------------------------	----

## Chapter 4

4.1 Methodology.....	54
4.1.1 Core Samples.....	54
4.2 Productivity Test Data.....	56
4.2.1 Drill Stem Test (DST) & Wireline Formation Tests.....	56
4.3 Well Logs.....	57
4.4 Rock Properties.....	59
4.4.1 Porosity.....	59
4.4.2 Permeability.....	60
4.4.3 Resistivity.....	61
4.4.4 Fluid Saturation.....	62
4.5 Characteristics of Selected Wireline Logging Tools.....	64
4.5.1 Gamma Ray Logs.....	64
4.5.2 Spontaneous Potential Logs.....	65
4.5.3 Induction Logs.....	67
4.5.4 Electrode Resistant Logs.....	69
4.5.5 Neutron Logs.....	70
4.5.6 Density Logs.....	72
4.5.7 Combination Density Neutron Logs.....	73
4.5.8 Sonic Logs.....	73
4.6 Electrosequence Analyses.....	76
4.7 Petrel.....	77
4.7.1 Modelling.....	77
4.7.1.1 Structural Modelling.....	77
A) Fault Modelling.....	78
B) Pillar Gridding.....	78
C) Vertical Layering.....	79
4.7.1.2 Correlation.....	79
4.7.1.3 Description of Correlation section.....	80
4.8 Reservoir Modelling.....	81
4.8.1 Facies Modelling.....	82
A) Stochastic Modelling.....	82
B) Deterministic Modelling.....	83
C) Interactive Modelling.....	83
4.9 Seismic Interpretation.....	83
4.10 Data Quality Control.....	84

## Chapter 5

5.1	Discussion and Results.....	87
5.1.1	Granulation Seams.....	87
5.1.2	Glaucconite.....	96
5.1.3	Facies Description.....	100
5.1.4	Fluvial Sequence.....	103
5.1.5	Bioturbation.....	113
5.1.6	Shallow Marine Facies.....	115
5.1.7	Porosity and Permeability Distribution.....	119
5.1.8	Structural Models.....	120
5.1.9	Facies Models.....	122
5.1.10	Cross Section East-West.....	128
	Conclusions and Recommendations.....	130
	Bibliography.....	134
	Appendix 1: Porosity and Permeability Distribution of the E-M Suite.....	142
	Appendix 2a: Porosity vs. Permeability over E-M 1.....	151
	Appendix 2b: Distribution of Granulation Seams (E-M 1).....	152
	Appendix 3a: Porosity and Permeability Distribution over E-M 2.....	154
	Appendix 3b: Distribution of Granulation Seams (E-M 2).....	155
	Appendix 4a: Porosity and Permeability Distribution over E-M 4.....	157
	Appendix 4b: Distribution of Granulation Seams (E-M 4).....	158
	Appendix 5A: Well Correlation of the E-M Suite .....	160
	Appendix 5B: Well Correlation of the E-M Suite .....	161

## List of Figures

Figure 2.1: Locality map of onshore and offshore basins explored for oil and gas courtesy of the Petroleum agency of South Africa. (PASA).....	28
Figure 2.2: Formation of a half-graben from a series of normal faults dipping in the same direction (modified from Houston 1986).....	29
Figure 2.3: Western, eastern and southern offshore zones of South Africa (Modified from Broad, 2004).....	30
Figure 2.4: Evolution of deep marine channel deposits (Van Wagoner 1988).....	32
Figure 2.5: The rift phase in the Late Jurassic – Lower Valanginian showing the break up of Africa, Madagascar and Antarctica (modified from Broad, 2004).....	34
Figure 2.6: <b>Top:</b> Early drift phase in the Valanginian (1At1) – Hauterivian (6At1) showing the movement of microplates: Falkland Plateau (FLK), Patagonia (PAT) and Maurice-Ewing Bank plates (MEB) past south coast of Africa (modified from Broad, 2004) <b>Bottom:</b> Late drift phase in the Hauterivian (6At1) onwards (Modified from Broad, 2004).....	35
Figure 2.7: Oblique rift half-graben sub-basins of Outeniqua Basin: Bredasdorp, Pletmos, Gamtoos, and Algoa (modified from Broad, 2004).....	37
Figure 2.8: Exxon model sequence (type 1) developed on a margin with a shelf slope break. (Van Wagner 1990).....	42
Figure 2.9: Parasequence stacking patterns (Van Wagner 1990).....	43
Figure 2.10: Schematic lithologic logs contrasting the facies seen in: (a) Gradational shoreface facies (b) Sharp-base shoreface facies (Plint, 1988).....	44
Figure 3.1: Delineation of study area courtesy PetroSA.....	48

Figure 3.2: Top: Seismic profile with identified sequence boundaries Bottom: Schematic cross section (modified from Broad, 2004).....	52
Figure 4.1: Non wetting oil (black) and water (blank) in a single water-wet pore (Modified from Levorsen, 1967).....	64
Figure 4.2: Gamma ray tool (modified from Serra, 1984).....	65
Figure 4.3: Spontaneous Potential logging tool (modified from Rider, 1996).....	68
Figure 4.4: Induction log equipment (modified from Schlumberger).....	67
Figure 4.5: Normal device with electrodes A, M, N (modified from Schlumberger).....	70
Figure 4.6: (A) Compensated neutron tool drawing, and (B) Schematic trajectories of a neutron in a limestone with no porosity and pure water (modified from Rider, 1996).....	71
Figure 4.7: Compensated density sonde (modified from Wahl, JPT, 1964).....	72
Figure 4.8: Sonic logging tool showing Receiver (R) and Transmitter (T) (modified from <a href="http://www.spwla.org/library_info/glossary">http://www.spwla.org/library_info/glossary</a> ).....	74
Figure 4.9: Damage core boxes courtesy of Petroleum Agency of South Africa .....	86
Figure 4.10: Damaged core boxes courtesy of Petroleum Agency of South Africa....	86
Figure 5.1: Porosity vs. Permeability (Berg and Avery, 1995).....	88
Figure 5.2: Seismic profile of the E-M structure, courtesy of the Petroleum Agency of South Africa (PASA).....	90
Figure 5.3: Two dimensional block diagram of granulation seam distribution courtesy ABA and associates Ltd.....	91
Figure 5.4: Core photos, courtesy of Petroleum Agency of South Africa E-M2, illustrating the affects of the granulation seams.....	91
Figure 5.5: E-M 1 core photo, courtesy of Petroleum Agency of South Africa illustrating the affects of the granulation seams.....	92
Figure 5.6: E-M 4 core photo, courtesy of Petroleum Agency of South Africa illustrating the affects of the granulation seams.....	92
Figure 5.7: E-M 2 core photo, courtesy of Petroleum Agency of South Africa illustrating the affects of the granulation seam .....	93

Figure 5.8: E-M 1 core photo, courtesy of Petroleum Agency of South Africa illustrating the affects of the granulation seam .....	94
Figure 5.9: Core photo, core 2 and courtesy of Petroleum agency, illustrating the orientation or the lack of consistent orientation of the granulation seams.....	94
Figure 5.10: Core photo, core 2 and courtesy of Petroleum agency, illustrating the orientation or the lack of consistent orientation of the granulation seams.....	95
Figure 5.11: E-M 2 core photo, core 2 and Courtesy of Petroleum Agency, illustrating the uniformities of the granulation seams in the sand horizon. ....	95
Figure 5.12: E-M 3 core photo courtesy of the Petroleum Agency of South Africa illustrating the occurrences of iron within the granulation seams.....	97
Figure 5.13: E-M 3 core photo courtesy of PASA.....	98
Figure 5.14: Optical image of a glauconitic sandstone (made at 20X magnification) showing formation of a pseudomatrix that occludes the original primary porosity (courtesy of Rob Lavinsky, Omni Laboratories, Inc).....	98
Figure 5.15: Examples of a scanning electron micrograph of pore-filling fibrous illite in sandstone. (Courtesy of the Rob Lavinsky, Omni Laboratories, Inc).....	99
Figure 5.16: Examples of a scanning electron micrograph of pore-filling fibrous illite in sandstone. (Courtesy of the Rob Lavinsky, Omni Laboratories, Inc).....	99
Figure 5.17: Core photo courtesy of Petroleum Agency of South Africa.....	101
Figure 5.18: Core photos of E-M 2, courtesy of Petroleum Agency of South Africa.....	101
Figure 5.19: Core photos of E-M 2 core 4, Courtesy of Petroleum Agency of South Africa.....	102

Figure 5.20: Core photo's of E-M 1 cores 1 and 2, courtesy of Petroleum Agency of South Africa showing woody encased in the core. ....	104
Figure 5.21: Core photo's of E-M 1 cores 1 and 2, courtesy of Petroleum Agency of South Africa showing woody material encased in the core.....	104
Figure 5.22: Core photo's of E-M 1 cores 1 and 2, courtesy of Petroleum Agency of South Africa showing woody material encased in the core .....	104
Figure 5.23: Core photo's of E-M 1 cores 1 and 2, courtesy of Petroleum Agency of South Africa showing encased woody material in very fine grained sand.....	105
Figure 5.24: Core photo of E-M 2 core 2, courtesy of Petroleum Agency of South Africa.....	105
Figure 5.25: Core photo of E-M 2 core 2, courtesy of Petroleum Agency of South Africa.....	106
Figure 5.26: Core photo of E-M 2 core 2, courtesy of Petroleum Agency of South Africa.....	106
Figure 5.27: Core photo, courtesy of Petroleum Agency of South Africa.....	107
Figure 5.28: Core photo showing a small scale fold, courtesy of Petroleum Agency of South Africa.....	108
Figure 5.29: Core photo's of E-M Suite, courtesy of Petroleum Agency of South Africa.....	108
Figure 5.30: Core photo showing dewatering feature, courtesy of Petroleum Agency of South Africa.....	108
Figure 5.31: Core photo's of E-M Suite, courtesy of Petroleum Agency of South Africa.....	109
Figure 5.32: Core photo's of E-M Suite, courtesy of Petroleum Agency of South Africa.....	109

Figure 5.33: Core photo's of E-M Suite, courtesy of Petroleum Agency of South Africa.....	110
Figure 5.34: Core photo's of E-M Suite, courtesy of Petroleum Agency of South Africa.....	110
Figure 5.35: Core photo showing oil stained sand, courtesy of Petroleum Agency of South Africa.....	111
Figure 5.36: Core samples of E-M Suite, courtesy of Petroleum Agency of South Africa, occurrence of the interbedded sandstone-siltstone facies which is limited to very thick sandstone intervals.....	110
Figure 5.37: Core samples of E-M Suite, courtesy of Petroleum Agency of South Africa, occurrence of the interbedded sandstone-siltstone facies which is limited to very thick sandstone intervals.....	112
Figure 5.38: Core photo's of E-M Suite, courtesy of Petroleum Agency of South Africa.....	113
Figure 5.39: Core photo's of E-M Suite, courtesy of Petroleum Agency of South Africa.....	112
Figure 5.40: Core sample of E-M Suite, courtesy of Petroleum Agency of South Africa showing traces of cross bedding visible within core photo.....	114
Figure 5.41: Core photo's of E-M Suite, courtesy of Petroleum Agency of South Africa.....	113
Figure 5.42: Core photo's of E-M1, courtesy of Petroleum Agency of South Africa.....	114
Figure 5.43: Core photo's of E-M Suite, courtesy of Petroleum Agency of South Africa.....	114
Figure 5.44: Core photo illustrates the poorly sorted conglomerate in the E-M Suite, courtesy of Petroleum Agency of South Africa.....	117

Figure 5.45: Core photo illustrates the poorly sorted conglomerate in the E-M Suite, courtesy of Petroleum Agency of South Africa .....	117
Figure 5.46: Core photo illustrates the poorly sorted conglomerate in the E-M Suite, courtesy of Petroleum Agency of South Africa .....	117
Figure 5.47: Core photo illustrates the poorly sorted conglomerate in the E-M Suite, courtesy of Petroleum Agency of South Africa .....	117
Figure 5.48: Core photo of E-M 4 Core 5, courtesy of the Petroleum Agency of South Africa.....	118
Figure 5.49: Well positions within fault model.....	121
Figure 5.50: Facies model displays the distribution of the up-scaled facies logs .....	122
Figure 5.51: Sand rich zone 1.....	123
Figure 5.52: Top Zone 2, showing the distribution of the confining shale layer .....	124
Figure 5.53: Sand rich bottom zone 3 showing possible re-entry points with incisions .....	125
Figure 5.54: Zoomed section of zone 2, E-M 1(Yellow), E-M 2(Green), E-M 3(Blue),E-M 4 (Orange).....	127
Figure 5.55: Illustrates the location of the wells within zones 1, 2 and 3.....	128
Figure 5.56: Compartmentalization by minor faults between zone 1 and 3.....	128

## List of Tables

Table 1: Porosity and permeability distribution through the E-M suite.....	51
Table 2: Porosity and permeability distribution through the E-M suite.....	119



## Preface

The Petroleum Oil and Gas multinational of SA (Pty) Limited, trading as PetroSA, is South Africa's nationalised oil company. It owns, operates and manages the South African government's commercial resources in the petroleum industry. The company operates as a commercial non-listed entity under South African law.

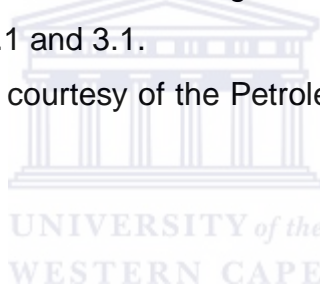
Sasol (Suid Afrikaanse Steenkool en Olie - South African Coal and Oil) and Petroleum South Africa (PetroSA) are the two main players in the synthetic fuel market where Sasol is the world's largest manufacturer of oil from coal, gasifying the coal and then converting it into a range of liquid fuels and petrochemical feed stocks.

PetroSA is active in two worldwide businesses:

Oil and gas exploration, and the production and marketing of petrochemicals. The company explores for oil and gas in preferred basins around the world, with a focus on Africa, and has producing fields off the coast of South Africa. Offshore petroleum production is a major technological triumph. The limits of oil and gas exploration in terms of water depth and other factors have been powerfully subjective by the recent trend in technological progression. It is only over the last few years that exploration under the current oil boom setting has become economically feasible. PetroSA is a pioneer in the field of gas-to-liquids (GTL) technology, recognized worldwide for producing the 'cleanest' fuels through an environmentally responsible GTL process that releases minimal emissions. A number of wells drilled offshore had gas shows and tested good gas flow rates and supply good substantiation for a gas province. South Africa's prospects for natural gas production increased significantly in 2000, with the discovery of offshore reserves close to the Namibian border. The reserve, named the Ibhubezi Prospect, contains three trillion cubic feet of

gas. In 2001, PetroSA completed a project to bring on stream the EM gas fields off shore of Mosselbay, giving the plant an additional eight years of gas life. PetroSA operates the Oribi/Oryx oil field and Sable oil field. The FA gas field was discovered in 1984, 85 kilometers south of Mosselbay, a harbor town some 400 km south of Cape Town. In 1992 gas from the FA field was brought onshore for the Mossgas refinery. Two nearby satellite fields, FAH and FAR, which are situated respectively 16 kilometers and eight kilometers northwest of the FA platform and were brought into production in May 1997. The EM gas field, 49 kilometers west of FA, and the smaller EBF field were commissioned in 2000. These fields will provide the Mossgas onshore plant with gas until 2006. Mossgas believes that further gas discoveries could extend gas supplies to the onshore production plant. Locality map of onshore and offshore basins explored for oil and gas can be found within text and locality map within figure 2.1 and 3.1.

Maps and figures supplied courtesy of the Petroleum agency of South Africa. (PASA)



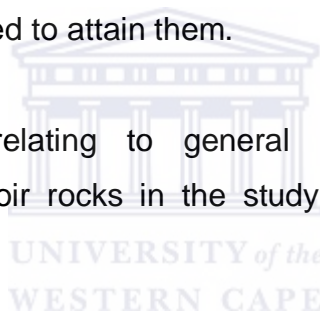
## 1.1 Thesis Outline

This thesis embodies the written report of the study work carried out to assess the hydrocarbon potential and production capabilities of Lower Cretaceous Aptian E-M suite reservoir sands in the central part of the Bredasdorp Basin.

### 1.1.1 Chapter 1

Chapter one gives the broad overview of what this thesis is about and presents the research framework background, aims and the flowchart of stepwise methods employed to attain them.

Consulted publications relating to general geology, stratigraphy and characterization of reservoir rocks in the study area are discussed under literature review.



### 1.1.2 Chapter 2

Chapter two begins with the presentation of the general description of the E-M suite with the location of the four wells used for the investigation in chapter three and leads into chapter four where lithologic units are correlated across all the wells covered by the available data by applying well log correlation techniques.

Subsequently, electrosequence analysis is carried out by integrating geological information which was extracted from post-mortem reports, well completion reports, seismic horizon picks, into the correlated well logs (image

format) to locate the successive planes of unconformities. The electrosequence analysis primarily helps to extract geological information from the correlated section. The log correlation and the electrosequence analysis section are presented in Appendix 5.

### 1.1.3 Chapter 3, 4, 5 and 6.

Chapters three delineates the study area and gives a broader perspective of the area of investigation.

Chapter four lays out the methodology which was used to obtain the results.

Chapter five is centered on the detailed reservoir characterization through petrophysical analyses of identified sandstone reservoirs. Schlumberger Petrel software is used extensively to carry out the petrophysical analysis. Digitized well and wireline log data are the input data.

In addition chapter five deals with the reservoir modeling (structural and property). The structural modeling in Petrel process steps comprises three dimensional faults and facies modeling where property modeling denotes the distribution of petrophysical parameters in the three dimensional (3D) window. Using Schlumberger Petrel software, models are built to reproduce within the limit of the quality of available data, the true 3D view of selected reservoir sands (facies) and the distribution in the subsurface of their respective petrophysical properties such as permeability (mD) and effective porosity (%).

The thesis ends with chapter six, conclusion and recommendations based on the observations made in the various phases of analysis.

## Impression of subsurface studies

The study of the subsurface has progressed enormously within the oil industry over the years with the use of geophysical methods. Measurements within a geographically controlled area are used to establish the share of physical properties that reflect the unique characteristics of the local subsurface geology. Once these methods predominantly seismic, gravity and magnetic methods have been used to locate positive geological conditions for feasible hydrocarbon accumulation an investigative well will be drilled. The potential structure will be explored to open way for a range of techniques of evaluating the resources.

Most of the oil and gas that is presently produced world wide comes from hydrocarbon accumulations in the pore spaces of reservoir rocks such as sandstones, limestones or dolomites. In order to have an idea of the commerciality of a revealed source or reservoir, some basic petrophysical parameters need to be generated. These include porosity, permeability, hydrocarbon saturation, thickness and area extent of reservoir formation (size of reservoir). The parameters can be derived or inferred primarily from electrical, nuclear and acoustic logs.

Well logging is the process of recording various physical, chemical, electrical or other properties of the rock/fluid mixture penetrated by drilling a well into the earth's crust (Crain, 2004).

The actual running of a log involves the probe/sensor on the end of the logging cable, the cable itself, and the surface electronics. A sensor and its associated electronics are housed in a sonde, which is suspended in the hole by an armored electric cable. The sensor is separated from the virgin formation by drilling mud, mud-cake, and often an invaded zone in the formation. The signals from the sensor are conditioned by down-hole

electronics for transmission up the cable to the surface electronics, which in turn conditions the signals for output and recording.

As the cable is raised or lowered, it activates a depth measuring device which provides depth information to the surface electronics and recording device. The data is recorded on digital tape, film, and paper.

Signatures displayed by diverse logging tools are an expression of the inherent physical properties, which they are intended to measure as acquired by the in-situ geologic units throughout individual processes of their formation and evolution. When these properties are cautiously calculated, studied, analyzed, corrected and suitably integrated into data sets from other sources, they could augment, to a good level of accuracy the imaging of the subsurface as well as specifically evaluating targeted resources.

Petrophysics encompasses standard log analyses and various techniques of characterizing reservoir rocks through derivation of conventional reservoir parameters. In standard log analyses, large volumes of log data are reduced to more manageable results as well as minimizing potential errors in the assumptions and in the log derived results. Petrophysical analysis is the combination of log analysis with other physical measurements such as core data, petrographic data and seismic data to enhance accurate prediction of reservoir characteristics and performance.

Petrophysics is by extreme one of the most imperative and useful fields of science available to a petroleum geologist. In conjunction with field development from its preliminary detection is generation of large volume of well log, seismic and production data. These are used to get an estimate of probable productive acres, which in combination with an estimated recovery factor will give an estimate of total recoverable oil in Barrel (bbl) and gas in Million Cubic Feet per Acre Foot (Mcf/acre-ft) from the reservoir.

In the early stages of planning exploration and development in a new area, surface seismic surveys are used broadly to outline prospective structural or stratigraphic traps. Improvements in digital filtering have led to high quality results under favorable conditions.

The resolution of the subsurface seismic survey, however, is still essentially limited by low operating frequencies at deeper levels. Seismic resolution is a measure of how large an object needs to be in order to be seen in seismic section (Rafaelsen, 2004). The frequency of the sound signal decreases with increasing depth while the velocity and wavelength increase, implying poorer resolution with increasing depth.

With the drilling of wells, opportunities subsist to prevail over the limitation in seismic data through the use of well logs. A merger of sonic log and density can be used to generate synthetic seismograms after editing and calibrating against check shots. Synthetic seismograms are valuable in verifying reflection events in a seismic section and relating seismic features to geological structures.

Reservoir characterization and evaluation has progressed beyond the predictable manual petrophysical analyses and their use in estimating recoverable hydrocarbons in reservoir rocks. Several Windows-based software packages for petrophysical analyses are available. When available well and seismic data are input into them in the correct format, they can be used to carry out petrophysical analyses and visualize the distribution of petrophysical parameters within a framework of a 3D reservoir model.

# Chapter 1

## Introduction

### 1.1 Background

Exploration in South Africa is managed by the Petroleum Agency of South Africa, whom soliciting bids for offshore acreage off the Southern and Western coasts of South Africa. To date South Africa's upstream has played a minimal role in the evolution of the South African oil industry. Extensive exploration over a period of more than thirty years has revealed no onshore hydrocarbons, however small oil and gas fields have been discovered offshore, particularly in the Bredasdorp Basin and off the West coast of South Africa near the Namibian border.

The F-A gas and condensate fields in the offshore Bredasdorp Basin are presently being exploited by Mossgas and an average of 194 million standard cubic feet of gas and 9,500 barrels of condensate are being produced daily, Broad 2004. A 91km pipeline conveys gas and condensate to the Mossgas synfuels plant located at Mosselbay, where petrol, diesel and kerosene are produced (Locality Map refer to figure 3.1)

PetroSA has discovered further gas and oil deposits offshore in Blocks 9 and 11A in the Bredasdorp basin. The gas deposits are separate from the Mossgas synfuels operation and from the current development of the E-BT oil field. PetroSA is seeking to farm out up to 40% in each of the sub units within Block 9, which surround the F-A, and E-M oil fields as part of increasing production above Oribi's present 20,000 bpd. The E-AR field, now dubbed the Oryx field, projected to be operational in 2000 to compensate for the declining output from Oribi field. The Oryx field is located only 6km away from the Oribi field.



Petroleum South Africa encountered problems within Block 9 of the Bredasdorp Basin with the E-M suite of wells. The prediction of flow rates and flow capacity of gas & oil, under cut expectations and further investigation were proposed to the suite.

It was for this reason the project set forward to assist PetroSA with the research and provide possible solutions to their current situation.

It is also the intentional endeavour of this research to present the estimated hydrocarbon reserve, which may fulfil the main objective of PetroSA and reinforce the overall petroleum reserves of South Africa.



## 1.2 Research Problems

The following list was provided as possible problems to solve:

- Calculating the orientation of the given wells and orientating them in their correct orientation for analyses.
- Provide answers on how granulation seams formed and if they are mechanically or hydrologically driven.
- If they are hydrologically driven where did the water come from?
- What restrictions these granulation seams has on flow and the flow rate within the reservoir if any.
- To model the seam mechanics as competent as possible & tying the results to the petrophysical data provided.
- Is there a possibility to exert a pull on possible investors into this section of the upstream sector through this study?

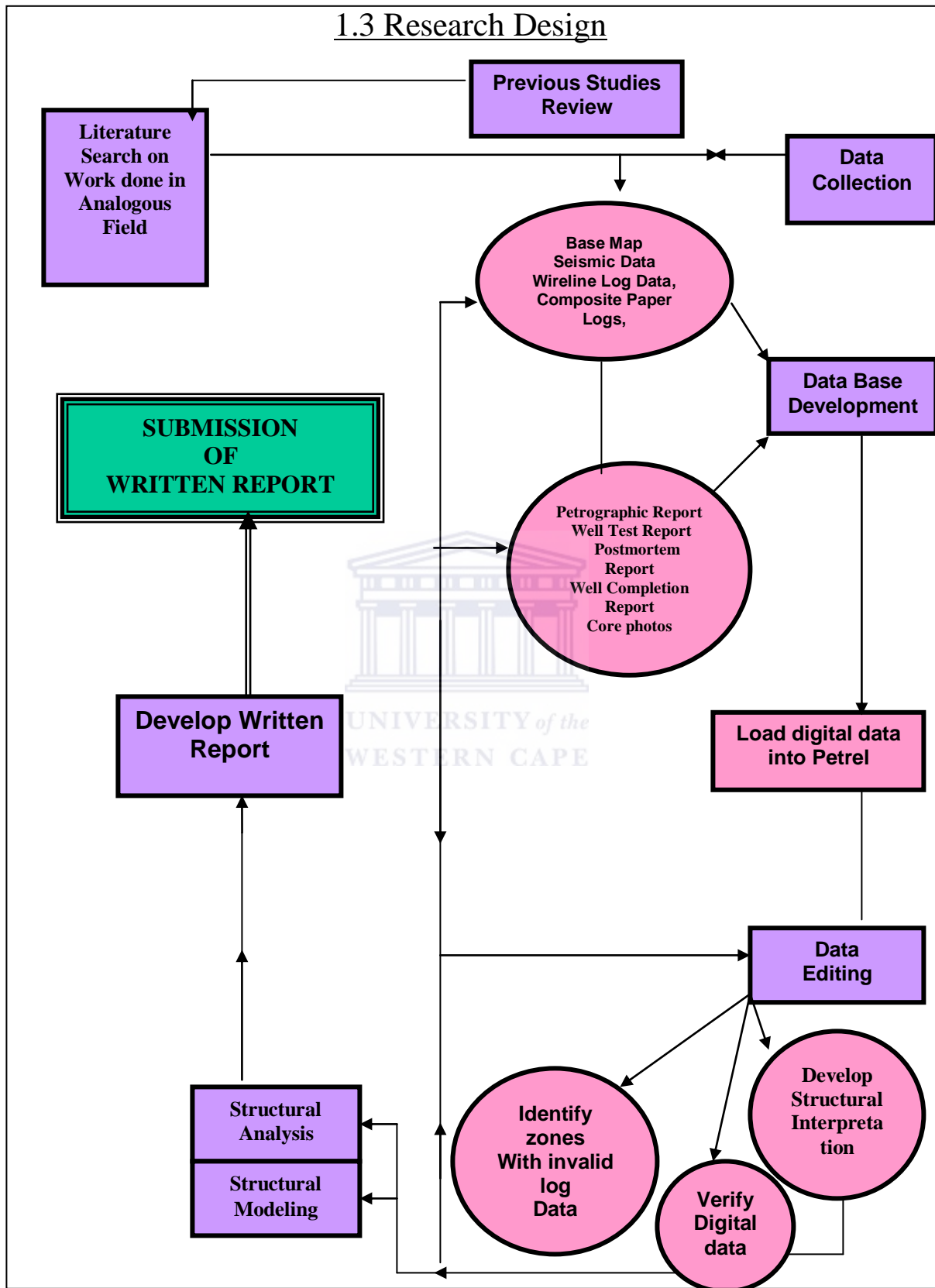
It is not entirely obvious if the problem is structural due to the structural history of the Bredasdorp Basin and the study hopes to elucidate this.

The research will attempt to comprehensively analyze core and thin sections cut from various parts of core to further evaluate the structural implications which may affect flow within the E-M suite located within the deep marine channel plays of the Bredasdorp Basin. It will also try to define physical rock characteristics such as lithology, porosity, pore geometry, permeability, water and hydrocarbon saturation.

Determine the formation, orientation and distribution of the granulation seams formed in the core as well look at the implications of compartmentalization.

Furthermore establish what causes the lowered production rates within the E-M field as well as the structural implications that the Bredasdorp Basin holds on the Suit.

### 1.3 Research Design



# Chapter 2

## 2.1 Description of the study area

The Bredasdorp basin covers approximately 18,000 km<sup>2</sup> beneath the Indian Ocean along the southern coast of South Africa, which is in the southwest of Mossel Bay. The basin is essentially filled with Upper Jurassic and Lower Cretaceous synrift continental and marine strata and post Cretaceous and Cenozoic divergent rocks.

The Infanta Arch bound the basin on the west and southwest by the Agulhas Arch and on the northeast the basin opens to the southeast to connect with the Southern Outeniqua Basin, which is terminated on the southeast by the Agulhas-Falkland Fracture Zone (Illustration in Figure 2.1). Reactivated rift faults are prominent along the margin of the Agulhas Arch and minor faults define the northeast margin of the Infanta Arch.

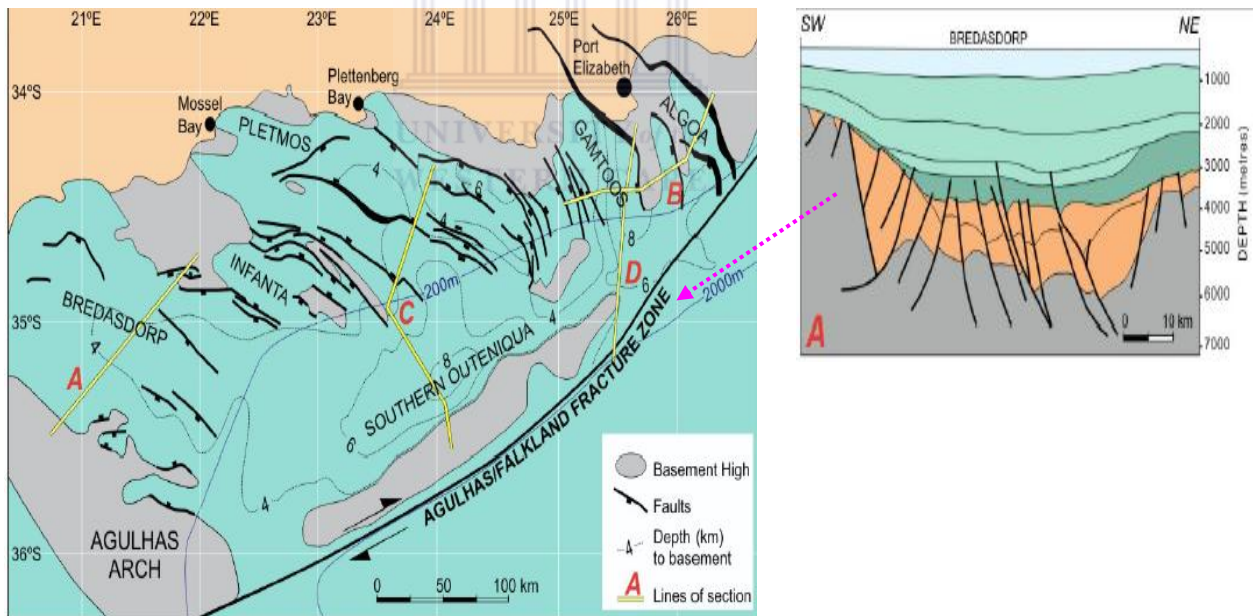


Figure 2.1: Locality map of onshore and offshore basins explored for oil and gas courtesy of the Petroleum agency of South Africa. (PASA)

Transtension generation along the Agulhas-Falkland Zone initiated Right Lateral movement which separated the South American and African plates and effected tectonic development of the Bredasdorp Basin

South Africa's offshore basins can be divided into three distinct tectono-stratigraphic zones. A western broad passive margin basin which is related to the opening of the South Atlantic in the early Cretaceous a south eastern offshore basin with a narrow passive margin that was formed due to the break up Africa, Madagascar and Antarctica.

This basin consists of a series of eon sub-basins which all consists of half grabens and is of an assortment of thicknesses.

The southern margins, known as the Outeniqua Basin, are essentially interplay of pull-apart basins and transform margins. The Bredasdorp, Pletmos, Gamtoos and Algoa basins are the sub-basins of the Outeniqua Basin (Figure 2.3). They display rift half-graben feature overlain by variable thicknesses of drift sediments.

Half-graben feature is formed when normal faults within a sedimentary basin are dipping in the same direction making adjacent fault blocks to slip down and tilt relative to the fault next to it (Figure 2.2)

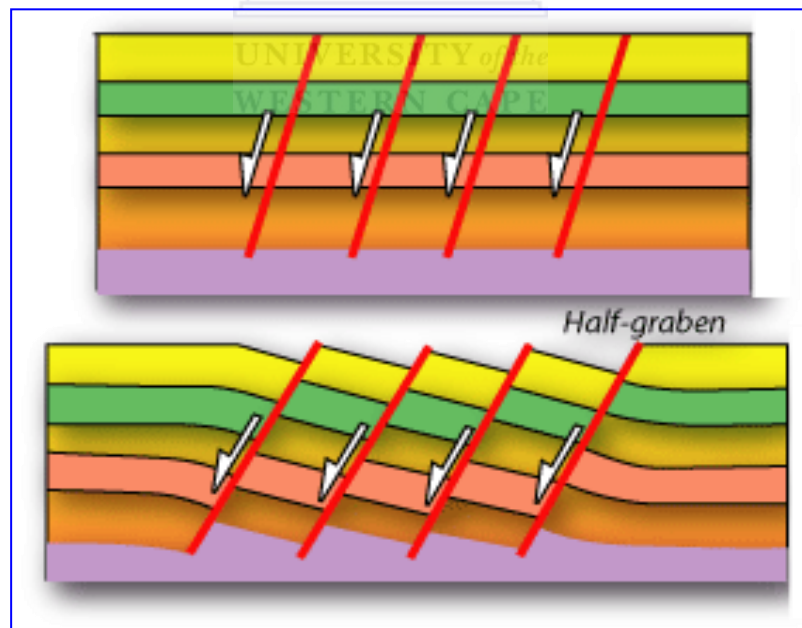


Figure 2.2: Formation of a half-graben from a series of normal faults dipping in the same direction (modified from Houston 1986)

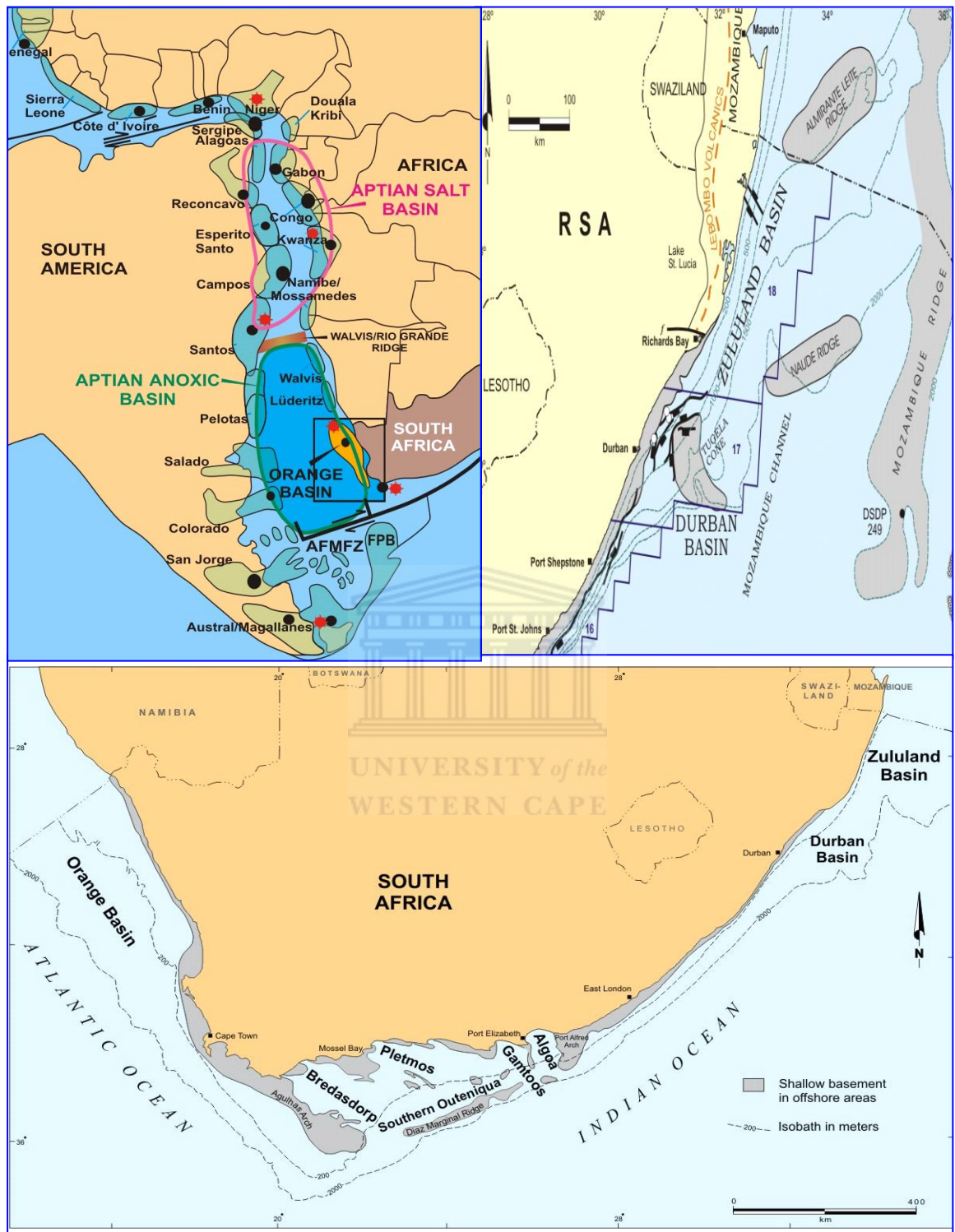


Figure 2.3: Western, eastern and southern offshore zones of South Africa  
(Modified from Broad, 2004)



Mid-Cretaceous lowstand systems tracts, containing varying thicknesses of sandstone and has been identified in the sub-basin, south-central Bredasdorp basin, offshore South Africa. These lowstand tracks overly a type 1 unconformity of Albian age, related to erosion of submarine channels into the lower continental slope.

Local tectonic activity of short duration along faults parallel to the Agulhas fracture zone may have contributed to gradient steepening.

The oldest rift fault does not replace the drift –onset unconformity. A second generation displaces the drift–onset unconformity and may involve the lower part of the post-rift sequence.

The youngest faults displace the unconformity at the Tertiary base. The interplay of diminishing rift tectonics, thermal cooling and inferred eustatic variations in global sea level reduced a distinctive series of repetitive cycled depositional sequences. This can be recognized in various elements of low stand systems tracts. Within these sequences it appears to contain potential reservoirs. Incised valleys and canyons provide surfaces on which mounded and sheet like submarine/basin floor fans and submarine channel fill with associated mounds and fans. Prograding deltaic/coastal lowstand wedges were also deposited within the area.

Figure 2.4 shows that the basin fill consists of cyclic sequences deposited in response to relative changes in sea level.

These fans, channel fills and wedges are top sealed and sourced by transgressive shale's and marine condensed sections, deposited at a time of regional transgressive shale's of the shoreline.

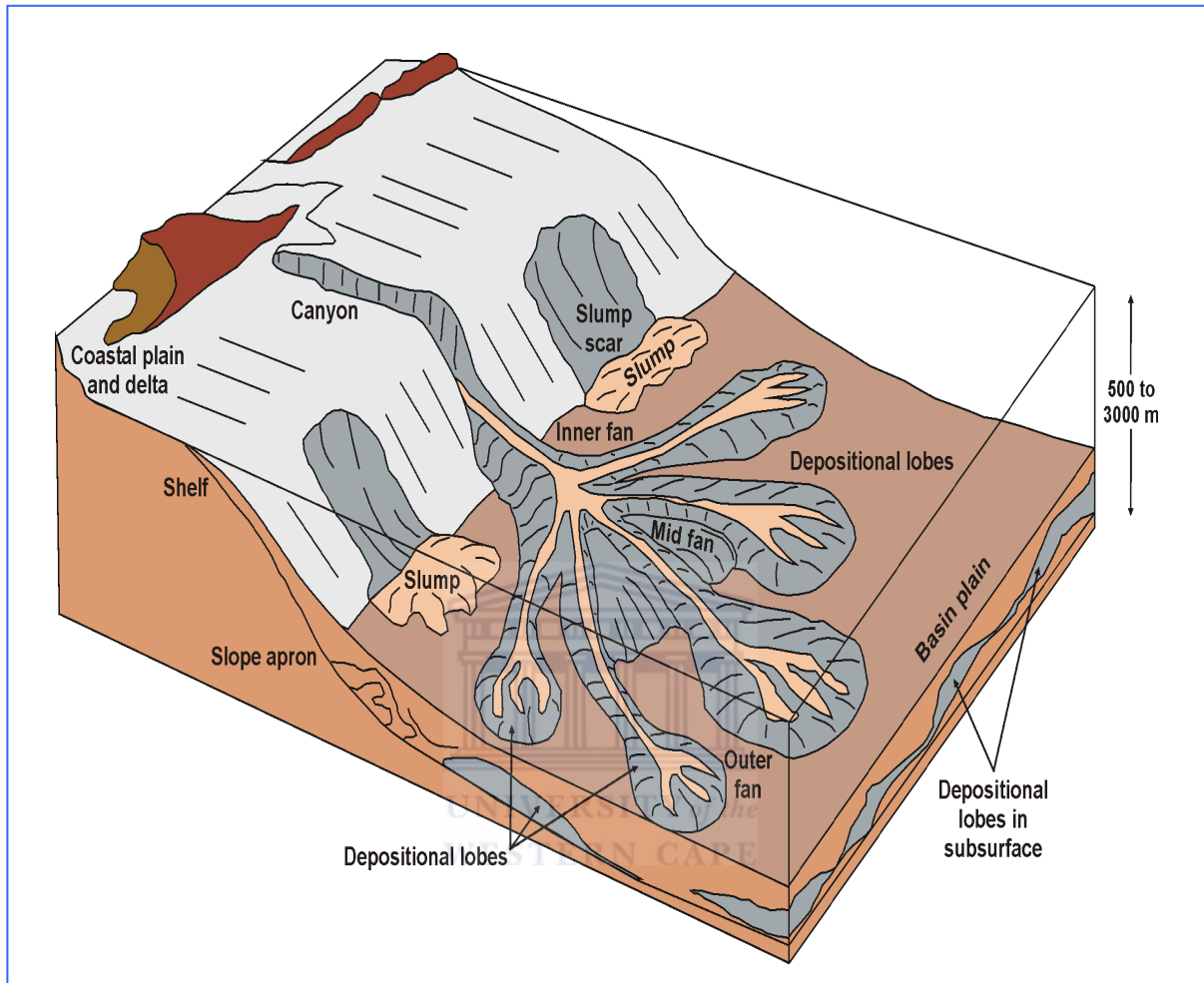


Figure 2.4: Evolution of deep marine channel deposits, (Van Wagoner 1988)

These features formed due to the erosion of incised valleys and submarine canyons, followed by channelized slope fans and deltaic/coastal lowstand wedges that prograded during a relative sea level rise. Flooding of the shelf as relative sea level rise accelerated and resulted in poorly defined transgressive systems tracks. With the relative sea level at a highstand extensively developed deltaic/coastal systems prograded basinward exhibiting well-defined clinoforms.



The major hydrocarbon plays in the lowstand tracts occur as mounded basin – floor turbidite fans, channel fills and draped sheets and is found in the up-dip pinch –out of deltaic /coastal sandstones.

## 2.2 Tectonic Setting of the Outeniqua Basin

The Outeniqua Basin, comprising of four sub-basins (Bredasdorp, Pletmos, Gamtoos and Algoa) was formed from dextral shearing processes of the South African margin, which began in the Early to Mid-Cretaceous. The rift phase of the south coast ended in the Lower Valanginian, which is associated with drift-onset unconformity (Petroleum Agency Brochure 2004/2005). The drift-onset unconformity is simultaneous to the earliest oceanic crust in the South Atlantic. A complex series of micro plates such as the Falkland Plateau gradually moved southwestwards, past the southern coast of Africa (Figure 2.5 Top). These movements created some oblique rift half-graben sub-basins including the Bredasdorp Basin which may be regarded as failed rifts. It is youngest in the west and oldest in the east (Figure 2.6).

Succeeding to the rift phase was a transitional rift-drift phase featuring at least three phases of inversion related to continuous shearing. Transitional rift drift ended in the mid Albian as the Falkland Plateau finally separated from Africa and was followed by the development of a true passive margin (Figure 2.5 Bottom).



Figure 2.5: The rift phase in the Late Jurassic – Lower Valanginian showing the break up of Africa, Madagascar and Antarctica (modified from Broad, 2004)

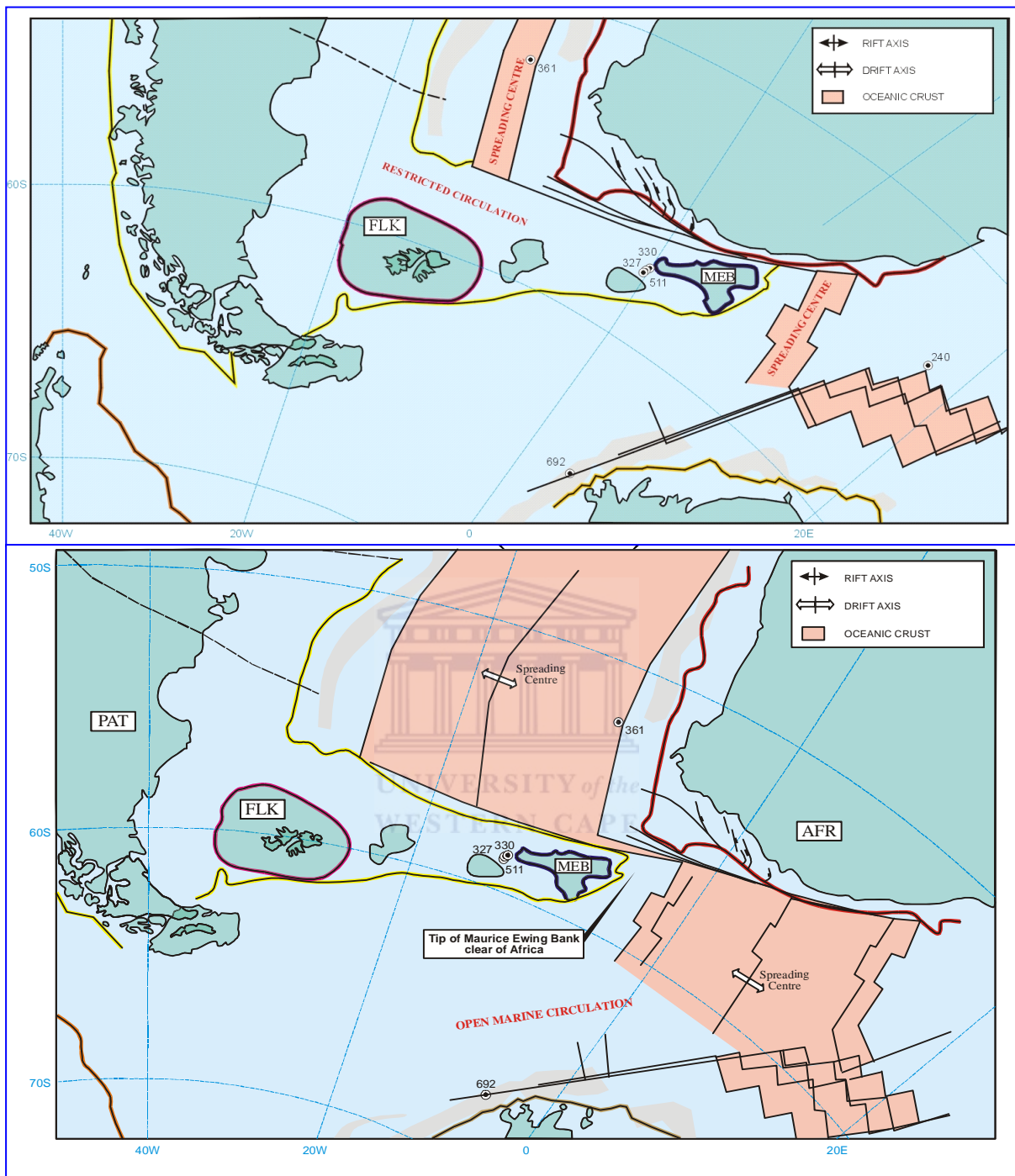


Figure 2.6 **Top:** Early drift phase in the Valanginian (1At1) – Hauterivian (6At1) showing the movement of microplates: Falkland Plateau (FLK), Patagonia (PAT) and Maurice-Ewing Bank plates (MEB) past south coast of Africa (modified from Broad, 2004)

**Bottom:** Late drift phase in the Hauterivian (6At1) onwards (Modified from Broad, 2004)

## 2.3 Tectonic History

The Bredasdorp as well as the adjacent Pletmos and Gamtoos basins experienced onset of rifting during the Middle-Late Jurassic. Dextral transtentional stress which was produced by the breakup of Gondwanaland which occurs to the east between the Falkland Plateau and the Mozambique Ridge, initiated normal faulting north of the Agulhas–Falkland fracture Zone. (R. A. Livermore 1999)

The principle normal fault bound elongate synrift graben and half graben basins up to  $\approx 10$  km wide. Deposition of thick synrift continental and marine sediments continued within the rift basin until  $\approx 126$  Ma when most extensional faulting ceased, the synrift deposition started and initiate postrift tectonics, erosion and deposition.

After the above mentioned took place widespread uplift of major bounding arches and less within the horst blocks in the region resulting in enhanced erosion of the lower Valanginian drift onset second order unconformity. Subsidence and deposition during the initial postrift supercycle that is composed of third order cycles were concentrated within the most central parts of the Bredasdorp Basin. Distribution of the early postrift Bredasdorp embayments closely coincides with the distribution of the late synrift basins, which continued to subside slowly along the rift faults during most of the supercycle. (R. A. Livermore 1999)

The Bredasdorp Basin resembles well-developed systems tracts and type 1 erosional unconformities. The supercycle ended with the final movement of the Falkland Plateau westward past the Agulhas platform. During the remainder of the Cretaceous the Bredasdorp Basin experienced four principle episodes of subsidence ranging from 9-12 m.y. in duration, each terminating by the uplift of basin margins and sub aerial erosion.



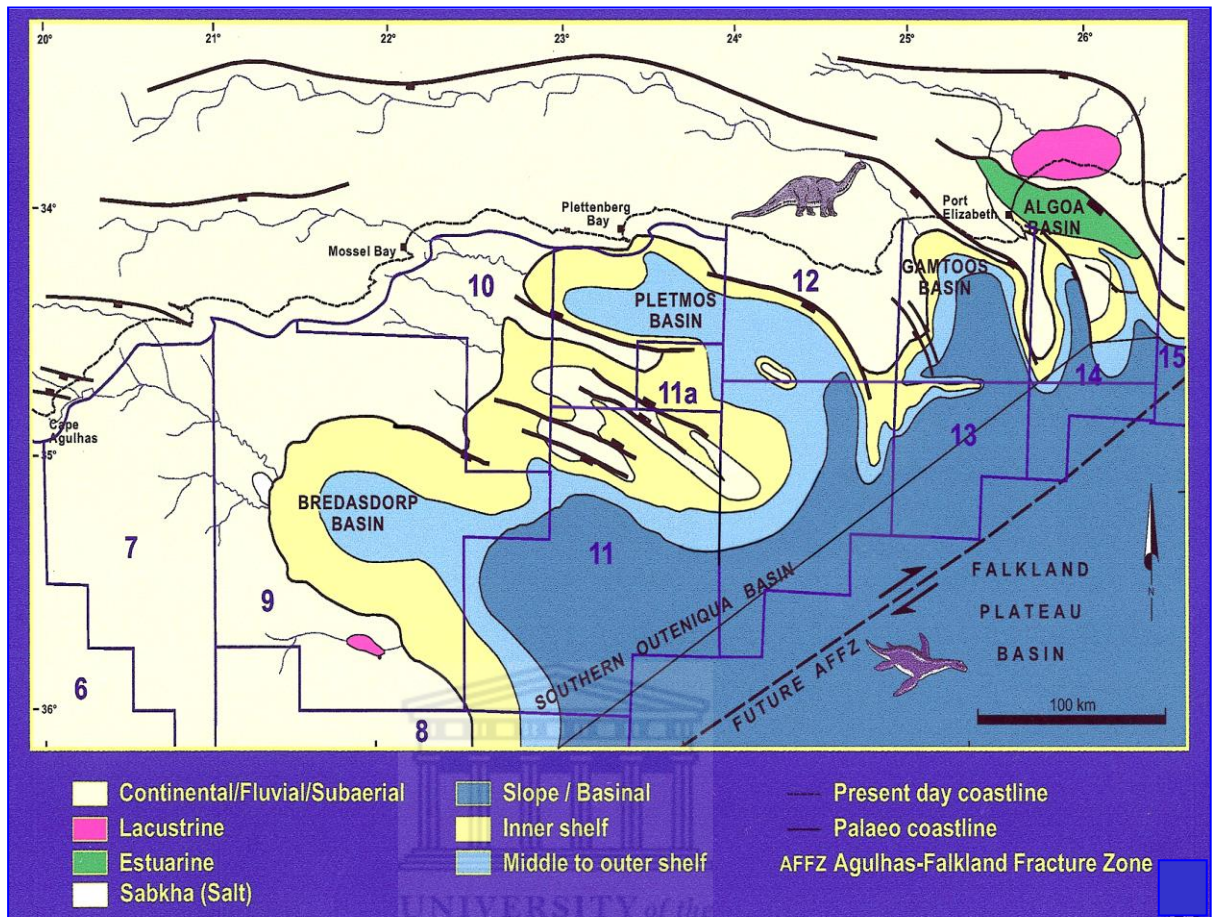


Figure 2.7: Oblique rift half-grabens sub-basins of Outiniqua Basin: Bredasdorp, Pletmos, Gamtoos, and Algoa (from Broad, 2004)

## 2.4 Depositional Systems

The Bredasdorp Basin evolved from fan deltas and river dominated to wave dominated deltas and also associated coastal systems. Slope and basin systems evolved from fine-grained density and suspension deposits to leveed slope and basin floor turbidite fans this has also been related to the fine-grained turbidite systems. The changes is due to the response to second order tectonic episodes which resulted in the variation in sediment supply

rates and subsidence or accommodation rates and increasing open ocean processes.

Four relative isolated fault bounded subbasins composing the Bredasdorp Basin during supercycle 1-5 (126-117.5 Ma) were supplied with sediments by high gradient fluvial systems. River dominated deltaic systems progrades southward across the northern margin of the central subbasin. (PASA brochure 2005)

During the second postrift supercycle 6-12 (117.5-112 Ma) well developed river dominated deltaic coastal systems prograded into the expanded basin. This deposition followed major uplift and erosion of second order erosion of the second order unconformity. Fluvial sediments were introduced to lowstand shorelines through small canyons and eroded into the shelf edge. The Upper Barremian 9A LST basin floors comprises of several individual submarine fans. The lowstand prograding wedges does not appear at all of the mouths of all of the entrances of the river systems. It only occurs where the sediment supply rates exceeded accommodation rates for the sediments.

## 2.5 Source Rock Maturity

The geologic elements necessary for oil and gas accumulation in sufficient quantities to create a pool large enough to be worth producing are:

- i. Organic-rich source rocks
- ii. Porous and permeable reservoir rocks to store the accumulated oil and gas
- iii. A system of trap and seal to prevent the oil and gas from leaking away

Petroleum source rock can be defined as fine-grained sediment which in its natural setting has generated and released enough hydrocarbons to form

commercial accumulation of oil or gas. For a rock to be referred to as petroleum source rock, it must have the quality and sufficient amount of dispersed organic matter otherwise referred to as kerogen and must be matured. The quality of oil generated by any source rock is dependent on the ease of degradation of the constituent kerogen and the time-temperature relationship.

Common petroleum source rocks are clays and carbonate muds.

The Bredasdorp basin is rich in gas and oil prone marine source rocks of the Kimmeridgian to Berriasian age. An oil prone Lower Cretaceous lacustrine source rock is present in the onshore Algoa sub-basin. Known oil and gas source rocks of deep marine origin is situated in a transitional rift-drift sequence. These are best developed in the Bredasdorp Basin. All the source rocks are mature over a large area.

Sandstone reservoirs are present in both the synrift and drift sections; the reservoirs are shallow marine to fluvial where the drift sandstones are deep marine turbidite deposits. The trapping mechanisms within the synrifts are structural as well as truncational. The drift marine shale's provide the main seals. Synrift seals also exist and are mainly tilted fault blocks. Prospect within the Bredasdorp Basin indicates a very high hydrocarbon potential and contains almost all of South Africa's proven hydrocarbons (Broad, 2004).

## 2.6 Tectonic Elements in the Bredasdorp Basin

The most abundant tectonic elements in the Bredasdorp Basin are normal faults but compressional structures are also developed. Normal faults have listric geometry and detach onto common décollement planes depth. Several normal faults have associated transfer faults and therefore the normal fault systems in the Bredasdorp Basin are typical linked Fault systems, defined by

(Gibbs 1990). Several different orientations of normal faults can be recognised which implies that the extension took place in different orientated stress fields at different geological times. The oldest faults in the area are rift faults that do not displace the drift onset unconformity 1At1. The second generation of normal faults displaced 1At1 and may involve the lower sequences of the post rift sequence. The youngest normal faults displace the base-Tertiary unconformity. Non-tectonic normal faults, which are not basement involved, are also recognised in the Bredasdorp Basin and these structures form as the result of differential compaction in the post rift sequence. Tectonic normal faults may also have components of differential compaction and is therefore possible that many of the younger normal faults are of compactional origin rather due to crustal extension.

## 2.7 Paleogeography



The post rift Cretaceous paleogeography of the basin clearly evolved in response to the changing tectonic history of the basin, which also in respect recorded the stacking of the third order sequences. An initial postrift basin exhibited several small embayments that closely conformed to the residual synrift subbasin. An enlarged basin that flooded and integrated the initial postrift embayments with connections to the proto Indian Ocean also evolved and gradually expanded the basin with an increasing connection to the early Atlantic Ocean.

The initial restricted postrift Bredasdorp Basin during supercycle 1-5 was composed of four major fault bounded subbasins, two of the subbasins were aligned a northwest–southeast axis and two others along a east and west axis through the central area which was bounded by the Infanta and Agulhas arches. Fluvial sediments entered the embayments mainly via the northwest along the axis of one of the existing synrift subbasins and from the north and northeast across the faulted northern margin of the restricted basin. Fluvial



sediments also entered the embayments via Agulhas Arch along the southeastern margin of the basin. The isolated embayments were connected by a narrow passage to the southeast with the Southern Outeniqua Basin and the early Indian Ocean. (Clifton 1969)

The Bredasdorp Basin expanded during supercycle 6-12 and thus mainly fluvial sediments continued to enter the basin from the north and northwest. The basin maintained the strong northwest–southeast elongation and inherited a synrift subbasin but was now open to relatively free marine circulation to the southeast with the Southern Outeniqua Basin and Indian Ocean. At the beginning estimated at ~112 Ma the Bredasdorp Basin was subjected to four 10 m.y. long thermal decay subsidence cycles that greatly enlarged the Cretaceous basin by coastal encroachment. Each of the transgressive regressive supercycle was terminated by basin margin uplift; intense erosion then took place and then renewed subsidence. The Falkland Plateau had by that time moved westwards past the Bredasdorp basin thus it was now fully open to the Southeastern Outeniqua Basin and in increasingly growing Indian Ocean. Opening of the basin resulted in the relatively high marine circulation and wave energy, which is also indicated by wave dominated delta systems and evidence of geostrophic erosion of slopes. During supercycles 13 and 14 fluvial sediments entered the basin mainly from the west and northwest but during this time supercycles 15, 16 as well as 17 and 20 entered the basin primarily from the northeast.

## 2.8 Sequence Stratigraphy

### 2.8.1 Cycles Frequencies and Sequence and Parasequence Sets

In the Bredasdorp Basin it has been established that a total of 24 seismically resolvable postrift Cretaceous unconformities and associated depositional sequences between the drift onset second order unconformity and third order

unconformity which is situated at 126Ma and 79Ma. All of the sequences are estimated to be of type 1, which six of the unconformities exhibit, intense tectonically enhanced erosion, which also coincide with the second-order and third-order surfaces. There is a total of 20 third order sequences composing of five second-order supersequences within the Bredasdorp Basin. Most of the sequences is poorly developed fourth order sequences.

Fundamental third order sequences, described by Mitchum and Van Wagoner 1988, comprise depositional tracks that are composed of parasequence sets which exhibits characteristic stacking patterns illustrated on below:

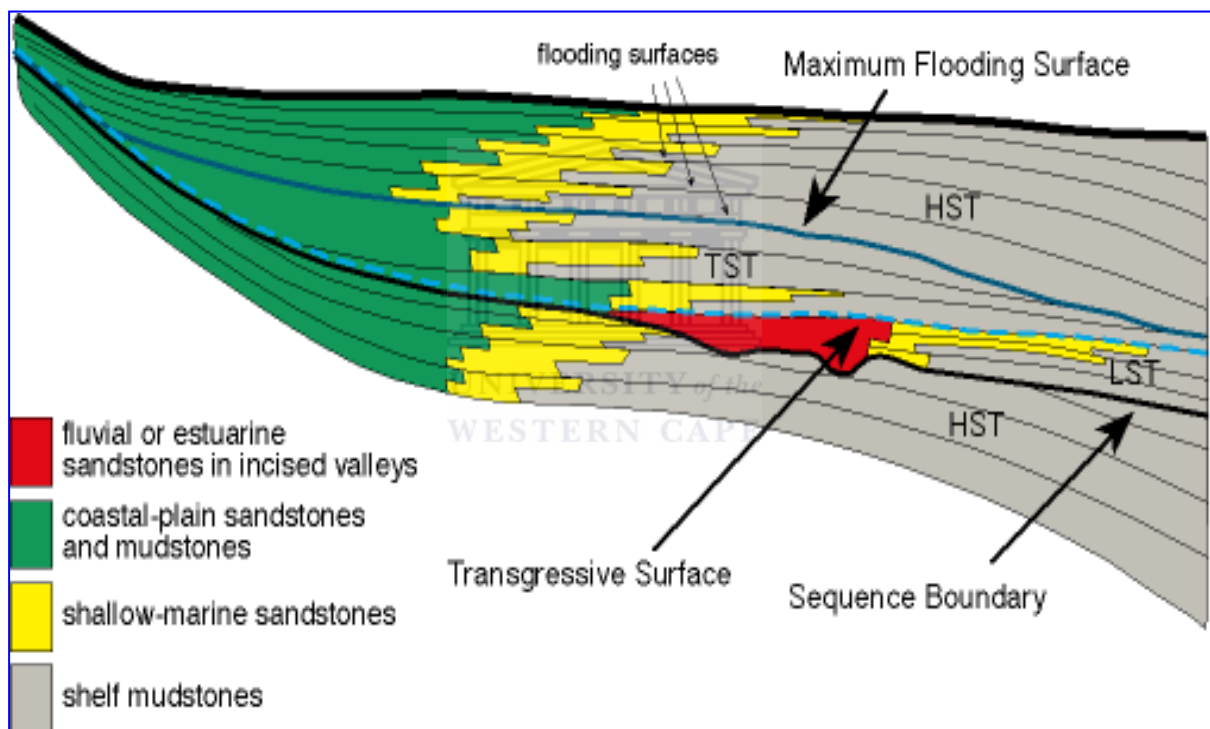


Figure 2.8: Exxon model sequence (type 1) developed on a margin with a shelf slope break (van Wagner 1990)

The location and nature of these depositional sequences are related to relative sea-level fluctuations. The rate of sea-level change is the parameter that largely controls the stratigraphic response. This is illustrated in the model on the following page:

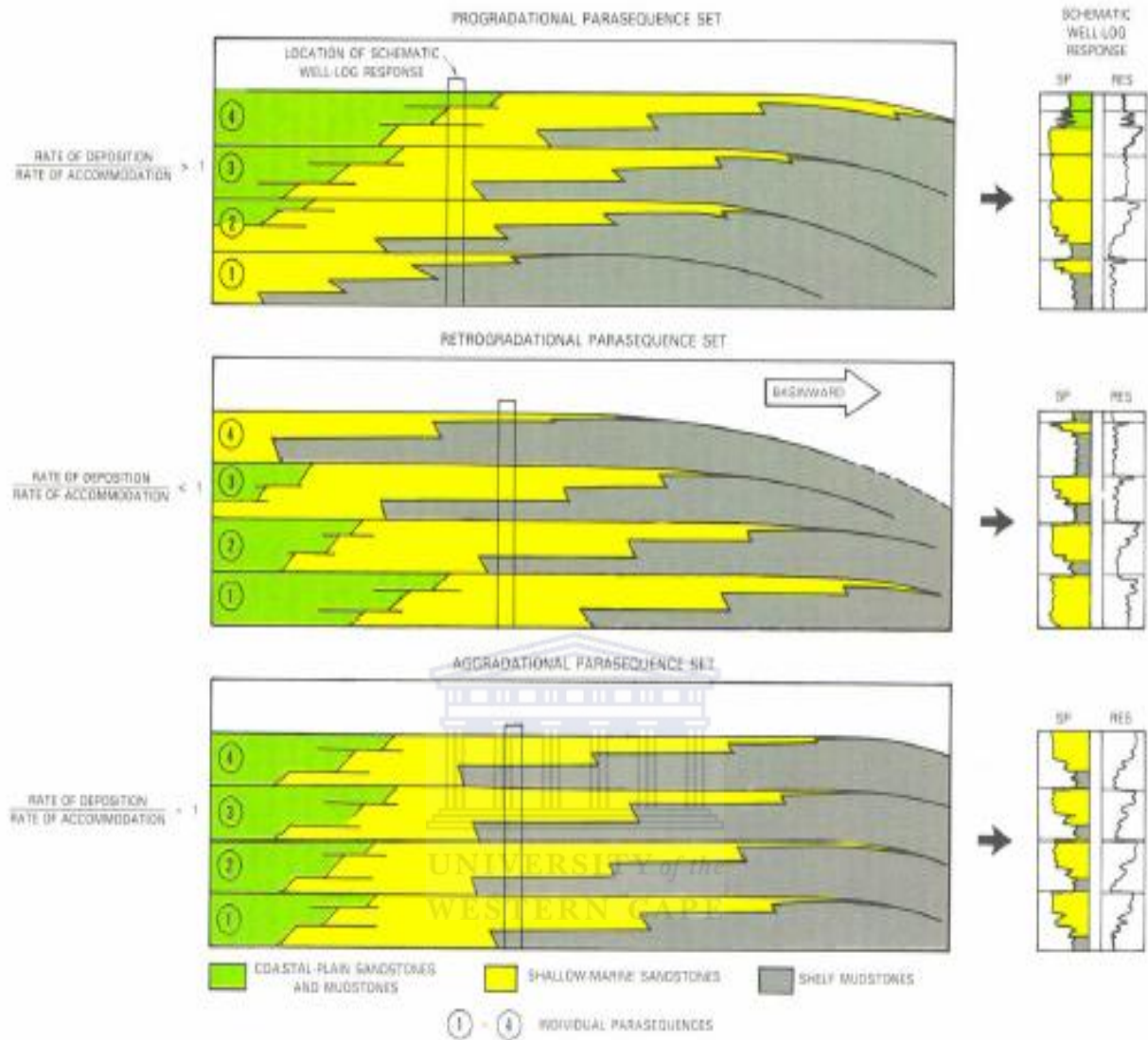


Figure 2.9 Parasequence stacking patterns (Van Wagner 1988).

The Bredasdorp Basin resembles the same type of depositional sequences as well as the sedimentary supply to the basin; it also correlates to the low and high systems tracks within the basin, which is illustrated by the models of Plint 1988.

In the Bredasdorp basin the postrift cretaceous third and fourth order sequences and most of the component systems tracts are seismically resolved between the lower Valanginian (126Ma) and the upper Campanian (77.5 Ma). The sequences are bounded by sub-aerial and submarine type 1

unconformities, which were correlated by PetroSA on all seismic profiles throughout the basin. The Drift sequences within the basin have a general lack of sand rich low stand reservoir facies.

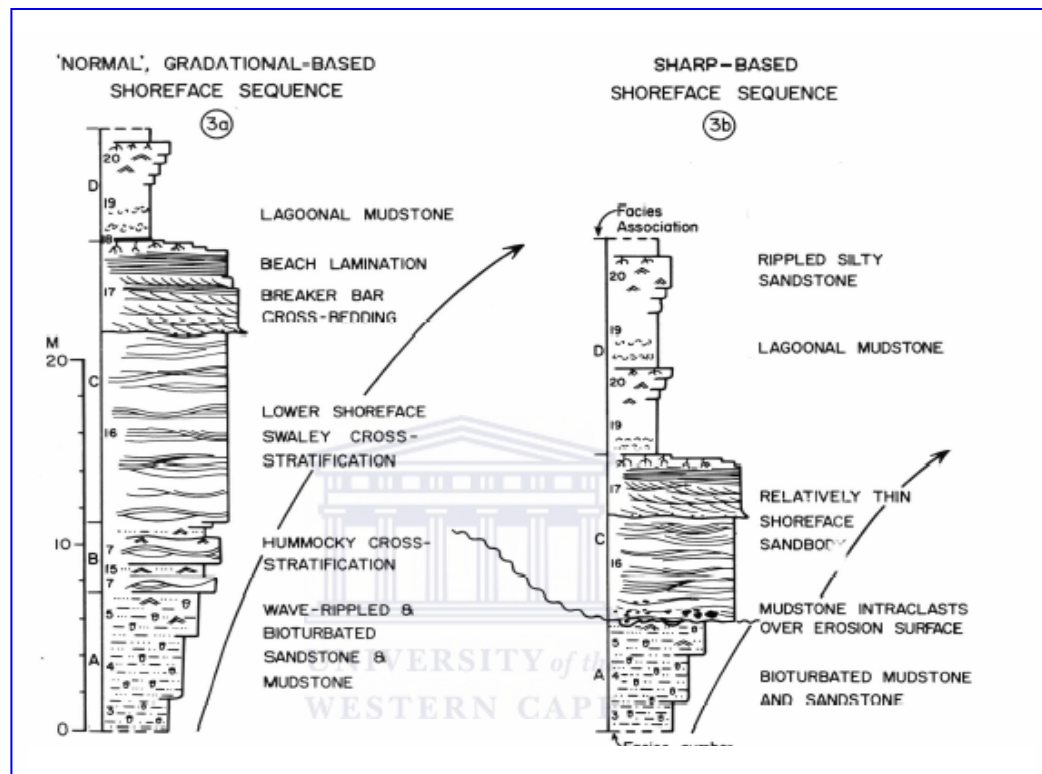


Figure 2.10: Schematic lithologic contrasting the facies sequence seen in: (a) gradational and (b) sharp-based shoreface sequence (Plint, 1988).

The Pre- 177.5 Ma sequences are mostly distal, fine-grained, deep water high-stand and low-stand facies. The sequences are all preserved within the central parts of the faulted sub-basin.

Some of the low-stand fan delta wedge systems were preserved on the downthrown sides of the reactive synrift faults on the northwestern and southwestern part of the basin margin and were progressively onlapped during coastal encroachment that characterized the first postrift sequence.

## 2.9 Lowstand Systems Tract (LST)

The lowstand systems tract develops after the formation of a sequence boundary. It is the set of depositional systems developed during the time of relative low sea level in which sediment production is reduced on rimmed shelves because a relatively small shallow water area is available for sediment production (Figure 2.7).

Provided relative sea level has fallen sufficiently and a distinct shelf-slope break exists, lowstand systems tract may include two distinct parts: lowstand fan and lowstand wedge. If the system lacks a distinct shelf-slope break and relative sea level does not fall sufficiently, only a lowstand wedge may form.

The lowstand fan consists of a basin-floor submarine fan which typically displays aggradational stacking and is overlain by the lowstand wedge. The river incises into the exposed shelf during the time of the lowest relative sea levels and the sediment get shunted directly off the shelf edge to feed submarine fans.

A lowstand wedge consists of a progradational set of parasequences building out from the pre-existing continental slope. The slow rise in relative sea level subsequent to its fall and production of a sequence boundary brings in a slow rate of accommodation coupled with a comparatively high supply of sediment and results in the progradational stacking of sediment typical of lowstand wedge.

## 2.10 Transgressive Systems Tract (TST)

The transgressive systems tract is made up of retrogradational sets of parasequences. It is separated from lowstand systems tract (LST) by the underlying transgressive surface (ts) or flooding surface and overlain by the maximum flooding surface (Figure 2.8). Flooding surfaces display strong facies contrasts, pronounced deepening, and a strong degree of sediment starvation, which makes it quite thin compared to other systems tracts.

The continuous relative sea level rise produces accommodation space at a faster rate than it can fill with sediments; hence a relatively minor amount of sand reworked along the shoreline (nearshore sand) and little sediment (thinner offshore deposit) is transported to the outer continental shelf.

## 2.11 Highstand Systems Tract (HST)

This consists of an aggradational to progradational set of parasequences that overlies the maximum flooding surface and is terminated at the top by the next sequence boundary.

The period of highstand systems tract is characterized by slowness in the rate of relative sea level rise and its fall prior to the next sequence boundary.

Seaward progradation of sediments may partially infill inner part of the outer shelf as a result of sea under the influence of high rate of sediment production. Slope and basinal environments also receive excess shelf and shelf-edge derived materials. Subsequently, a new sequence boundary is gradually formed and begins to erode into the underlying highstand systems tract (Figure 2.8)

The Bredasdorp basin is a basin that underwent a series of structural deformation during the break up of Gondwanaland and the rest of the continents within the southern hemisphere. The structural deformation within the area with the addition of sediment influx from the coastal region was sufficient in the formation of average to good source. The area mainly consists of half grabens which dip slightly towards the south with structural pinchouts completing the trapping mechanisms for hydrocarbons within the basin.





## Chapter 3

### 3.1 Delineation of the E-M Suite E-M Suite

The Mossgas E-M field is an offshore gas field located approximately 50 km to the west of the existing F-A platform on the Agulhas Bank. The E-M was planned to use an 18" subsea pipeline approximately 49 km long, linked to the F-A platform.

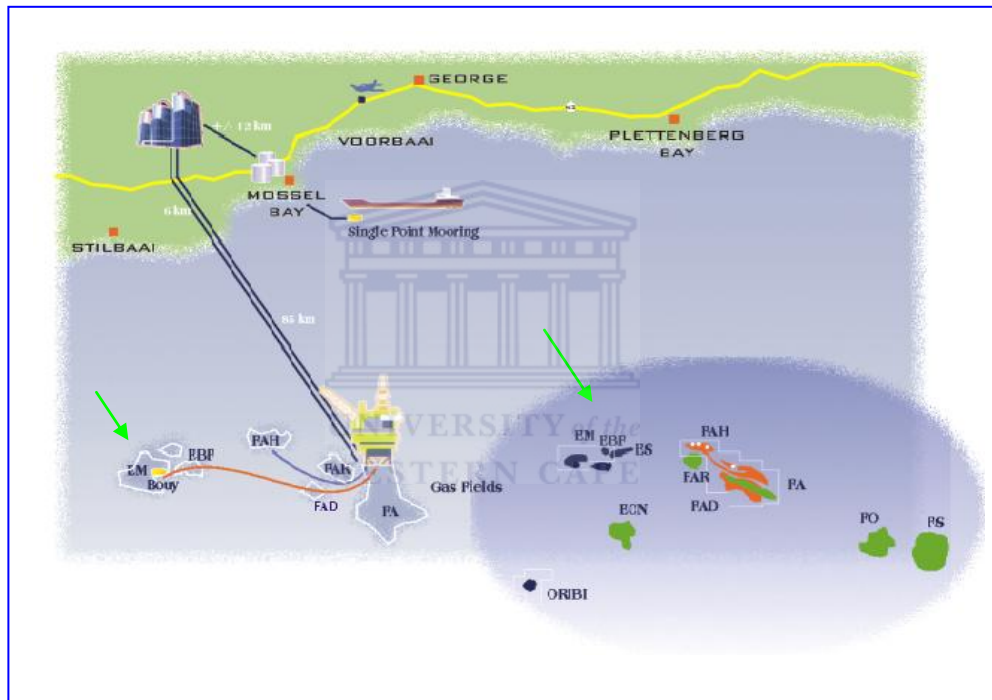


Figure 3.1: Delineation of study area courtesy Petroleum South Africa

E-M 1 was the first well drilled on the E-M structure which has an aerial closure of 10 km<sup>2</sup>. The upper 45 meters of the reservoir section is formed by shallow marine sandstone and the lower 80m is formed by fluvial sandstones with interbedded claystone. There is good quality source rocks situated between 2310m to 2440m and has approximately 32 m of interbedded green claystone and siltstone.



The absence of the shallow marine sandstone in E-C1 could suggest that there is a possibility of stratigraphic pinchouts to the west and north of E-M1 which in turn may suggest effective hydrocarbon traps. There might be the possibility of a second channel affecting the reservoir with a different sequence of events. E-M 1 is thus a gas recovery well.

E-M 2 is situated approximately 1.7 km north-east of E-M 1 and has good quality mature source rocks present in the lower parts of the succession between 2315m to 2410m and between 2500m to 2530m. The submarine fan sequence is a very poorly developed sequence. The sequence situated below 2567m is a 34m fluvial succession and overlies a reduced thickness of shallow marine sandstone (Appendix 5). A thick column of green claystone is present immediately but is much shallower than that in E-M 1. The fluvial sediments continue to 2759m and continue to the base at where drilling recommenced. The fluvial succession is interbedded with a thick sandstone unit. The well was stimulated with acid in an attempt to get the well clean; the acid caused damage in the well through fines migration and causing the reduction of the permeability even more. The submarine sandstone allocated within the well is a very poorly developed sandstone sequence. The sequence that is just below 2567m consists of mainly fluvial sediments and continues to 2759m.

The geophysical logs indicate a net hydrocarbon bearing sandstone between 2607m to 2646m (Appendix 5). The average poroperm is approximately 17 % and 340mD throughout the gas and oil bearing zones but the permeability increases in the latter parts of the well.

The hydrocarbon in this well is approximately 15 meters deeper than in E-M 1 caused trough faulting. Results within Appendix 5

E-M 3 lies approximately 1.75km south of E-M 1, 3.25km south-south-east of E-M 2 and is located in a fault block down throw to the south on the southern flank of the domal closure. The well was abandoned due to the fact that the sandstone/ reservoir sand was too thin and too tight to have any economical value or potential. The top of the primary sandstone targeted is at the same depth as the hydrocarbon water contact (HwC) for the rest of the domal structure and so concludes that all this sandstone is non hydrocarbon bearing but instead water bearing. At depth 2564m marine sediments are located rather than the fluvial marine transition.

E-M 4 is situated approximately 1.88km west of E-M 1 and falls within the domal closure of the E-M structure and is 95 km south-south-west of Mosselbay. The well has moderate quality mature source rocks capable of generating oil and wet gas and this is present within the lower parts of the well situated between 2375m and 2450m. Just below that sequence two intervals of shallow marine sandstone are evident and are situated at 2559.5m to 2610m and 2749m to 2821m the rest of the succession is made up of fluvial sediments.

The reservoir is porous to slightly porous and glauconitic sandstone is present from 1994m to 2055m. From the geophysical logs it can be safe to say that the reservoir interval is situated or exists between 2558m to 2630m. Average porosities and permeability are 14% and 53md respectively where the maximum's are 18.5% and 697md respectively.

The shallow marine sandstones are underlain by non glauconitic channel sandstones and green and red claystone interbeds. In Table 1 below a comparison of the mean porosity and permeability for the shallow marine sandstone for the four wells in the E-M structure:

	<b>E-M 1</b>	<b>E-M 2</b>	<b>E-M 3</b>	<b>E-M 4</b>
<b>Porosity (%)</b>	<b>15.5</b>	<b>13.5</b>	<b>11.7</b>	<b>14</b>
<b>Permeability (mD)</b>	<b>210</b>	<b>66</b>	<b>2.5</b>	<b>53</b>

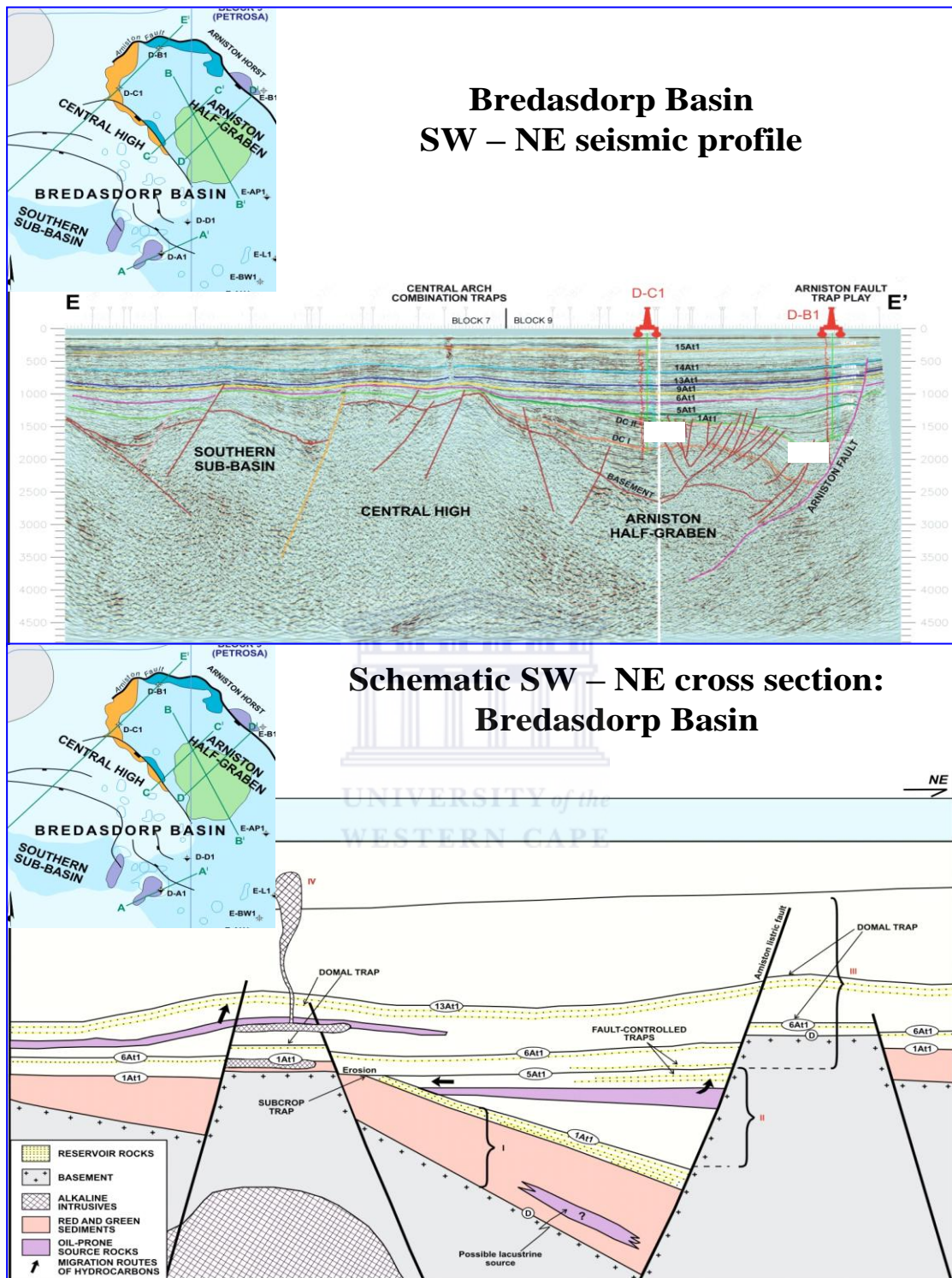
Table 1: Average porosity and permeability distribution over the E-M suite

Table 1 shows a clear indication of a drop in permeability within the E-M structure but an almost unwavering porosity is maintained. The gas saturated shallow marine sandstone is located between 2558m to 2617m with the oil zone occurring between 2617m to 2634m. From the geophysical logs it can be observed that this unit is situated in the oil water transition zone. The base of the shallow marine sandstone is underlain by non glauconitic channel sandstone and green and red claystone interbeds.

The shallow marine sandstone corresponds closely to that of E-M 2 that can be observed in Appendix 3 and 4. The hydrocarbon-water contact (HwC) at 2634m is very consistent with that found within the E-M 2 well. The top of this reservoir is found to be approximately 53m deeper.

The schematic drawing within Figure 5.2 shows the sequence boundaries as well as the domal closures within the E-M suite.

These features formed contemporaneously with the erosion of incised valleys and submarine canyons, followed by channelized slope fans and deltaic/coastal lowstand wedges that prograded during a relative sea level rise. Subsequent flooding of the shelf as relative sea level rise accelerated resulted in poorly defined transgressive systems tracts. Extensively developed deltaic/coastal systems prograded basinward, thus exhibiting well-defined clinoforms; the relative sea level at a highstand.



**Figure 3.2: Top:** Seismic profile with identified sequence boundaries  
**Bottom:** Schematic cross section (modified from Broad, 2004)

Sandstone reservoirs in the Bredasdorp Basin are characterized by a range of stacked and amalgamated channels and lobes. They originated from the materials eroded from pre-existing highstand shelf sandstones and transported into the central basin by turbidity current (Petroleum Agency of South Africa Brochure 2005).

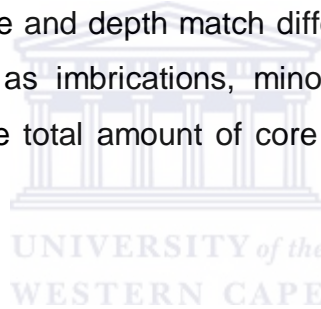
Channelized reservoirs are more abundant in the western and southwestern play areas as a result of their proximity to the base of the slope relative to the eastern area where fan lobes predominate. They are not directly affected by faulting although there is evidence to suggest that deep-seated basement structures related to synrift faulting influenced palaeo channel trend of the Aptian and Albian sequences. Generally, sandstone reservoirs are present in both synrift and drift sections (Petroleum Agency South Africa Brochure).

Marine shales and condensed sections developed during the transgressive phase act as seals. Traps are feasible from Late Cretaceous to Early Tertiary. Structural and truncational traps are noticeable within shallow marine to fluvial synrift reservoirs while drift reservoirs are trapped by a wide variety of low relief closures such as compactional drape anticlines, stratigraphic pinch-out traps and inversion-related closures (Petroleum Agency of South Africa Brochure 2004)

## Chapter 4

### 4.1 Methodology

Data for this project was collected over the period March to May 2005 obtaining well completion reports and other hard copied data as well as digital data from the Petroleum Agency of South Africa (PASA). The E-M suite consists of four primary wells, which are situated, in close proximity to each other. The selected cores by Petroleum South Africa were laid out within a core shed supplied by PASA and approximately 4 - 5 hours were spent daily physically investigating the cores of each well. The extensive time was spent to describe, correlate and depth match different horizons. Log different geological features such as imbrications, minor faults and folds to their corresponding depths. The total amount of core recovered is 372m from all four wells.



#### 4.1.1 Core Samples

These are cylindrical samples of rock taken from a formation in situ for analysis purposes. This is done by substituting a conventional drill pipe core barrel and core bit for the drilling bit to obtain samples as it penetrates the formation.

Usually cores are cut using a special coring bit and are retrieved in a long core barrel. The core barrel is a hollow cylindrical device 7.6m to 18m in length with a hollow drill bit which can be attached to the bottom of the drill pipe for the purpose of recovering continuous samples of the formation while the hole is being drilled. The samples recovered are cylindrical cores and can be as long as the core barrel, Reifentstahl 2002 .



Core samples provide a full sample of rocks penetrated. It is used both for qualitative (visual lithology) and quantitative analysis, which is a laboratory analysis of recovered reservoir formation samples for the purpose of measuring porosity, directional permeability, residual fluid saturation, grain size, density, and other properties of the rock and contained fluids. It is also used to calibrate wireline logs.

Additional coring methods such as sidewall coring could be carried out when extra rock samples are necessary after the well has been drilled and before it has been cased. Sidewall cores are obtained with a wireline tool from which a hollow cylindrical bullet is fired into the formation and retrieved after each bullet has been fired into the formation wall by a free pull by wires connecting the barrel to the gun. Core barrels are accessible for piercing formations of different hardness. The type of barrel and size of charge are varied to optimize recovery in different formations.

The problem with coring lies in the tendency of the formation samples to undergo physical changes on its way from the bottom of the well to the surface. More sophisticated coring mechanisms that can preserve the orientation, pressure and original fluid saturations of the core samples have been developed.

The cores are held within core boxes delineating the location and the depth to which each recovered core belongs to. Parts of core were still encased within waxed cylinders to preserve the original environmental fluids as well as the original sediment from the subsurface. These waxed units are randomly selected on basis of how important certain units of core were to the study. Certain parts of the waxed units visually obscured the investigation of the core and obstructed conformation to contacts between sedimentological units and grain size distribution between different sections of the core and were left

to proficient decision making as well as assumption on the continuum of the stratigraphic sequence.

Random core plugs were selected within each well to further evaluation to grain size distribution and the porosity and permeability traits each core attained.

## 4.2 Productivity Test Data

Productivity Test Data include: Formation Tester and Drill Stem Test (DST). Obviously, not all of these measurements are made in just any single well. A careful selection of a specific measurement is made in order to completely identify and evaluate the commercially productive hydrocarbon bearing zones.

Formation testing presents collection of data on a formation to determine its potential productivity before installing casing in a well. If a well flows hydrocarbons on a drill stem test, no amount of log or core samples analyses can deny that a productive zone has been found.

### 4.2.1 Drill Stem Test (DST) and Wireline Formation Testing

Drill-Stem Test, which is defined as a temporary completion of a well, is a procedure for testing a formation through a drill pipe. Incorporated in the drill-stem testing tool are packers, valves, or ports that can be opened and closed from the surface, and a pressure-recording device.



The formation fluid is recovered in the drill pipe through temporary relief of back-pressure imposed on the formation. Hydrostatic, flowing and shut in pressures are recorded against time.

A DST not only provides the proof that hydrocarbons exist in the formation and that it will flow, but it also supplies very important data concerning both the size of the reservoir and its capability to produce. Interpretation of pressure records from drill stem test adds greatly to the overall formation evaluation.

Wireline Formation Testing complements drill stem test by their ability to sample several different zones encountered by the well. They provide fluid samples and detailed formation pressure data that is almost impossible to obtain from DST alone, Reifenstuhl 2002.

### 4.3 Well Logs

Well logs are a class of the most useful and important tools available to petroleum geologists. They are products of survey operations consisting of one or more set of digitized data or curves, which display an array of permanent record of one or more physical measurements as a function of depth in a well bore. They are used to identify and correlate underground rocks, determine their mineralogy, generate their physical properties and the nature of the fluids they contain.

During drilling a well, relatively little can be learned about the potential of the penetrated formation. The analyses of the returned cuttings, sometimes referred to as Measurement While Drilling (MWD), reveal the general lithology.

Geological sampling during drilling leaves a very imprecise record of the formation encountered. Mechanical coring is slow and expensive. Even though geophysical logs need interpretation to bring it to the level of geological or petrophysical experience, there strong points are in there precision and ability to bridge the gap between well cuttings and core samples. Levorsen 1967.

The geophysical wireline logs are the continuous records of geophysical parameters along a borehole. They are products of wireline logging which involves inserting a logging sensor or a combination of (Sonde) in the drill collar is lowered into the well bore by a survey cable and a continuous physical measurements (electrical, acoustical, nuclear, thermal and dimensional) are made. A sensor and its associated electronics are housed in a sonde, which is suspended in the hole by an armored electric cable. The sensor is separated from the virgin formation by the drilling mud, mud cake, and often by an invaded zone in the formation.

Signals from the sensor are conditioned by down-hole electronics for transmission up the cable to the surface electronics, which in turn conditions the signals for output and recording. As the cable is raised or lowered, it activates a depth measuring device which provides depth information to the surface electronics and recording devices. The data is recorded on digital tape, film or paper. Levorsen 1967.

Necessary geophysical measurements are obtained to allow a quantitative evaluation of hydrocarbon in place. It is very important to get accurate, well calibrated and complete data. The cost of Wireline logging generally amount to less than 6% of the total well budget.

Once a well is cased and in production, data missed in the original logging phase cannot be recovered anymore and costly work-over would be needed to find out what went wrong and where.

Some well logs are made of data collected at the surface; examples are core logs, drilling-time logs, mud sample logs, hydrocarbon well logs, etc. Other types such as movable oil plots, computed logs, etc. show quantities calculated from other measurements.

## 4.4 Rock Properties

Rock properties or characteristics, which affect logging measurements include:

### 4.4.1 Porosity



This is defined as the ratio of void space to the bulk volume of rock containing the void space. It can be expressed as a fraction or percentage of pore volume in a volume of rock and has a symbol  $\Phi$ . It is represented with the formula stated below:

$$\text{Porosity } (\Phi) = \frac{\text{Volume of Pores}}{\text{Total Volume of Rock}}$$

The amount of internal space in a given rock volume is a measure of the amount of fluids the rock will hold. The amount of interconnected void space excluding isolated pores and pore volume occupied by adsorbed water available to free fluids is referred to as effective porosity

The effective porosity can also be defined as the fraction or percentage of interconnected pore or void space volume in a volume of rock. It excludes isolated pores and pore volumes occupied by water adsorbed on clay minerals or other grains.

The total porosity is all void space in a rock and matrix whether effective or non effective. It includes porosity in isolated pores, adsorbed water on grains or particle surface and associated with clay. Levorsen 1967.

Porosity in sedimentary rocks can be primary or secondary. Primary porosity refers to the porosity remaining after the sediments have been compacted but without considering changes resulting from subsequent chemical action or flow of water through the sediments. Secondary porosity on the other hand is the additional porosity resulting from fractures, vugs, solution channels, diagenesis, and dolomitization. The three common types of secondary porosity are: fracture porosity, shrinkage porosity and dissolution porosity.

#### 4.4.2 Permeability

This is the property a rock has to transmit fluids. It is related to the effective porosity but not always dependent on it. Permeability is controlled by the size of the connecting passages (pore throats or capillaries) between pores. It is measured in darcies, more commonly in millidarcies and represented by the symbol  $K_a$ .

A measure of the ability of a rock to conduct a single fluid through its interconnected pores when it is 100% saturated with that fluid is called absolute permeability while effective permeability refers to the ability of a rock to transmit a fluid in the presence of another fluid when the two fluids are immiscible.

The ratio of the effective permeability of a fluid at partial saturation to its permeability at 100% saturation (absolute permeability) is the relative permeability. It is also defined as the ratio of the amount of a specific fluid that will flow at a given saturation, in the presence of other fluids, to the amount of the same fluid that will flow at a saturation of 100%, other factors remaining the same. It ranges in value from zero at low saturation to 1.0 at 100% saturation of the specific fluid.

Since different fluid phases inhibit the flow of each other, the sum of the relative permeability's of all phases is always less than unity.

#### 4.4.3 Resistivity

This is the rock property on which the entire science of logging was initially developed.

The resistance of a material which is its ability to resist the flow of the electric current at a particular temperature is directly proportional to its length ( $\ell$ ) and decreases with increasing cross-sectional area ( $A$ ). The proportionality constant is the resistivity ( $\rho$ ) of the material.

The resistivity of a material is its resistance ( $R$ ) over a specified length and cross sectional area. It is defined by:

$$\text{Resistivity } (\rho) = \frac{RA}{\ell}$$

In log interpretation, hydrocarbon, the rock, and fresh water all act as insulators and are therefore non-conductive and highly resistive to electric flow. The resistivity recorded on a resistivity well log may differ from true

resistivity because of the influence on the measured response caused by the presence of the mud column, invaded zone, adjacent beds and borehole cavities. This is referred to as apparent resistivity and may need correction prior to use in any computation.

The measured units are ohm-meters (ohm-m).

#### 4.4.4 Fluid Saturation

This is the fraction or percentage of the pore volume occupied by a specific fluid (oil, gas, water). It is generally defined by:

$$\text{Fluid Saturation } (S_f) = \frac{\text{Formation fluid occupying pores}}{\text{Total pore space in the rock}}$$

The fluid in the pore spaces of a rock may be wetting or non wetting. In most reservoirs, water is in the wetting phase while few reservoirs are known to be oil wet. The wetting phase exists as an adhesive film on the solid surfaces.

Water saturation is an important log interpretation concept because hydrocarbon saturation of a reservoir can be determined by subtracting water saturation value from a unit value (1), where a unit value (1) equals 100% water saturation. Water saturation  $S_w$  is measured in percentage. Underhill, J. R

Irreducible water saturation  $S_{w_{irr}}$  is the term used to describe the water saturation at which the water is adsorbed on the grains in the rock, or held in capillaries by capillary pressure. At irreducible water saturation, water (wetting phase) will not move implying a zero relative permeability and the non wetting phase is usually continuous and is producible under a pressure gradient of the well bore.

The occupation of fluids in a pore may take different forms:

- i. Funicular saturation. A form of saturation in which the non wetting phase exists as a continuous web throughout the interstices, which make it to be mobile under the influence of the hydrodynamic pressure gradient. The wetting phase may or may not be at irreducible saturation. Figure 4.1A illustrates the oil (non wetting phase) as funicular.
- ii. Pendular saturation. Here the wetting phase exists in a pendular form of saturation in which an adhesive fluid film of the wetting phase coats solid surfaces, grain to grain contacts, and bridges pore throats. The wetting phase may or may not be at irreducible saturation. In Figure 4.1, water (wetting phase) in A and B is pendular.
- iii. Insular saturation. A type of saturation in which the non wetting phase exists as isolated insular globules within the continuous wetting phase. Here it is uncertain that a decrease in pressure may cause the insular globules to collect into a continuous phase. Illustration in B and C of Figure 4.1 show that the oil (non wetting phase) is insular. Levorsen, 1967.

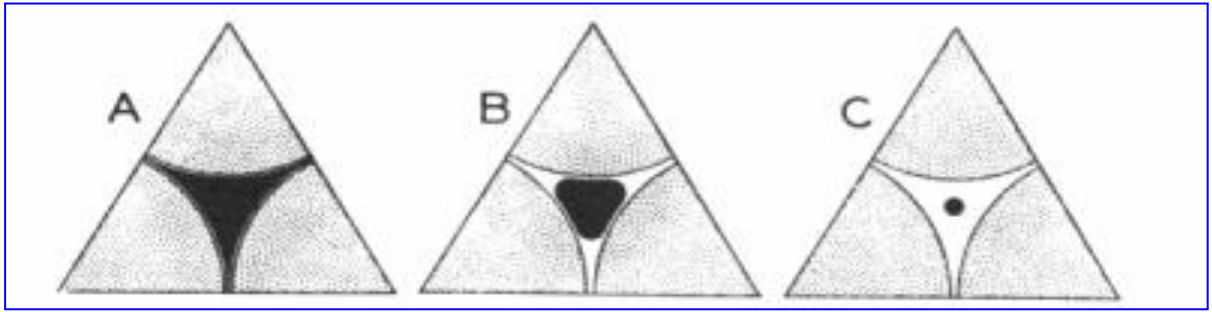


Figure 4.1: Non wetting oil (black) and water (blank) in a single water-wet pore (from Levorsen, 1967)

## 4.5 Characteristics of Selected Wireline Logging Tools

Wireline logging tools are numerous and new models designed to handle specific logging restrictions. Therefore for the purpose of this study, a few logging tools have been selected for short description of their distinctiveness.

### 4.5.1 Gamma Ray Logs (GR)

Gamma ray logs are designed to measure the natural radioactivity in formations (Figure 4.2). The number of energy of the naturally occurring gamma ray in the formation is measured and distinguished between elements of parent and daughter product of the three main radioactive families: uranium, thorium and potassium.

In sediments the log mainly reflects clay content because clay contains the radioisotopes of potassium, uranium, and thorium. Potassium feldspars, volcanic ash, granite wash, and some salt rich deposits containing potassium (e.g. potash) may also give significant gamma-ray readings. Shale-free sandstones and carbonates have low concentrations of radioactive materials and give low gamma ray readings. The standard unit of measurement is API (American Petroleum Institute)



High gamma ray may often not imply shaliness, but a reflection of radioactive sands such as potassium rich feldspathic, glauconitic, or micaceous sandstones. Gamma ray log is usually preferred to spontaneous potential logs for correlation purposes in open holes nonconductive borehole fluids, for thick carbonate intervals, and to correlate cased-hole logs with open-hole logs.

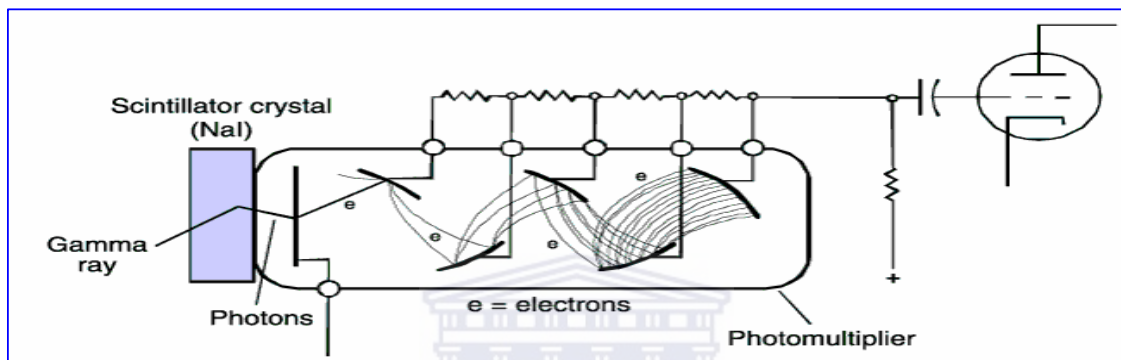


Figure 4.2 Gamma ray tool (modified from Serra, 1984)

## 4.5.2 Spontaneous Potential Logs (SP)

Also known as self potential logs, it measures potential (DC voltage) difference between a movable electrode in the borehole and a distant reference usually at the surface (Figure. 4.3). The SP results from the measurable voltage drop in the borehole produced by the flow of SP currents generated by electrochemical and electrokinetic potentials in the hole.

The SP tends to follow a fairly constant shale base line in impermeable shales while in permeable formations; the deflection depends on the contrast between the ion content of the formation water and that of the following:

- i. Drilling mud filtrate
- ii. Clay content
- iii. Bed thickness and resistivity
- iv. Hole size
- v. Invasion
- vi. Bed boundary effect.

In thick permeable, thick non-shale formations, the SP value approach the fairly constant value (static SP), which will change if the formation water salinity changes. It varies in dirty reservoir rocks and a set of pseudo-static SP value is recorded.

SP is most useful when:

- i. Drilling mud is fresher than the formation water
- ii. A good contrast exists between mud filtrate and formation water resistivity
- iii. Formation resistivity is moderately low

The SP curve becomes featureless when the mud column becomes so conductive that it fails to display a demonstrable voltage drop which the tool can support.

SP response of large negative deflection in permeable beds enhances easy sand-shale discrimination, correlation, and under favorable conditions estimation of formation water resistivity (Rider, 1996)

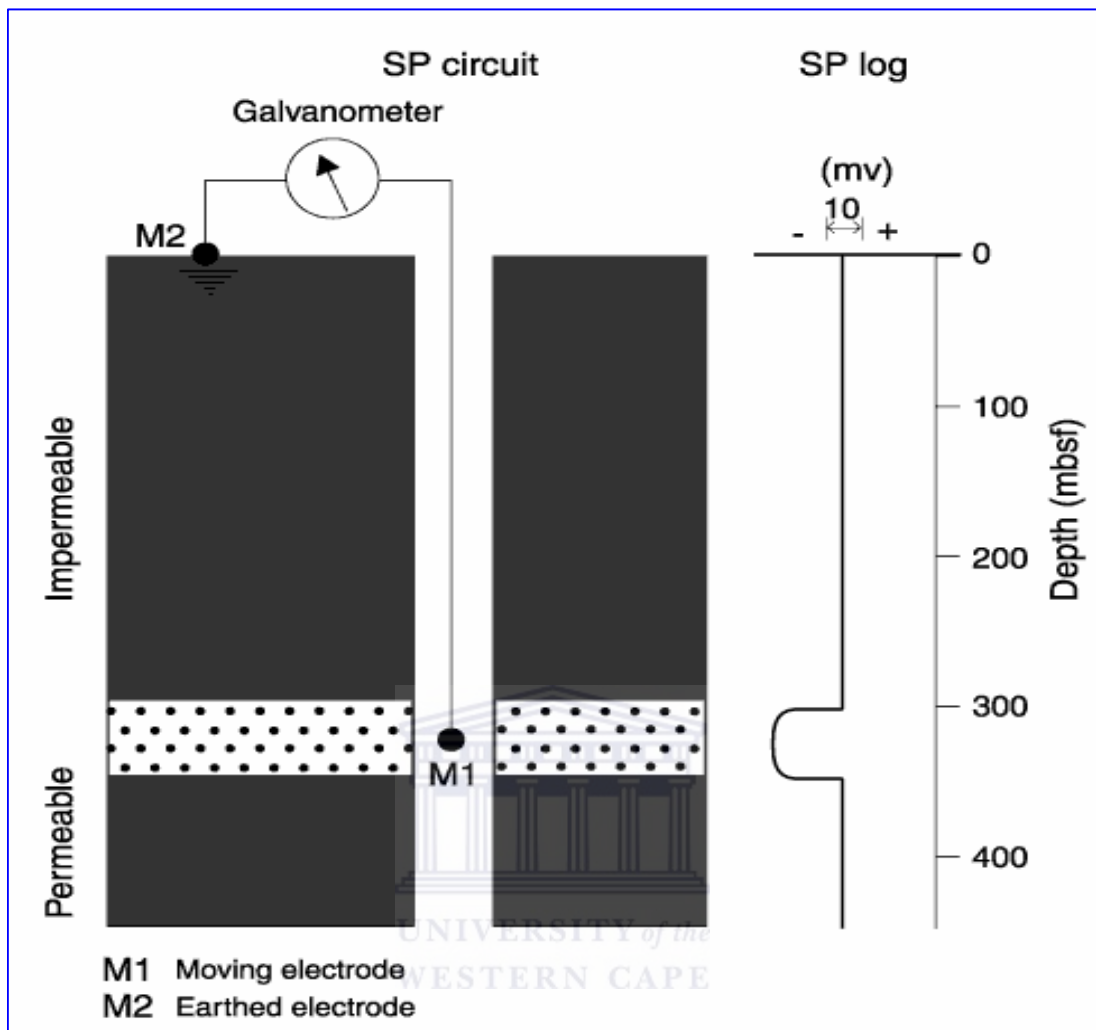


Figure 4.3 Spontaneous Potential logging tool (modified from Rider, 1996)

### 4.5.3 Induction Logs

Induction logs are a class of resistivity logs which are recorded in uncased boreholes and involve the application of electromagnetic induction principles for the measurement of formation resistivity or conductivity. It has an advantage of being used in nonconductive borehole fluids such as air, oil, and gas in which other electrical resistivity logging tools cannot be easily used. It works well with electrically conductive drilling mud provided the mud is not too saline and the borehole diameter not too large (SPWLA Glossary, 1984-97).

Practical induction tools include an array of several transmitter and receiver coils designed to provide focusing and deep investigation to minimize borehole and adjacent formation effect (Figure 4.4).

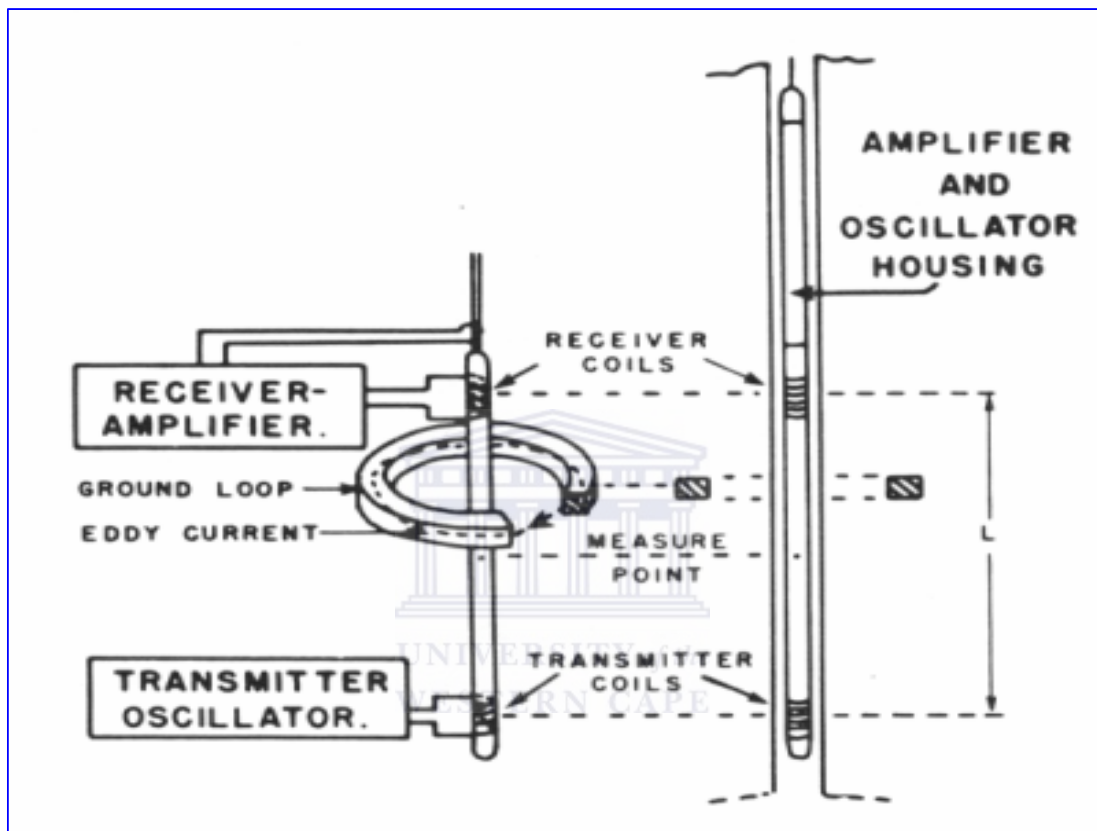


Figure 4.4 Induction Log equipment (modified from Schlumberger)

The transmitting coils emit a high frequency alternating current of constant intensity resulting in an alternating magnetic field which in turn induces secondary current in the formation. The multiple coils are used focus the resistivity measurement to minimize the effect of materials in the borehole, invaded zone, and other nearby formation. The induced current flows in circular ground-loop paths coaxial with the sonde. These ground loop current also generate their own magnetic fields, inducing signals in the receiver coils

which at low conductivities are essentially proportional to formation conductivity. However at high conductivities, the magnetic fields of the ground-loop currents induce additional eddy currents in adjacent ground loops which are superimposed on those induced by the transmitter coil field. This is referred to as skin effect and affects the reading.

Induction tools can be run separately or combined with other devices. Integrated tools such as the induction device with a deep depth of investigation (ILD) with another induction device having shallower depth of investigation (ILM) and invaded zone investigative devices (short normal device, short laterolog or spherically focused logging device) are common examples.

#### 4.5.4 Electrode Resistivity Logs

The second class of resistivity measuring device is the electrode log. Electrodes in the borehole are connected to a power source (generator) and the current flows from the electrodes through the borehole fluid into the formation and then to remote reference electrode (Figure 4.5). Examples of electrode resistivity tools include: Normal Devices, Lateral Logs, Laterolog, Microlaterolog, Microlog, Proximity Log, and Spherically Focused Logs.

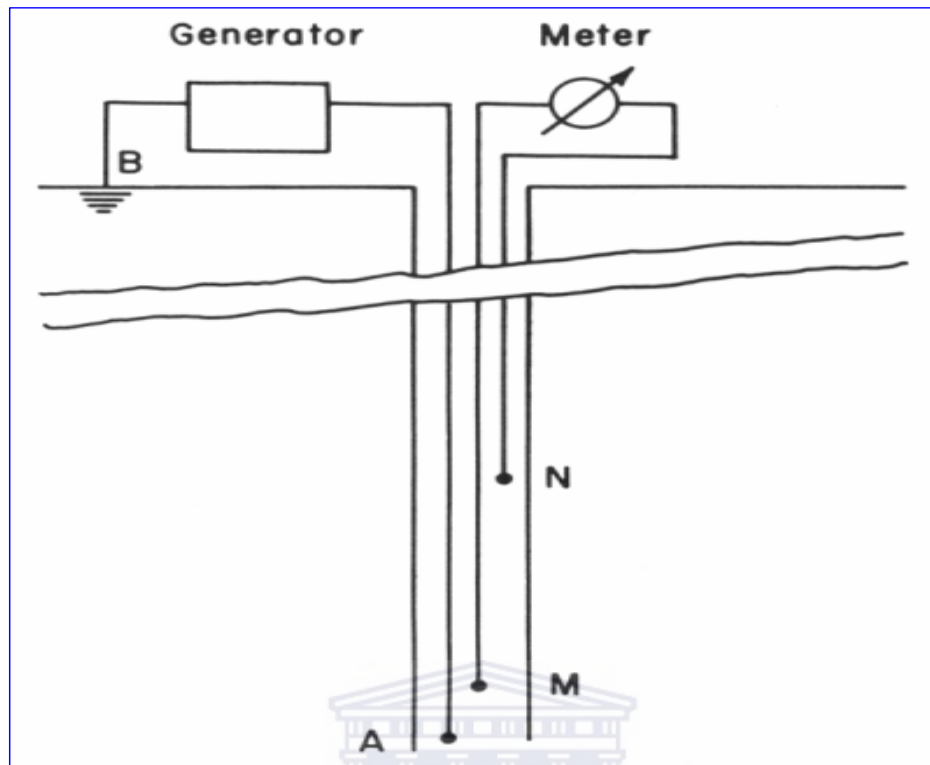


Figure 4.5: Normal Device with electrodes A, M, N (modified from Schlumberger)

Boreholes filled with salt-saturated drilling muds require electrode logs such as Laterolog or Dual Laterolog to determine accurate true resistivity values of the uninvaded zones.

#### 4.5.5 Neutron Logs

Neutron logs are porosity logs that measure primarily the hydrogen ion concentration in a formation but also affected by mineralogy and borehole effects. In clean formations, where the porosity is filled with water or oil, the neutron log measures liquid-filled porosity. Whenever pores are filled with gas rather than oil and water, neutron reads low values. This occurs as a result of less concentration of hydrogen in gas compared to oil or water. The lowering of neutron porosity by gas is called Gas effect.

The tool contains a continuously emitting neutron source and could either be a neutron (neutron-neutron tool) or a gamma ray detector (neutron-gamma tool). High energy neutrons from the source are slowed down by collisions with atomic nuclei (Figure 4.6). The hydrogen atoms are by far the most effective in the slowing down process because their mass is nearly equal to that of the neutron. Hence, the distribution of the neutrons at the time of detection is primarily determined by the hydrogen concentration.

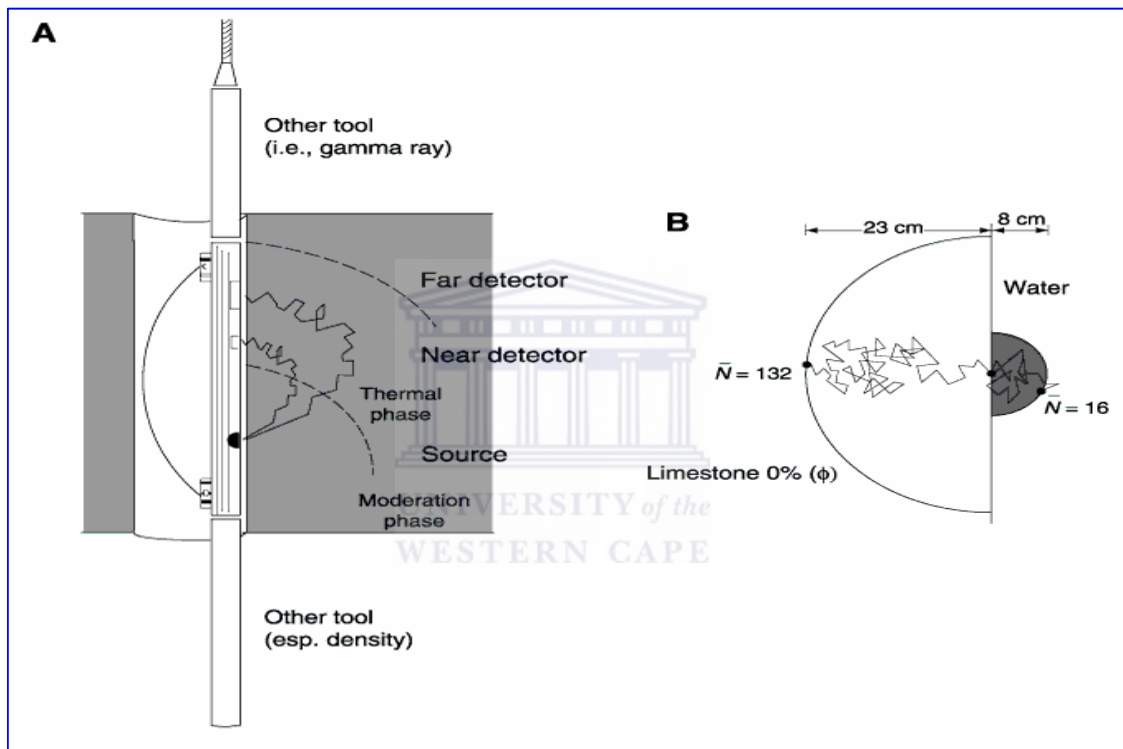


Figure 4.6: (A) Compensated neutron tool drawing, and (B) Schematic trajectories of a neutron in a limestone with no porosity and pure water (modified from Rider, 1996)

Neutron log responses vary, depending on: difference in detector types, spacing between source and detector, and lithology (i.e. sandstone, limestone, and dolomite).

### 4.5.6 Density Logs

This is a well log that records formation density. The logging tool consists of a gamma ray source (e.g.  $\text{Cs}^{137}$ ) and a detector shielded from the source so that it records backscattered gamma rays from the formation depending on the electron density of the formation (Figure 4.7). The formation electron density is proportional to its bulk density. Like in neutron tool, the source and the detector are usually mounted on a skid which is pressed against the borehole wall.

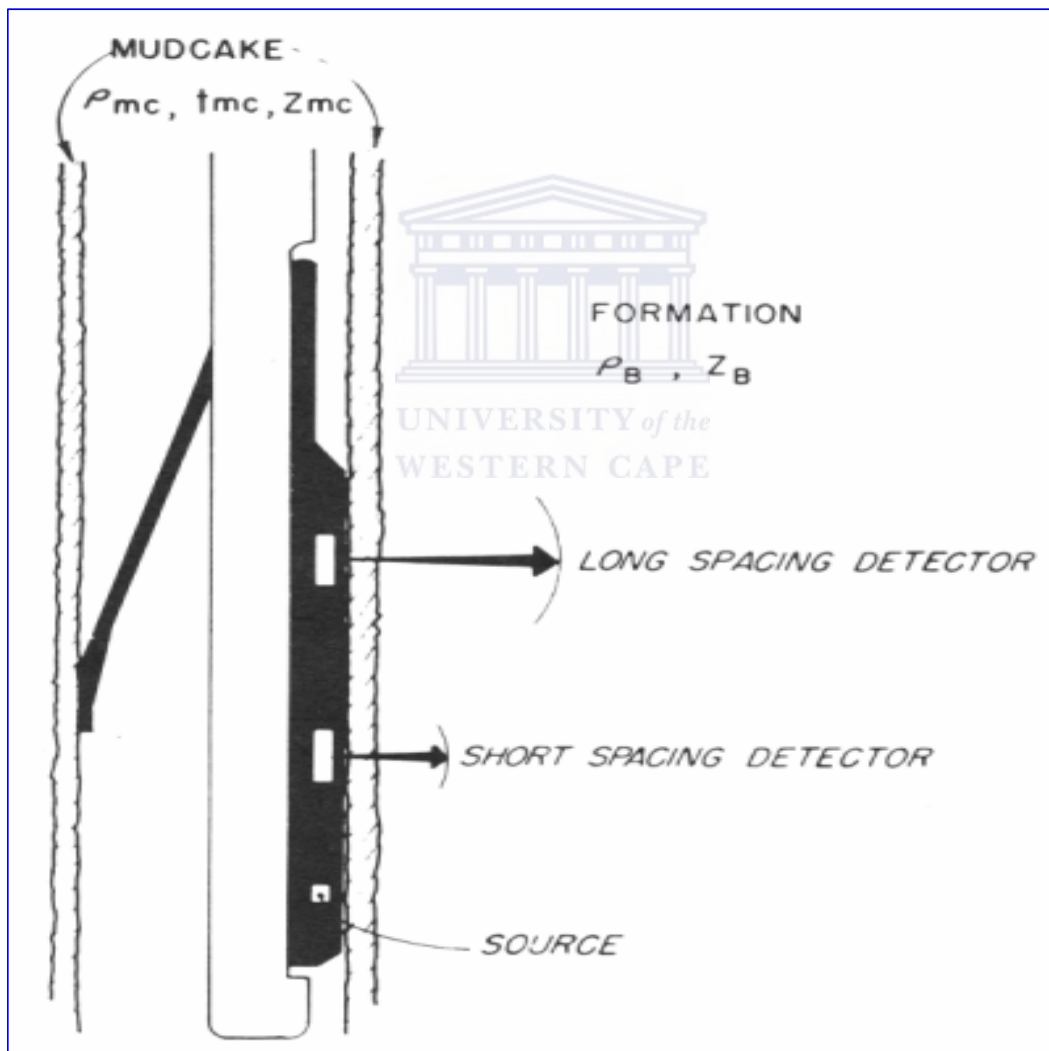


Figure 4.7: Compensated Density Sonde (modified from Wahl, JPT, 1964)



The compensated density logging tool includes a secondary detector which responds more to the mud cake and small borehole irregularities. The response of the second detector is used to correct the measurements of the primary detector. Density log is applied primarily to uncased holes.

#### 4.5.7 Combination Neutron-Density Log

This is a combination porosity log. Besides its use as a porosity device, it is also used to determine lithology and to detect gas bearing zones.

Both the neutron and density curves are normally recorded in limestone porosity units with each division equal to either two percent or three percent porosity. Limestone and dolomite porosity units can also be recorded.

An increase in density porosity occurring with a decrease in neutron porosity indicates a gas bearing zone usually referred to as Gas Effect. Gas Effect is created by gas in the pores as it causes the density log to record too high a porosity (i.e. gas is lighter than oil or water) while the neutron log record too low a porosity reflecting lower concentration of hydrogen atoms than oil or water.

#### 4.5.8 Sonic Logs

A sonic log measures interval transit time ( $\Delta t$ ) of a compressional sound wave in feet per second and hence, a reciprocal of the compressional wave velocity.

The sonic log device consists of one or more transmitters and two or more receivers (Figure 4.8). The time for the acoustic energy to travel a distance through the formation equals to the distance spanned by the two receivers is the desired measurement and the unit expressed as microseconds per foot. The interval travel time can be integrated to give the total travel time over the logged interval.

Borehole compensated sonic log consists of two transmitters located above and below the receiver, which are pulsed alternately to produce an improved log. Errors due to sonde tilt or changes in the hole size are minimized by averaging the measurements.

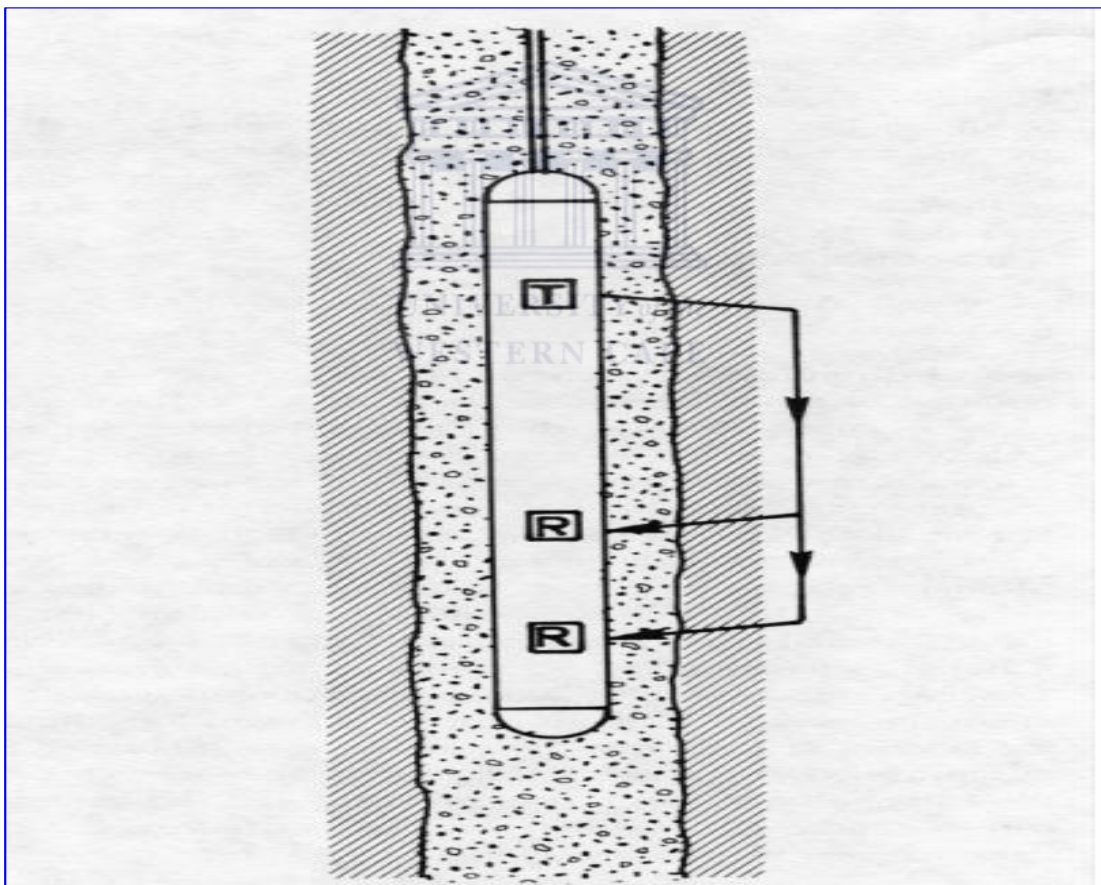


Figure 4.8 Sonic logging tool showing Receiver (R) and Transmitter (T)  
(Modified from [http://www.spwla.org/library\\_info/glossary](http://www.spwla.org/library_info/glossary))

The sonic log is used in combination with other logs (e.g. density and neutron logs) for porosity, shaliness, and lithology interpretation. Integrated transit time is also helpful in interpreting seismic records.

A simpler but efficient approach is taken to evaluate the core, using a measuring tape a handlens and a digital camera it was able to compile imperative information from the cores such as:

- + mineral inhibition
- + grain size distribution
- + changes in facies
- + fining sequences
- + contacts between facies successions
- + environments of deposition
- + sequence alternation

Most importantly the structural implications of the granulation seam distribution as well as the facets of compartmentalization within the different core sections.

The granulation seams had no specific orientation within the cores and in some areas they were chaotic and occurred as areas which were highly fractured. During the investigation it was discovered that the granulation seams actually accompanied a distinct sequence, which in this case was a thinly bedded shale unit which stretched straight through all the cores.

This specific shale layer stepped up or down within a few meters within the cores and at this stage it was pure speculation that shale units had been affected by faults running between the wells.

With further examination of data supplied by PASA, it retained no information of the granulation seam inhibition within the core consequently there was no relevant data within the well completion reports stipulating orientation,

distribution and the thicknesses these granulation seams possess. Thus no specific data occurred that could be used to model this seams. It was for this reason it was decided to track and model these shale's due to the implication it may hold to the reservoir recovery rates and the reservoirs ability to produce oil and gas at an economically viable rate.

The granulation seam mechanics is an important aspect that had to be kept in mind; they are generally stress indicators through compaction of the sand as well as indicators of the movement of the sand. The granulation seams has a close relation to the shale layers through the alternation of the sand shale facies, the shales where affected by the granulation seam mechanics by causing micro fractures within the shale.

Due to the difficulty to model these granulation seams in 2D as well as 3D and the lack of data, it has been determined to focus on the shale and claystone units which accompanies these granulation seams in close proximity and take into account the impact and severity the granulation seams has on the overall structure.

## 4.6 Electrosequence Analyses

Electrosequence analyses were used to help with the objective to extract as much geological information as possible. With the use of this analyses it was possible to extort information regarding the porosity, resistivity and density the cores enclosed. The analyses indicated a clear cyclic sequence within the sand units. Two main facies was identified during this analyses which was a shallow marine facies and a fluvial facies. With this information it provided a starting point for further analyses.

## 4.7 Petrel

Petrel was chosen to model this reservoir because it is window based software for 3D visualization with a user interface based on the Windows Microsoft standards as well as shared earth modeling tool bringing about reservoir disciplines through common data modeling. This is one of the best modeling applications in the world and it was for this reason that it was chosen to apply within the given aspects of the project. A data base was created within petrel clearly delineating the different information and data needed to complete this project. The geophysical, geological and petrophysical data was imported to petrel within the main data base and through this it was possible to generate and visualize the imported data in 2D as well as 3D.



### 4.7.1 Modeling

Three dimensional (3D) modeling in Petrel is broadly classified into two interdependent steps. These are structural and stratigraphic modeling.

#### 4.7.1.1 Structural Modeling

Structural modeling is the first step in building a geological model in Petrel. It is subdivided into three processes:

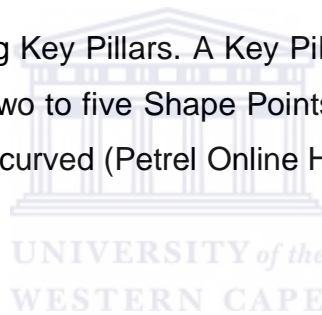
- (A.) Fault modeling
- (B.) Pillar gridding
- (C.) Vertical layering

All the three operations are attached together into one single data model - a three dimensional grid.

### (A.) Fault Modeling

This is the first step in building structural models in Petrel. The processes are used to construct linear, vertical, listric, S-shaped, reverse, vertically truncated, branched and connected faults. Fault modeling processes are used to create structurally and geometrically correct fault representations within horizon one two and three. The model consists of 8 primary faults but due to the lack of data the additional fault could not be added.

These faults are built using Key Pillars. A Key Pillar is a vertical, linear, listric or curved line defined by two to five Shape Points; two for vertical and linear, three for listric and five for curved (Petrel Online Help 2005).



### (B.) Pillar Gridding

A grid is simply a way of storing XYZ locations which describe a surface. Pillar Gridding is used to generate the 3D framework. A 3D grid divides space up into boxes (cells) within which it assumes material is essentially the same. Therefore, each grid cell will have a single rock type, one value of porosity, one value of water saturation etc. These are referred to as properties of a cell.

The grid is represented by pillars (coordinate lines) that define the possible position for grid block corner points.

### (C.) Vertical Layering

The Make Horizons process step is the first step in defining the vertical layering of the 3D grid in Petrel. This is a true 3D approach in the generation of 2D surfaces; all are gridded in the same process, taking the relationships between the surfaces into account (erosion, on-lap, etc), as well as honoring the fault model to ensure proper fault definitions in the surfaces and keeping the well control (well tops).

The 3D grid could have as many main layers as number of horizons inserted into the set of pillars. This is shown as horizons in the Models window of the Petrel Explorer.

The Make Zones and Make Sub Zones processes are the two last steps used in defining the vertical resolution of the 3D grid. The Make Sub Zones process allows the definition of the final vertical resolution of the grid by setting the cell thickness or the number of desired cell layers.

The next step was to start the interpretation of the well logs to stipulate contacts between different facies identification of unconformities, I had to identify the top and bottom of this specific unit within the well sections and insert well tops to display within the well section in 3D. With this I decided to identify the sand units above and below the shale for the main reason that this sand contains the granulation seams (Appendix 5)

#### 4.7.1.2 Correlation

The development of geologic pattern display by structural and stratigraphic units that are equivalent in time, age, or stratigraphic position through the use of electric wireline logs is generally referred to as log correlation (Rider 1996). It is a product of basic geological principles, which include sound

understanding of depositional processes and environment, concepts of logging tools and measurements, reservoir engineering fundamentals, and qualitative and quantitative log analyses.

Based on the depth range covered by the available data, stratigraphic units within the interval in the study area have been correlated using composite logs.

#### 4.7.1.3 Description of Correlation Section

The correlation section of the study area along North West – South East direction is shown in Appendix 5. The thicknesses of these units vary from well to well generated in Schlumberger Petrel.

A column of shale with thin intercalation of sands separating upper sandstone unit from the lower sandstone units and can be recognized across all the wells in the correlation section (Appendix 5). Its thickness ranges from 70m in E-M 1 to about 13m in E-M 4 showing a thinning towards the confines of the E-M structure. Core samples taken within this interval has been reported in the geological well completion report provided by PetroSA to contain good quality source rocks. The formation seems to amalgamate and thin out to the boundaries of the reservoir which will also entail it could be that there are pinchouts as well as stratigraphic traps along the margins/boundaries of the reservoir.

The major sandstone unit in the shallower part (below 2600m depth in E-M 1) of the correlation section exhibit a fairly uniform thickness and characteristics across the wireline logs section unlike the top sandstone unit (above 2550m depth in E-M 1) which varies from well to well. However the resistivity curves fairly display similar trend generally.



These behaviors could be explained in the sense that geologic province like the Bredasdorp Basin generally display low dipping structures towards shallower depth. An additional reason is that geologic structures tend to be less intricate towards the shallower part as a result of faults terminating upward which in turn make their effect on stratigraphic units being correlated less apparent particularly at the upper part of the correlated section.

## 4.8 Reservoir Modeling

Reservoir modeling generally refers to the techniques of constructing hypothetical three dimensional representations of the observed and anticipated characteristic of the recognized subsurface reservoir. The reliability of a model depends on quantity, quality, distribution and accuracy of data.

Geostatistical or stochastic methods generates samples of the sequence of data interpretation from probability distribution. It involves interpolation between data measurements through a random draw from a cumulative data distribution function to simulate the value at a given location. (Schlumberger 2004. Petrel Online Help, Petrel 2004 Version)

Schlumberger Petrel's in-built geostatistical methods are used in constructing models of the identified sand rich reservoirs (facies modeling) and the distribution of their matching petrophysical properties.

## 4.8.1 Facies Modeling

Facies modeling is a means of distributing discrete facies throughout the model grid. Normally the well logs with discrete properties are up-scaled into the model grid having defined necessary trends.

Seven different facies modelling approaches are available in Petrel. They are classified under three major methods: stochastic, deterministic and interactive.

### (A.) Stochastic

- i. Object Modelling: allows users to populate a discrete facies model with different bodies of various geometry, facies code and fraction.
- ii. Sequential Indicator: allows a stochastic distribution of the property, using the pre-defined histogram. Directional settings such as variogram and extensional trends are also honored.
- iii. Facies Transition Simulator: allows a stochastic distribution of the facies based on a given transition between facies, and a trend direction. The trend shape and direction are set interactively in the dialog and a range given for the variogram.

Facies models of BRED-C and BRED-D are generated using Sequential Indicator Simulation technique.

## (B.) Deterministic

- i. Indicator Cringing: allows a discrete distribution of the property, honoring the pre-defined histogram.
- ii. Assign Values: gives four different options to choose from: Undefined, constant, other property and surface. For each of these, the user may keep or overwrite the original values of the up-scaled logs.
- iii. User Defined Algorithm: allows the user to export files (ASCII) from Petrel in a standard Geo-EAS format. The user can use this information to run his/her preferred algorithms outside Petrel and import the results into Petrel, once the simulation has been completed.

(C) Interactive: allows the user to paint facies directly on the model in 3D

## 4.9 Seismic Interpretation

Seismic interpretation is the analysis of seismic data to generate reasonable models and predictions about the properties and structures of the subsurface. This is done by mapping reflection events matching to well tops reliably on a cropped seismic section and then correlating each event across all the other cropped seismic sections. Only three events were tracked through the steps listed below:

1. Seismic sections are visualized in 3D window
2. Conduct seismic correlation and mis-tie correction
3. Crop the interested two-way time interval of the seismic section to work on
4. Generate instantaneous phase attribute for all the seismic sections to enhance the continuity of weak events and to distinguish small faults and dipping events

5. Display well tops in 3D together with seismic sections and locate respective event corresponding to specific well top
6. Carry the event through all the available seismic sections using manual picking

Repeat the process for other well tops and their respective seismic event

#### 4.10 Data Quality Control

Due dates was difficult to maintain mainly through the continued impediment to retain documents and signatures from adjoined parties as well as requested data at requested times thus hampering the continuity of the project.

Parties involved were not available for lengthy periods of time with no forwarded warning of their absence or who the next contact person was in there absence. The little communication that there was between Petroleum South Africa (PetroSA) and the Petroleum Agency of South Africa (PASA) also added to the uncertainty to what data I am inclined to receive. Delays of up to two weeks were encountered at times where no contact could be established with the relevant parties to attain signatures for specific data needed.

The seismic data received from PASA had coordinates omitted which hampered the possibility for these data sets to be launched within the petrel window. The files lacked navigation data which could not be recognized within the UKOOA navigation to seg y axis utility file within petrel thus impossible to be displayed within the petrel work station. A further major setback was detected later within the modeling stage whereby the X and Y coordinates were inaccurately recorded on the borehole location map thus the wells could not be launched together with the seismic data. The data were displayed imperfectly in petrel window and the process steps had to be

cancelled and restarted having corrected the coordinate error that was earlier identified.

Seismic data passed from the Petroleum Agency of South Africa (PASA) did not correspond/correlated with the lines displayed in the petrel window. The extent of the lines shown on the base map did not retain the same information displayed in the petrel window. The lines were much more uninterrupted on the base map and had all lines that were selected crossing each other. When the seismic lines were displayed within petrel only 3 lines intersected each other out of a total of eight lines. This made the tracking of different horizons very difficult, two thirds of the interpretation and tracking of the different horizons had to be done on assumption and auto tracking.

Not all the fault systems could be mapped on the seismic lines mainly due to the fact that the most of the seismic lines did not intersect and it was extremely difficult to continue with the fault mapping due to the lack of data at critical intersection.

It was almost impossible to map the faults around the well section due to the absence of information displayed within these regions.

A number of cores within the E-M suite had units missing giving an incomplete representation of the original cores thus leaving it up to conjecture and skilled interpretation to complete the well correlation physically. Information tags on the core boxes had incomplete depth information or no data displayed on them thus making it difficult to correlate the continuity of the cores depth with stratigraphic sequences:

Shown within figures 4.9 and 4.10 below:



Figure 4.9



Figure 4.10

Figures 4.9 and 4.10: Damaged core boxes, courtesy of Petroleum Agency of South Africa



## Chapter 5

### 5.1 Discussion & Results

#### 5.1.1 Granulation Seams

Brittle failure in the earth's crust is generally not simple planar surfaces of detachment and slip, but is typically composed of heterogeneous volume of small scale fractures, slip surfaces which in time could also include granulation seams as well. Burhannudinnur and Morley, 1997

With core evaluation in faulted sandstones it has shown that numerous small scale faults, especially in more porous (and therefore potentially productive) sandstones, occur as granulation seams that have a significantly lower permeability than their host rock.

The presence of networks of granulation seams throughout faulted sandstone reservoirs may lower the bulk permeability of the reservoir, and an understanding of this is a crucial part of the input to reservoir simulation and estimates of reservoir productivity. Granulation seams are permeability barriers within the reservoir. The impact on bulk reservoir permeability will depend on the actual permeability of the granulation seams, and the density of these seams throughout the rock. Berg and Avery, 1995

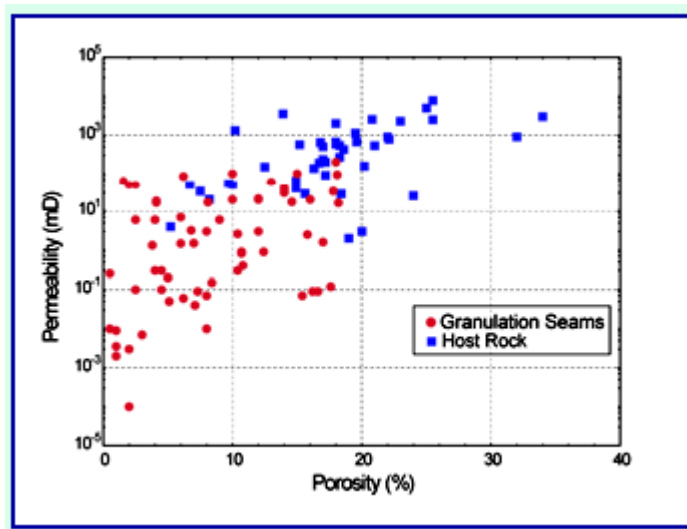


Figure 5.1: Porosity vs. Permeability (Berg and Avery, 1995)

Granulation seams are individual quasitabular bands of crushed rock, commonly less than 1 cm in thickness, which are characterized by intense grain size reduction, grain rotation and compaction (Fowles and Burley, 1994).

They are thought to form under conditions of high deviatoric stress, low confining pressure (i.e. at relatively shallow depths in the crust), and low temperature (Mitra, 1988) and typically accommodate small shear offsets which are generally less than a few millimeters in dimension (Antonellini and Aydin, 1995), causes cataclasis and reduces porosity and permeability in indurated quartz sandstones.

Figure 5.1 presents a porosity-permeability plot of host rock sandstone and granulation seams clearly showing the affect that the granulation seams has on the porosity and permeability within a rock.

The granulation seams was mainly found within the sand units in the reservoir, there cause was through the rolling of sand grains over one another creating seal like fractures within the sand beds.



Quartz overgrowths lead to a bimodal distribution of grain sizes: sub angular to well-rounded, fine- to medium-grained quartz in an angular silt- and clay-sized quartz matrix. This mechanical reduction in pore aperture size creates the potential for fault-sealing traps. Granulation occurs along individual or anastomosing seams up to a few millimeters thick and is more pervasive near major faults.

Undisturbed blocks, up to 30 cm across, of porous and permeable sandstone commonly are bounded in three dimensions by planar seams of tight granulated rock. Remobilization may result in tighter or looser packing of grains and in the precipitation or dissolution of material from fluids flowing through the injections.

Analysis on non-cemented injected sands shows that sands with high primary porosities (25-40%) get packed to give porosities below 20% due to remobilization. Post-depositional remobilization of sands greatly diminishes porosity of sands, either by tighter packing or by the precipitation of cements from fluids flowing through the injection structures (Beach 1999).

This cellular nature influences the entrapment of hydrocarbons, because of the abundance of granulated material associated with major faults; it appears possible that faults may serve as seals even when sandstone is faulted against sandstone. In friable sandstones studied, the clay coatings binding the grains are disrupted, fragmented, and then rearranged by grain rotation along insignificant faults with about 15-cm throw, leading to a pronounced decrease in porosity and permeability as well as significant reduction in pore aperture size (Panda and Lake 1994)

The presence of networks of granulation seams throughout the faulted sandstone reservoir may lower the bulk permeability of the reservoir.

Due to the location of the E-M suite it could be safe to say that the amount of faulting within the region could have contributed to the formation of the granulation seams and now instantaneous acting as barriers to fluid movement within the reservoir.

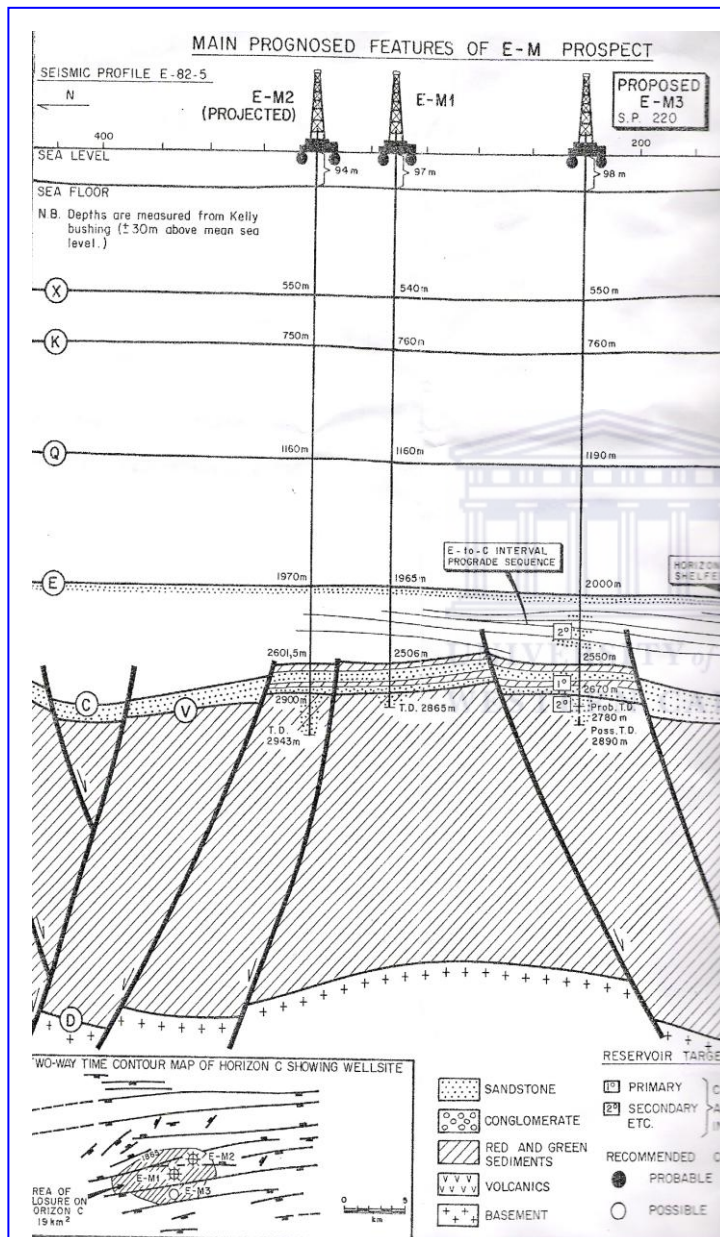
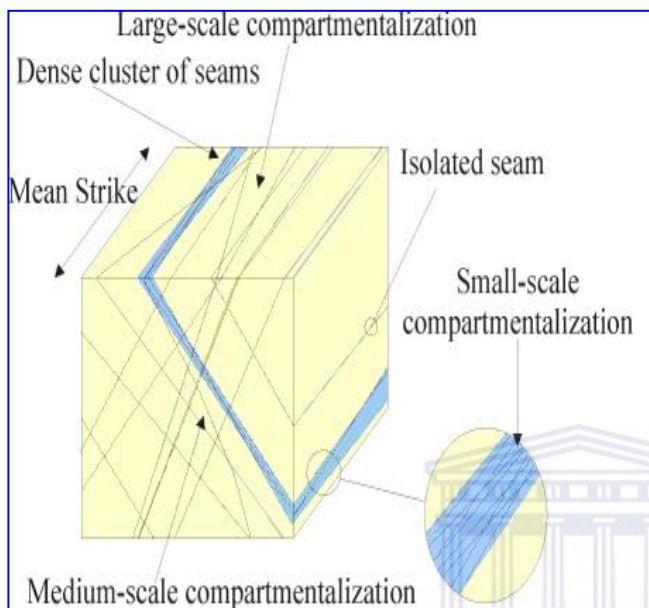


Figure 5.2: Seismic profile of the E-M structure, courtesy of the Petroleum Agency of South Africa (PASA)

Opposite insert is of E-M 1, 2, 3 and showing the position of the wells. The wells are all located within tilted fault block. Structural events caused the area to buckle and forced the arch shape domal closure thus strata within the area is displaced by a certain degree of ductile deformation.

The granulation seam formation was assisted by fault movement or linear movement of the faults, cutting across sand units which internally caused the mobilization or remobilization of the sand granules, causing grain rotation and compaction.

Importantly, these isolated compartments occur at a range of scales, from sub-millimeter size compartments within dense clusters of seams to compartments several tens of meters in dimension formed between dense clusters



Schematic diagram depicting the typical 3D geometries exhibited by granulation seams at outcrop level. Note the conjugate orientations and compartmentalization on a wide range of scales. ABA and associates Ltd.

Figure 5.3 Two dimensional block of granulation seam distribution, courtesy ABA and associates Ltd.



Illustration of the granulation seams that causes the compartmentalization within the wells. The seams have no real orientation but seem to be dipping  $5^{\circ}$ - $40^{\circ}$  respectively within all affected core.

Figure 5.4 Core photos, Courtesy of Petroleum Agency of South Africa E-M2, illustrating the affects of the granulation seams.

2D distribution of effective permeability in such systems is highly anisotropic and is controlled, not only by spatial density, but by the connectivity and compartmentalization of the network.



Illustrations of the granulation seams that causes the compartmentalization within the wells. The seams have no real orientation but seem to be dipping  $5^{\circ}$ - $40^{\circ}$  respectively within all affected core.

Figure 5.5 and 5.6

Figure 5.5: E-M 1 Core photo, Courtesy of Petroleum Agency of South Africa illustrating the affects of the granulation seams.

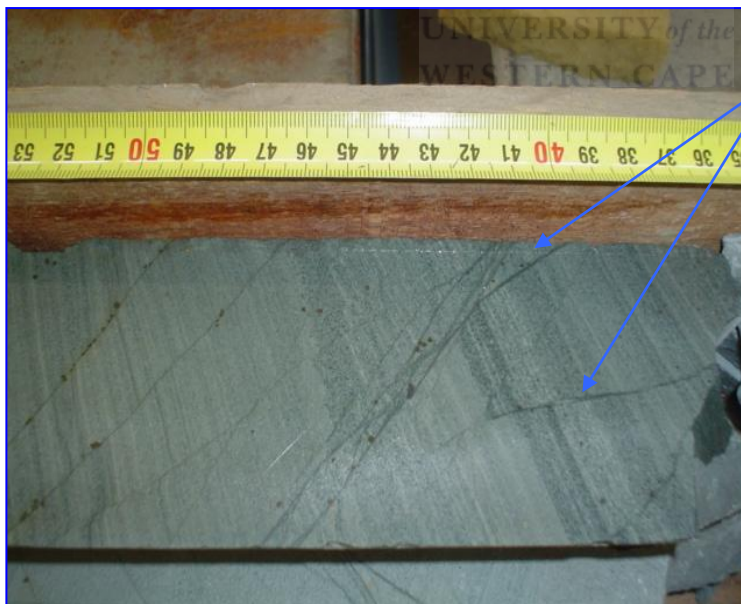


Figure 5.6: E-M 4 Core photo, Courtesy of Petroleum Agency of South Africa illustrating the affects of the granulation seams.



The compartmentalization of porous reservoir sandstone by granulation seams in fault damage zones is likely to lead to severe permeability reduction and flow anisotropy on the production time scale. Importantly, effective permeability appears to be independent of spatial clustering. This is visible within Appendix 1 where the porosity (%) and permeability (mD) is visibly reduced within the demarcated areas in the Tables 1 and 2. E-M 4 has a short affected area but is still affected by the compartmentalization.

The formation of the granulation seams is concentrated only within the sand units, mostly the clean sand, which makes the most logical sense. All four wells drilled within the area are affected causing compartmentalization within the sand and acting as barriers for fluid flow. These seams are all located over a 100m depth range in the four wells ranging from the shallowest dept of 2530m which is in E-M 1 to the deepest affected area located in E-M 3 at 2660m. The faults on the anticline act as permeability/fluid barriers to hydrocarbon migration producing a series of small compartmentalized accumulates in the suite.



Visible fractures within the core sample causing the compartmentalization of certain units within the stratigraphy

Figure 5.7: E-M 2 Core Photo, Core 5 Courtesy of Petroleum agency

These granulation seams also affected the inter-bedded /alternating shale units which vary in thicknesses, causing this unit to display fractures



The adjacent photo illustrates the affects that the granulation seams hold on the sandy units but also causing faulting/fractures within the shale layers. The arrow indicated the fracture causing the displacement and the broken line the displacement of the shale units.

Figure 5.8: E-M 1 Core Photo, Core 3 and Courtesy of Petroleum agency

These shale units are thought to acts as barriers causing the reservoir to be compartmentalized even more. In some core section these granulations seams....



....are in a chaotic state with no apparent orientation and just cause the whole section of rock to be divided into compartments as shown below in figures 5.8 and 5.9:

Figure 5.9 Core photo, Core 2 and Courtesy of Petroleum agency, illustrating the orientation or the lack of consistent orientation of the granulation seams.

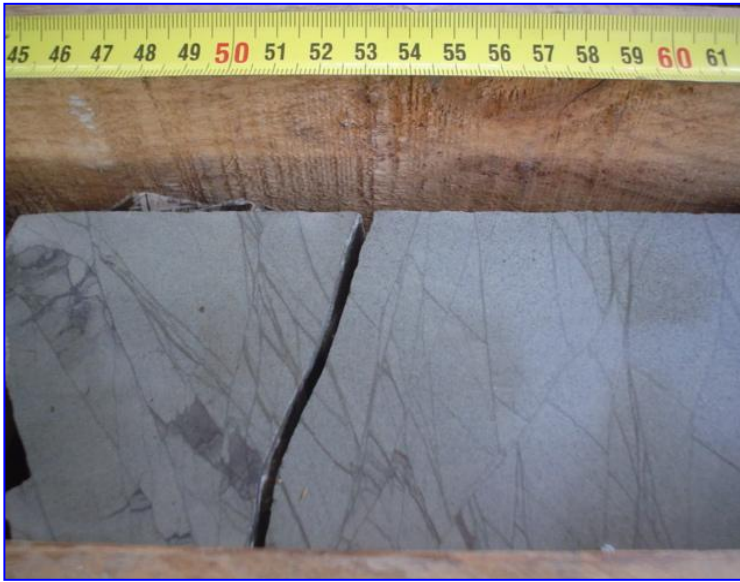


Figure 5.10: Core photo, Core 2 and Courtesy of Petroleum agency, illustrating the orientation or the lack of consistent orientation of the granulation seams.



Figure 5.11: E-M 2 Core Photo, Core 2 and Courtesy of Petroleum agency, illustrating the uniformities of the granulation seams in the sand horizon.

The photos illustrates that in some section of the core the granulation seams are uniformly distributed and then in contrast on the right the chaotic state of the granulation seam distribution within the same core just meters apart from

each other located between the depths of 2625m - 2628m in E-M 2. The cause of these sections is due to compression from the redistribution of the sand granules and thus causes fracturing within the sand units.

Faults often present barriers to migration of hydrocarbons, or trap hydrocarbons by either offsetting the pay zone against non-reservoir or through deformation processes that reduce pore throat radii within the fault zone. For a fracture network, there are additional geometrical properties such as fracture spacing, fracture orientation, spatial correlation among fractures, and interconnectivity of the fractures. The pore pressure and the fluid flow cannot be realistically modeled from one dimensional modeling (1-D) and it is generally not possible to obtain enough information about the permeability distribution for 3-D modeling. In the North Sea the Haltenbanken faults, depending upon the degree of juxtaposition or clay smearing, are relatively sealing to flow across the fault. However, the permeability along the fault plane is nearly nul. (Knut Bjorlykke, 1999)

Compartmentalization of hydrocarbon reservoirs by faults is a widely observed phenomenon in the North Sea and in the Gulf of Mexico oil fields (Matthai, 1998)

### 5.1.2 Glauconite

Most of the sandstone units contain glauconite which is Fe-rich dioctahedral mica. The name is derived from the Greek *glaucos* for the blue green color. Its color ranges from olive green, black green to bluish green. The relative density range is 2.2 - 2.8. It is normally found in dark green rounded nodules of sand size dimension. It can be confused with chlorite or with some clay. Normally, glauconite is considered diagnostic of continental shelf marine depositional environments with slow rates of accumulation. It develops as a



consequence of diagenetic alteration of biotite micas or volcanic glass. Glauconite forms under reducing conditions in sediments and is commonly found in nearshore sandstones (Burruss, 1987)

The sand-sized aggregate of clay-sized particles is easily broken apart into its component clay size when disturbed. It is rich in iron compounds and will release the iron if weathered in an anaerobic environment (visible in figure 5.12 and 5.13). As water levels change over geologic time, iron moves from a dissolved anaerobic state (ferrous) to an oxidized precipitate.

Because glauconite is easily disturbed (for example, eroded off a stream bank) and breaks apart into clay sized particles, it increases both the amount and the duration of the turbidity in the water column. Because of its high cation exchange capacity, it increases the likelihood that phosphorous, heavy metals or bacteria present in the water column and sediment will bond to it. Given that glauconite compacts so easily its permeability can be reduced to 1/100 (Antonellini, M. and Aydin, A. 1995).



Photos illustrate the iron oxidation occurring within the granulation seams within E-M 3. Glauconite which is Fe-rich dioctahedral mica, when exposed in oxidized condition this iron precipitates and causes rust on the surface of the cores, a prominent feature with the cores. Figures 5.12 and 5.13

Figure 5.12: E-M 3 Core Photo Courtesy of the Petroleum Agency of South Africa,



Figure 5.13: E-M 3 Core Photo Courtesy of the Petroleum Agency of South Africa

Although glauconite tends to exist as grains and as such is part of the rock framework, under moderate overburden pressure, these grains are easily compacted and may form a pseudomatrix that occludes the original primary porosity

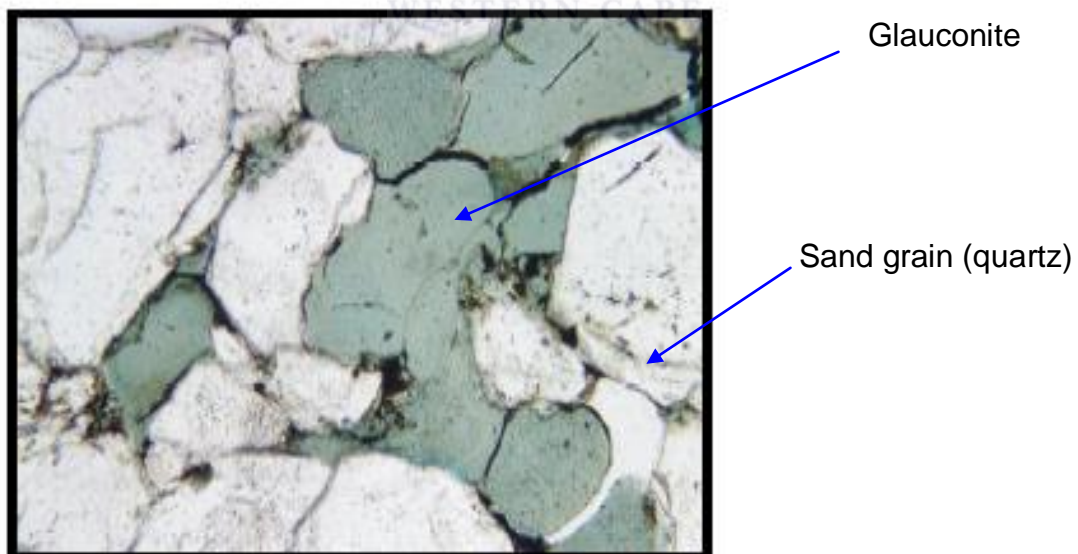


Figure 5.14: Optical image of a glauconitic sandstone (made at 20X magnification) showing formation of a pseudomatrix that occludes the original primary porosity (courtesy of Rob Lavinsky, Omni Laboratories, Inc)

Accompanying clay with glauconite is fibrous illite and this reduces permeability more than most clay minerals because it extends into or bridges the pore spaces.

Illite may precipitate in the pores of sandstone reservoirs, impeding fluid flow. The percent of illite typically increases with depth and temperature in most of the world's sedimentary basins and with geologic age. The clean sandstones consisting only of sand-sized grains sometimes lack this depositional clay in the suite.

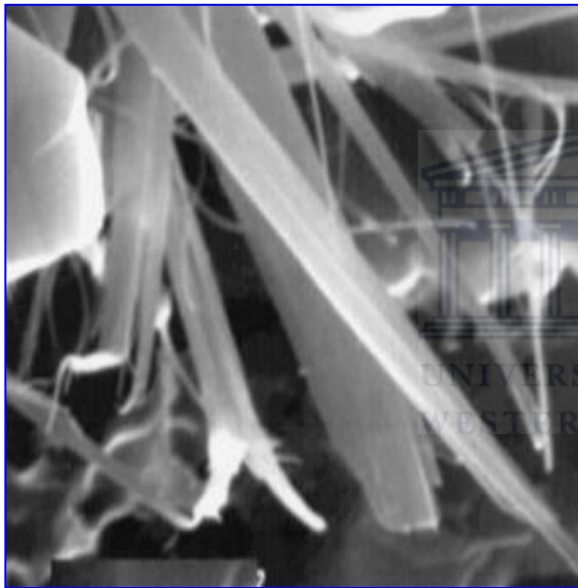


Figure 5.15

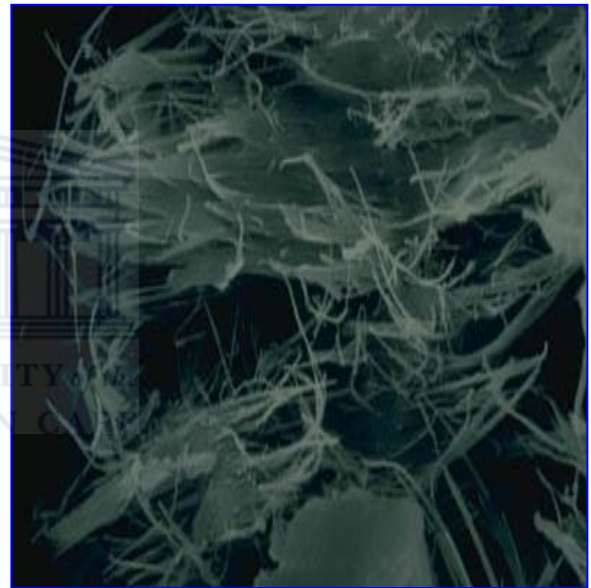


Figure 5.16

Examples of a scanning electron micrograph of pore-filling fibrous illite in sandstone.  
(Courtesy of the Rob Lavinsky, Omni Laboratories, Inc)

They are deposited in a high-energy environment in which the fines are winnowed away. During diagenesis, feldspars and other rock constituents may react with pore fluids to precipitate illite or other diagenetic clays and it is for this reason, the fine material in these sandstones tends to be mostly diagenetic, and more so than for shales. This may reduce permeability's by

blocking pore throats without reducing pore volumes. Traces of illite and glauconite have been picked up within these sands and the formation of illite is generally favored by alkaline conditions and by high concentrations of Al and K.

There are regions within the four wells where permeability drops significant but there is no evidence in the wavering of the porosity, demarcated areas stipulated within Appendix 2, 3 and 4. This can be attributed to the illite impediments which blocks off the fluid passages which causes the drop in permeability but not porosity. This with the addition of the granulation seams causes immense problems for the fluid flow within the reservoir.

### 5.1.3 Facies Description

Two main facies were identified, the one being a fluvial sequence and the other a shallow marine sequence which contained most of the fine grained sand.

The sand is interbedded with abundant of shale and siltstone where the thicknesses varied. A thick column of tightly packed red and green shale observed within the cores at varied depths was also seen to be of great importance. The shale is dense and very tightly packed and can be looked at as a confining layers or seal to any fluid above or below this specific unit.





The adjacent photo illustrates the very fine grained green shale units which is situated within the cores and is an indication of the change in the environmental energy. This unit was deposited under very low energy.

Figure 5.17: Core Photo courtesy of Petroleum Agency of South Africa



The adjacent photo shows a clean sand unit with no imposed structural damage. This is one of the prominent features of the shallow marine sequences which are alternating with a very distinct shale sequence shown in the next photo.

Figure 5.18: Core photos of E-M 2 core 4, Courtesy of Petroleum Agency of South Africa



Figure 5.19 Core samples of E-M 2, Core 4, and Courtesy of Petroleum Agency of South Africa

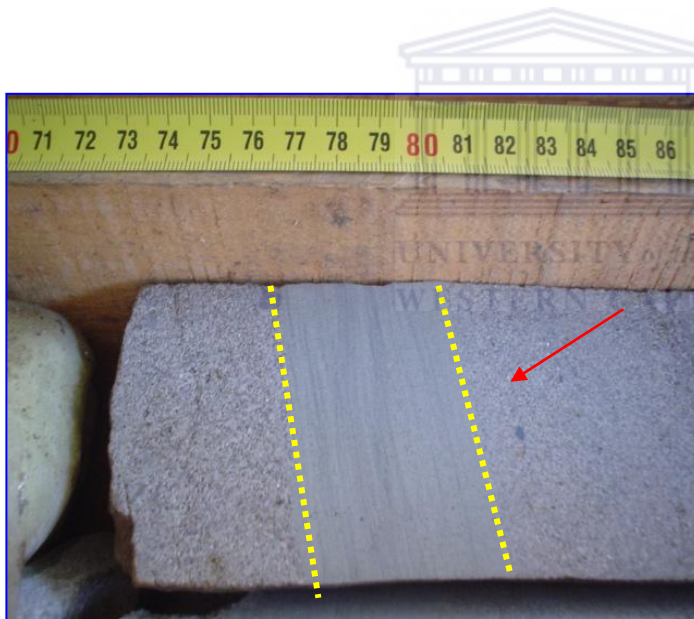


Figure 5.20

Core sample of E-M 2, Core 4, Courtesy of Petroleum Agency of South Africa

The photos above, Figures 5.19 and 5.20 are just to show the alternation between the sand packages with an alternating shale unit which is very

prominent feature within the sand body. These shale units vary in thicknesses and can be observed within the photos.

#### 5.1.4 Fluvial Sequence

The fluvial sequence strongly suggests a Meandering Fluvial River Streams and is characterized by single, highly sinuous channel with cohesive banks. Meandering streams form on lower slope gradients than braided systems; they commonly form downstream of braided fluvial systems and upstream of delta systems. Sandstone, a conglomerate channel deposit as well as fine grained floodplain deposits is normally associated with this type of sequence. Fluvial environments are typically controlled by stream power and grain sizes, but also by bank stability and the amount of bed load (Bathurst, 1971)

Morphologic elements of meandering fluvial systems are controlled by the development of helical flow as water moves towards the inside of the meander or bottom, carrying sediment across stream channel and up sloping banks of adjacent point bar. Deposits include channel sediments (principally lag deposits); point bars (upward-fining; with large dunes on lower part, ripples on upper part); natural levees (thickest and coarsest near channel bank); fine-grained flood basin deposits; and sandy crevasse splay deposits interbedded with floodplain fines. The cores are dominated by the deposition of shale's and siltstone alternating with thinly bedded sand sequences which is oxide stained and is black. The black color is from the carbon and organic constituents (plant fossil remains) which is also a very prominent feature within certain parts of the cores where it is still in its preserved fossil form.

The bedding is thin and the sedimentary structures that is common within the sections are:

- coal layers
- fossil plant material

The sequence is almost always abruptly terminated by sandy channel cuts or scours associated commonly with river channel deposits and consequently with conglomeratic units with an erosional base



Figure 5.21: Core Photo's of E-M 1 cores 1 and 2, Courtesy of Petroleum Agency of South Africa showing woody material encased in the core.



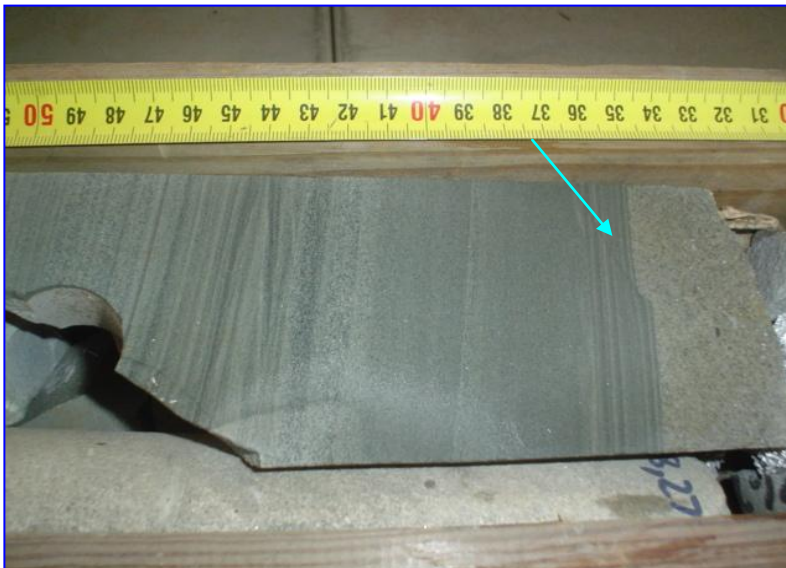
Figure 5.22: Core Photo's of E-M 1 cores 1 and 2, Courtesy of Petroleum Agency of South Africa showing woody material encased within the core unit.





Figure 5.23: Core Photo's of E-M 1 cores 1 and 2, Courtesy of Petroleum Agency of South Africa showing encased woody material in very fine grained sand.

The above photo's shows the biomaterial found within E-M 1 which is indicative of the fluvial sequence which retained most of the plant fossils and biomaterial during deposition and is located at depth between 2606 m-2627m. The material is to some extent incased within very fine grained sand as is visible within the photo furthest to the right.



Shown within the adjacent photo, the abrupt discontinued thinly bedded shale unit. The contact is exceptionally sharp and distinct between the two sequences, associated commonly with river channel deposits

Figure 5.24: Core Photo of E-M 2 core 2, Courtesy of Petroleum Agency of South Africa

Channels show erosive bases and contain cross-beds that are heterolithic and fine upwards within each set. Shown within the photos below, which is a collage of the deeper part of the core shown in figure 5.25, the shallower part of the core, figure 5.26, clearly showing fining upward sequence within E-M 2



Figure 5.25: Core sample of E-M 2 core 2, Courtesy of Petroleum Agency of South Africa



Figure 5.26: Core sample of E-M 2 core 2, Courtesy of Petroleum Agency of South Africa

Post-depositional structures include platy, sub-angular-blocky, or angular-blocky mudstone “clods” and rare columnar- and prismatic-shaped mudstone “clods”, all of which may commonly be clay coated (i.e., cutanic).



Based on these criteria, the shale facies is interpreted as being deposited by suspended sediment fallout and periodic low-energy currents

Figure 5.27: Core sample, Courtesy of Petroleum Agency of South Africa

Sedimentary structures typically include thin (1-3 mm) to very thin (<1 mm) parallel, horizontal or slightly inclined (<5°) laminae. Relatively rare, thin (1-3 mm), slightly lenticular siltstone laminae were observed, but are more abundant in the heterolithic siltstone facies. Thin to very thin, repetitive, fining-upward laminae sets were observed in parts. Laminae can be fissile.





Figure 5.28: Showing a small scale fold indicated by the arrow.

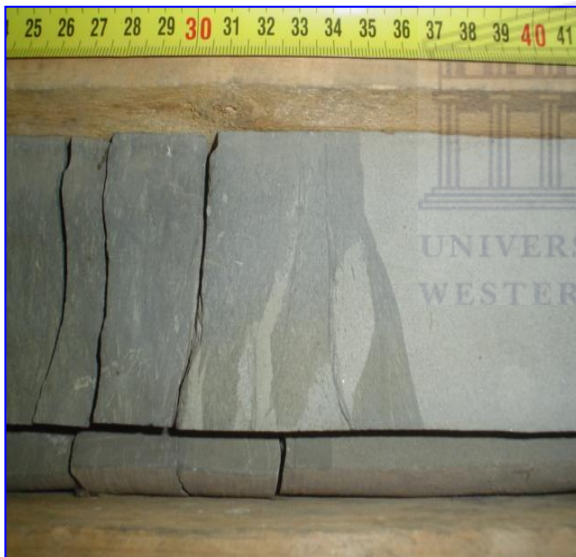


Figure 5.29:

Core samples of E-M Suite, Courtesy of Petroleum Agency of South Africa



Figure 5.30: Showing dewatering feature indicated with red arrow.

Based on the coarse and imbricated nature of grains, unidirectional inclination of bedding, and strata relationships to overlying finer-grained facies (e.g. underclay, cross-bedded sandstone, and heterolithic sandstone), the conglomerate is interpreted as bar deposits in a fluvial channel forming from

high-energy unidirectional traction currents and bed load deposition. Sharp, irregular lower contacts suggest erosion into underlying strata as shown in Figures 5.31 and 5.32.

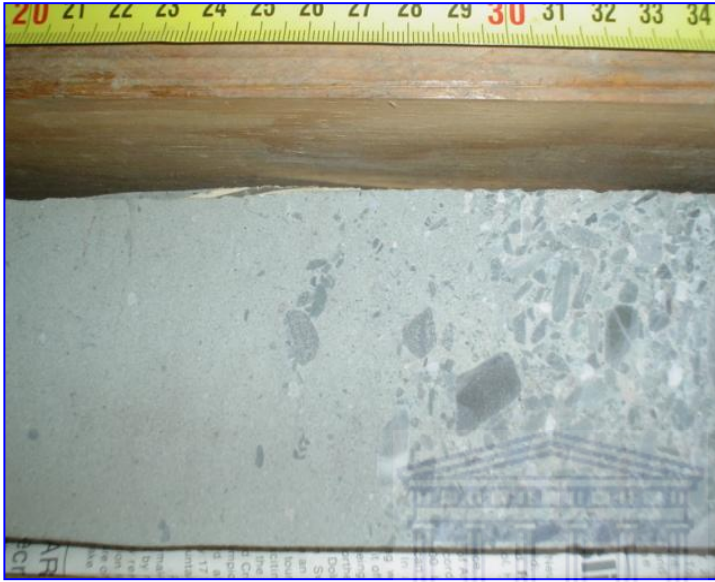


Figure 5.31: Core sample of E-M Suite, Courtesy of Petroleum Agency of South Africa



Figure 5.32: Core sample of E-M Suite, Courtesy of Petroleum Agency of South Africa

The sandstone facies is composed of light- to medium-gray, fine- to coarse-grained, very well- to well-sorted sandstone. Mud clasts (up to 1 cm diameter) are scattered and not uniform within the sand. The interbedded sandstone and siltstone facies consists of medium brown sand, were oil-stained Figure 5.35. The interbedded sandstone-siltstone facies is interpreted as forming from variable velocity.



Figure 5.33 Core sample of E-M Suite, Courtesy of Petroleum Agency of South Africa



Figure 5.34 Core sample of E-M Suite, Courtesy of Petroleum Agency of South Africa



Oil Stain



Figure 5.35

Core samples of E-M Suite, Courtesy of Petroleum Agency of South Africa

These processes differ from previous tide-related facies in that tidal indicators such as mud drapes, bundles and bundle sequences, and reactivation surfaces are absent, signifying relatively constant flow direction. In addition to the absence of tidal indicators, other evidence supporting these processes include the absence of trace fossils (except for possible bioturbation in structureless portions), suggesting constant sediment supply; and convolute fine-grained strata, implicating soft-sediment slumping. The multiple coarsening upward sequences are suggestive of several episodes of progradational sediment deposition. Based on these features, the interbedded sandstone-siltstone facies is interpreted as being deposited in prodelta and delta front settings for siltstone and sandstone lithologies, respectively. Based on well log interpretation, occurrence of the interbedded sandstone-siltstone facies is limited to very thick sandstone interval deposits shown in figures 5.36, 5.37 and 5.38 respectively.



Figure 5.36: Core samples of E-M Suite, Courtesy of Petroleum Agency of South Africa, Occurrence of the interbedded sandstone-siltstone facies which is limited to very thick sandstone intervals.

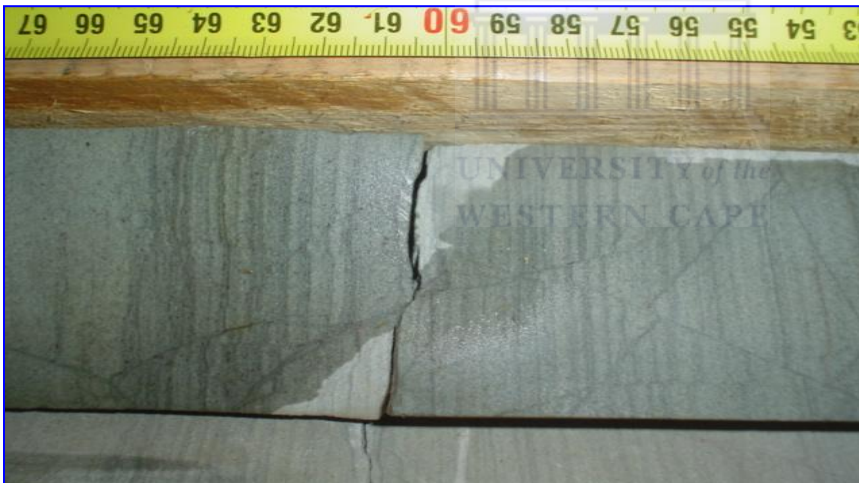


Figure 5.37: Core samples of E-M Suite, Courtesy of Petroleum Agency of South Africa, Occurrence of the interbedded sandstone-siltstone facies which is limited to very thick sandstone intervals.





Figure 5.38: Core sample of E-M Suite, Courtesy of Petroleum Agency of South Africa

### 5.1.5 Bioturbation

E-M 3 as well as E-M 4 contained a highly bioturbated facies which was absent within the other two wells this was a very short and abrupt event which terminated against a very fine grained sandstone.

It was composed of very micaceous and organic-rich, medium- to dark-gray, very fine-grained (vfL-vfU; fining upward), moderate to well-sorted sandstone. Thickness ranges from 0.15m to 0.6m being average. Other than faint thin 1-3 mm laminae, sedimentary structures were not observed. The lateral extent of the facies is unknown.

This facies is characterized by a high degree of bioturbation, including lighter-colored vertical and horizontal burrows giving the facies a “mottled” appearance. Burrows are difficult to identify, but include *Planolites*. The bioturbated sandstone facies is considered a transgressive lag or storm deposit forming following either high-energy current deposition due to marine flooding or storm currents that is subsequently bioturbated. This interpretation is evident by the comparison to overlying and underlying facies. The bioturbated sandstone facies caps a

shoaling-upward cycle—typically heterolithic siltstone, gray shale or underclay facies—but may also be interbedded.

The bioturbated sandstone facies is overlain by finer-grained, deeper water facies such as shale or minor heterolithic siltstone grading into shale. These relationships suggest a period or episode of higher energy current deposition brought about by marine flooding or storm reworking. Marine conditions are indicated by fossil content and by pyritic and calcitic cement or nodule formation.

The photos below illustrate the above mentioned:

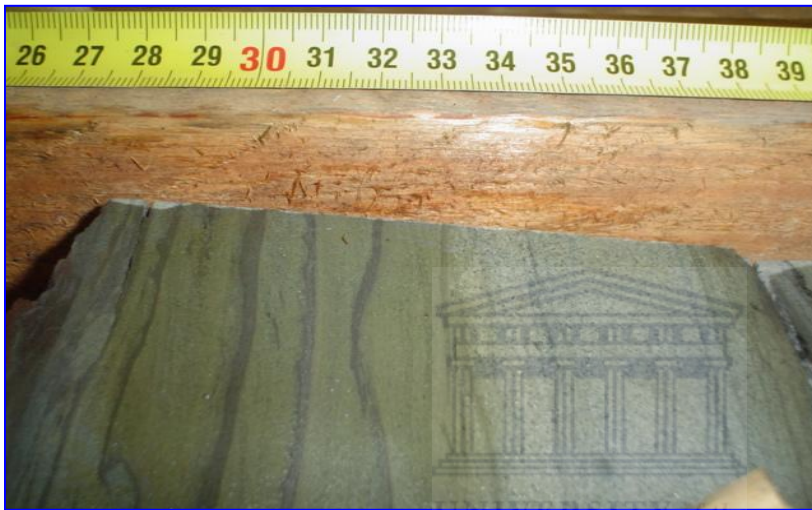


Figure 5.39: Core sample of E-M Suite, Courtesy of Petroleum Agency of South Africa



Figure 5.40: Core sample of E-M Suite, Courtesy of Petroleum Agency of South Africa  
traces of cross bedding visible within core photo.



Figure 5.41: Core sample of E-M Suite, Courtesy of Petroleum Agency of South Africa

### 5.1.6 Shallow Marine Facies

Sediment size on continental shelves decreases offshore, but grain sizes generally range from sand to mud. The deposits present both above and below the conglomerate bed consist of poorly to very poorly sorted, fine to very coarse grained yellow sandstone (coarse is the average grain size) with occasional scattered granules and pebbles. Broken and partially broken shell fragments distributed through the sandstone.

The sandstone appears to be massive, partially due to weathering. Where sedimentary structures are present they include well developed horizontal to sub-horizontal stratification and probable low angle cross-stratification often picked out by pebble- and granule-rich horizons shown in the illustrations below.

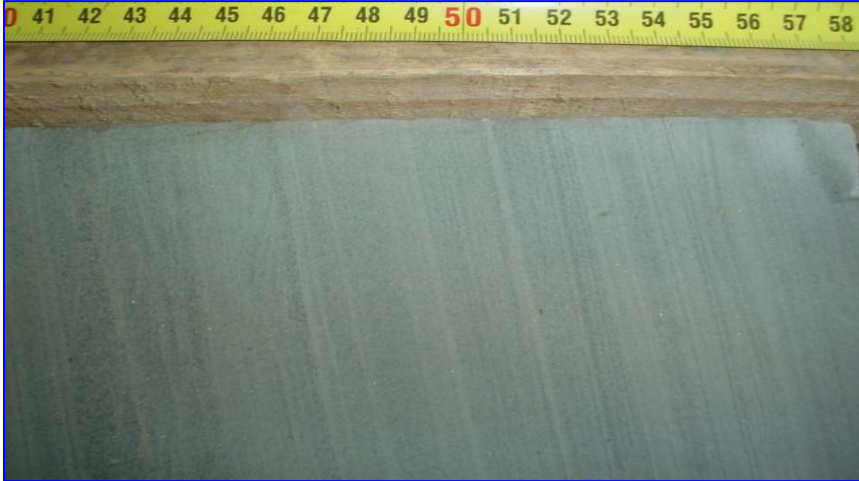


Figure 5.42: Core sample of E-M Suite, Courtesy of Petroleum Agency of South Africa

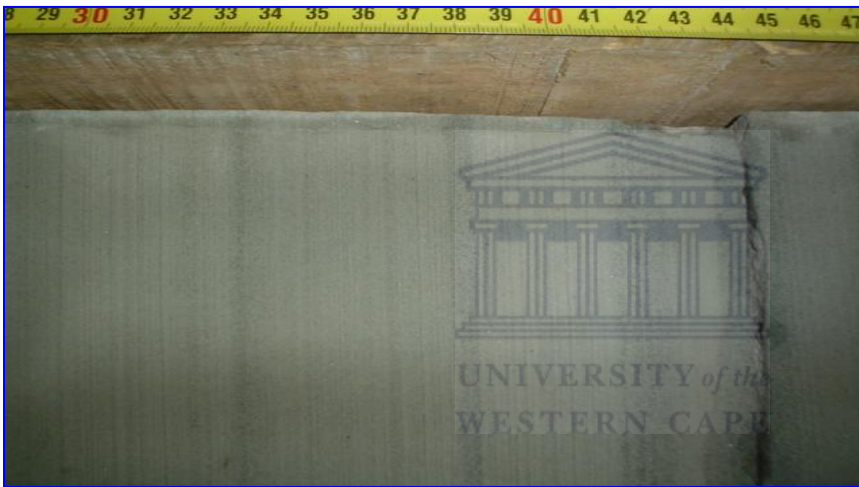


Figure 5.43: Core sample of E-M Suite, Courtesy of Petroleum Agency of South Africa (E-M 1)

The absence of trough cross-stratification representing bar development in the shoaling wave to breaker zone of the shoreface (e.g., Hunter *et al.*, 1979) indicates that these sediments do not represent upper shoreface deposits. In addition the lack of mm-scale, low angle ( $6^\circ$ ) planar to sub-horizontal lamination with heavy mineralized horizons and inverse grading (e.g., Clifton, 1969) suggests that they do not represent foreshore deposits. Consequently a mid-shoreface environment, seaward of the breaker zone, is envisaged.



The conglomerate bed has an erosional contact with the underlying shallow marine sandstones. The dip of this contact varies from less than 10° to sub-vertical. In some areas the contact appears to have been disrupted by post-depositional soft-sediment deformation. The conglomerate is extremely poorly sorted and is clasts or matrix-supported, displayed in Figures 5.44, 5.45, 5.46, 5.47.



Figure 5.44

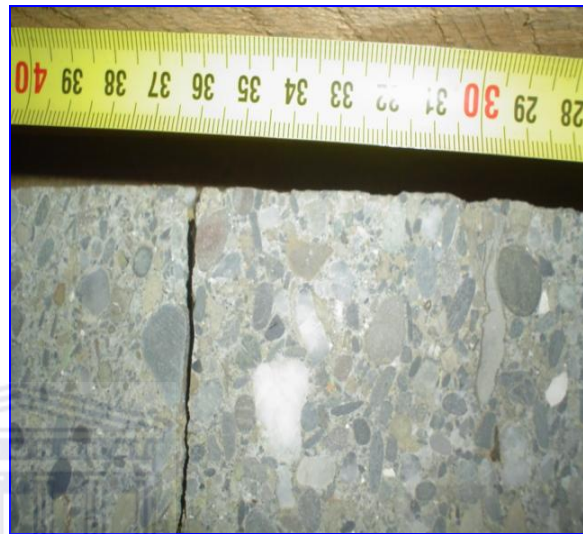


Figure 5.45



Figure 5.46



Figure 5.47

Core sample of E-M Suite, Courtesy of Petroleum Agency of South Africa, figures above illustrates the poorly sorted conglomerate within the core.

The photos is illustrations of the different types of support matricides that is exhibited within the cores from E-M 1 to E-M 4

Clasts within the conglomerate comprise 3 types: 1- angular to very angular clasts, ranging from granules to large cobbles up to 6cm in diameter; 2- very well rounded pebbles and cobbles of granodiorite; 3- blocks of shallow marine sandstone identical to the underlying sediment. Sandstone clasts long-axes range in length from 0.05 to 10 cm and often coincide with the original bedding fabric. Larger clasts may be folded and lie parallel or sub-parallel to the regional bedding. The conglomerate matrix consists of very poorly sorted fine to very coarse grained sandstone with numerous broken shell fragments, scattered granules and small pebbles of granodiorite. Matrix-rich areas appear massive in most parts; although in some cases poorly defined horizontal to sub-horizontal stratification can be observed.



The adjacent photo is an illustration of the pebble size and pebble distribution of a high energy environment.

Figure 5.48: Core sample of E-M 4 Core 5 Courtesy of the Petroleum Agency of South Africa

The thickness, variety of clast sizes, as well as the ungraded and unsorted nature of the conglomerate bed suggests that it represents a single depositional event. The sandstone clasts represent intraclasts derived from erosion of the underlying sandstone. This interpretation is based on an analogy with modern day pebbly shorelines in northern Chile, where very well rounded pebbles of granodiorite form small beach cusps (Hartley, 1999). The conglomerate matrix is

identical to that of the encompassing shallow marine sandstones, comprising very poorly sorted, shell-rich sandstone, indicating derivation from unconsolidated shoreface sediment. Thus the matrix, well rounded pebbles and sandstone intraclasts all indicate derivation of material from the shoreface and foreshore environment.

### 5.1.7 Porosity & Permeability Distribution

A total amount of 26 cores were cut throughout the E-M structure with a total length of 364m. With the average porosity and permeability displayed within the table below:

	E-M 1	E-M 2	E-M 3	E-M 4
Porosity (%)	15.5	13.5	11.7	14
Permeability (mD)	210	66	2.5	53

Table 2: Porosity and permeability distribution through the E-M suite

A total of eight cores were drilled within E-M 1 with the gas water contact located at 2360m, 60m below the confining shale. A trend line was included within the plot to indicate a drop in permeability within the well. (Appendix 2a)

This is to be expected due to the fact that permeability decreases with depth through compaction and through the loss of pore spaces. This will have a significant impact on production rates. The rest of the permeability depletion can be attributed to illite which occupies the pore throats and isolate pore spaces within the clean sand units.

Due to the nature of granulation seam its occurrence is mostly within the sand units and as can be observed they affected the areas with the greatest sand packages causing compartmentalization of these regions. With the compartmentalization of these sections it caused restriction of fluid flow within these sections or between compartments. (Illustrations in Appendix 2b, 3b, 4b)



The affected area just below the confining shale at 2560m (Appendix 2b), affected the shale layer, with the rolling of the sand grains it caused compaction and caused minor faulting and fracturing; the shale had to adjust to the compaction of the sand body.

Only four cores were drilled within E-M 2. The permeability within E-M 2 is of an increasing nature. This is in contrast to the fact that it should have had a trend of a decreasing nature due to the degree of compaction that should decrease the porosity but this is not the case within E-M 2.

As is shown within the plotted (Appendix 3a) area the biggest or greatest permeability occurs just below the confining shale and to contribute to that below the hydrocarbon water contact as well. The little reservoir to work within is also affected by compartmentalization through the affects of the granulation seams which is noted within the subsequent graph (Appendix 3b). There is little or no variation within the porosity showing once more that the granulation seams is affecting the area much more through compaction.

A total of six cores were drilled within E-M 4 with cores five and six just below the hydrocarbon water contact. E-M 4 has a permeability which also increases with depth and is not greatly affected by compaction through depth. The confining shale is just below 2600m within an area of the reservoir which has the highest peaks in permeability. Once again the porosity is consistent with variability in certain area but stays homogeneous. As evident within the plot (Appendix 4b), the granulation seam activity is once again affecting some of the regions with the greatest permeability. The compartmentalization within E-M 4 is approximately 20m above the hydrocarbon water contact and could pose a problem within flow of hydrocarbons or the recovery of hydrocarbons within E-M 4.

### 5.1.8 Structural Models

The 3D window with grid lines shows: on X and Y axis are UTM coordinates while sub-sea true vertical depths (SSTVD) are shown on Z axis. The green

arrow at the bottom right hand corner points to the geographical north direction. The wells have ball shape symbol and are displayed in distinct colors.

The relief of the model seems to imply that the possibility of the sediments being sourced from the west or south-western part of the basin. Four Major faults are identified within the modeled area. They have northwest-southeast (NW-SE) trend and divide the reservoir into blocks or segments. These faults gradually die out as they extend vertically.

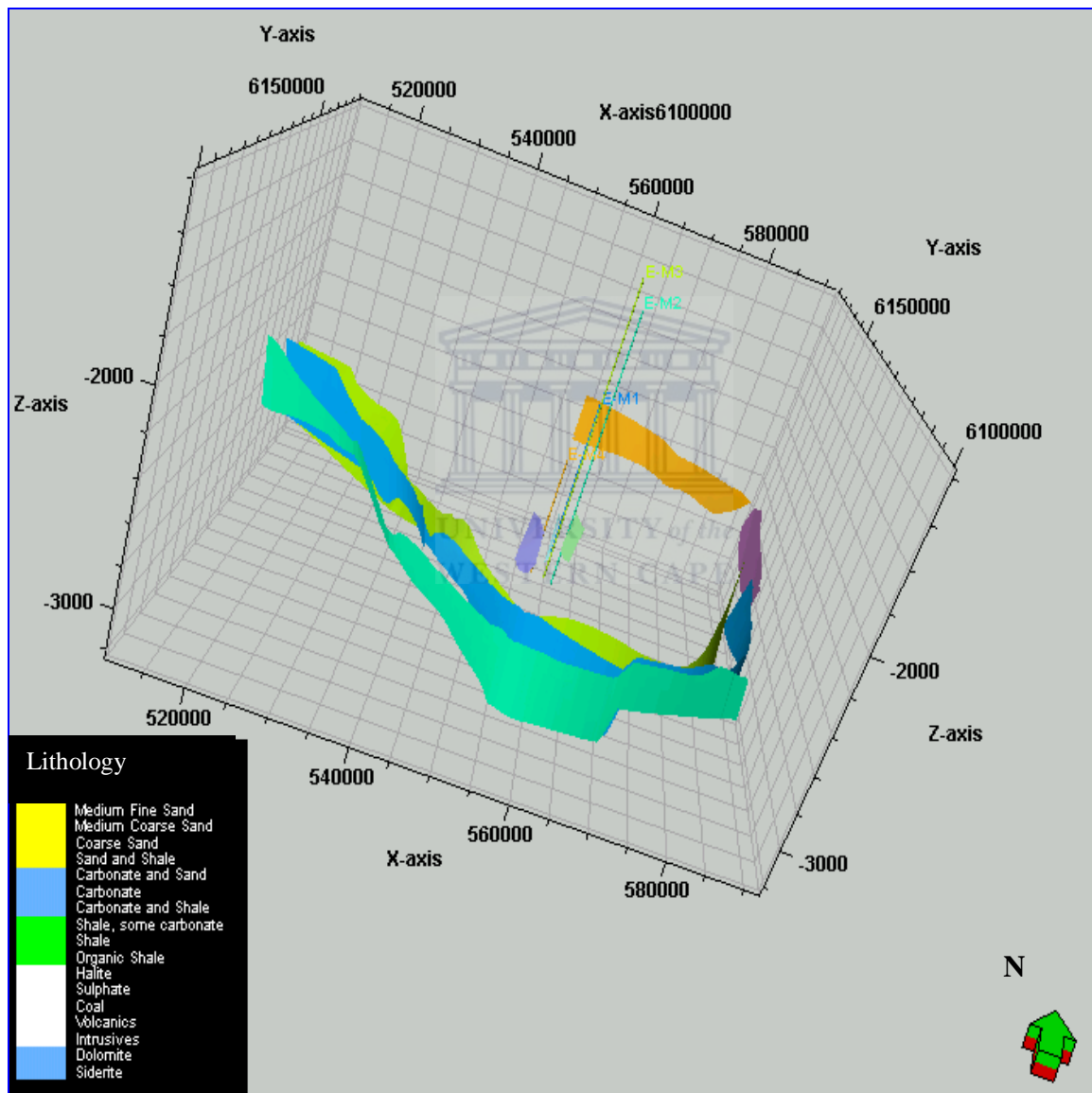


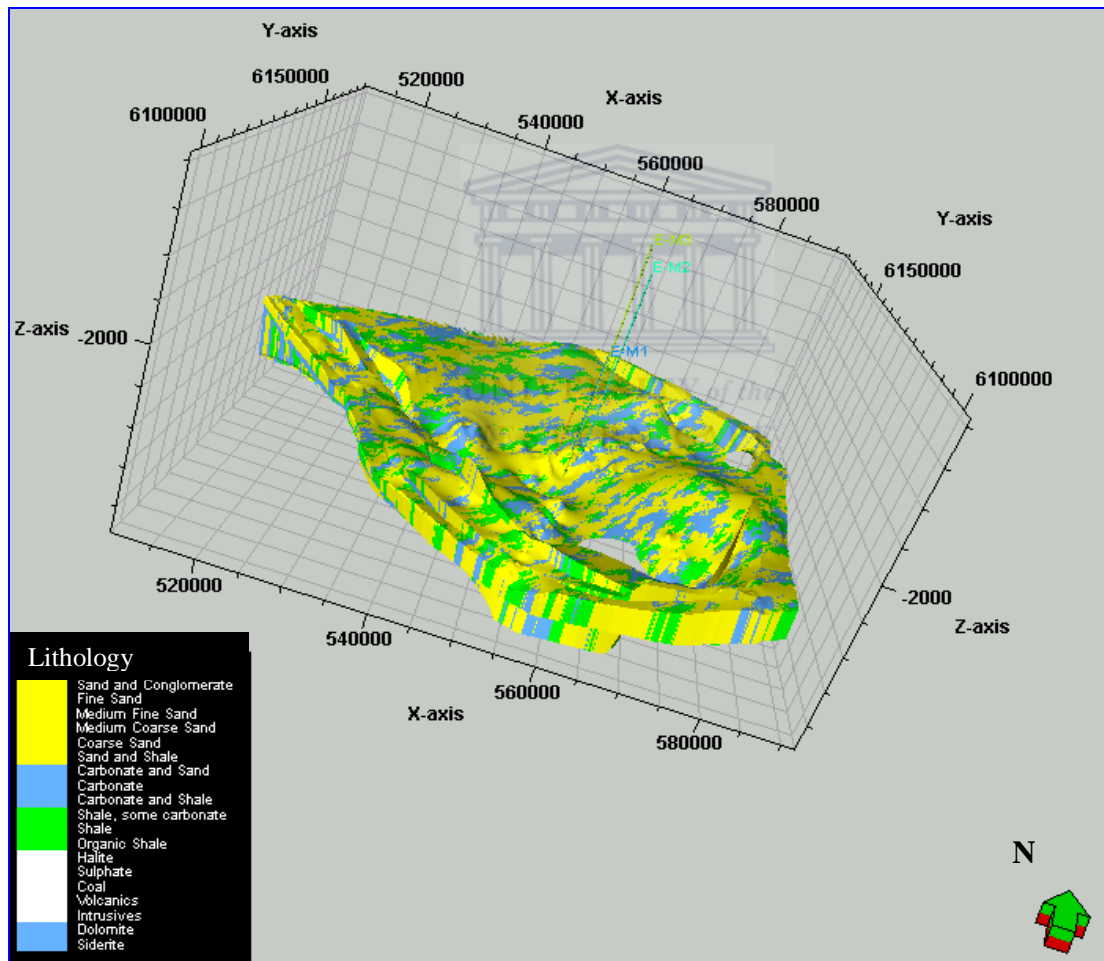
Figure 5.49: Well positions within fault model (arrow points to the north)



### 5.1.9 Facies Models

The facies model displays the distribution of the up-scaled facies logs in the 3D grid using Petrel's in-built Sequential Indicator Simulation algorithm. Four facies types are modeled: sand, silty sand, shaly sand, and shale. The facies pattern and distribution show northwest-southeast trend. Relatively high permeability areas are depicted with green/yellow/orange colour while areas with blue colour have low permeability values. The green arrow points to the north direction.

The observed incised valley features are filled with permeable sands. These areas may be selected for detailed study as they could be rich in hydrocarbon resources.



The reservoir is particularly rich in reservoir sand depicted with yellow coloration. A relatively thin zone comprising mostly of shale, divides/separates these sand rich zones.

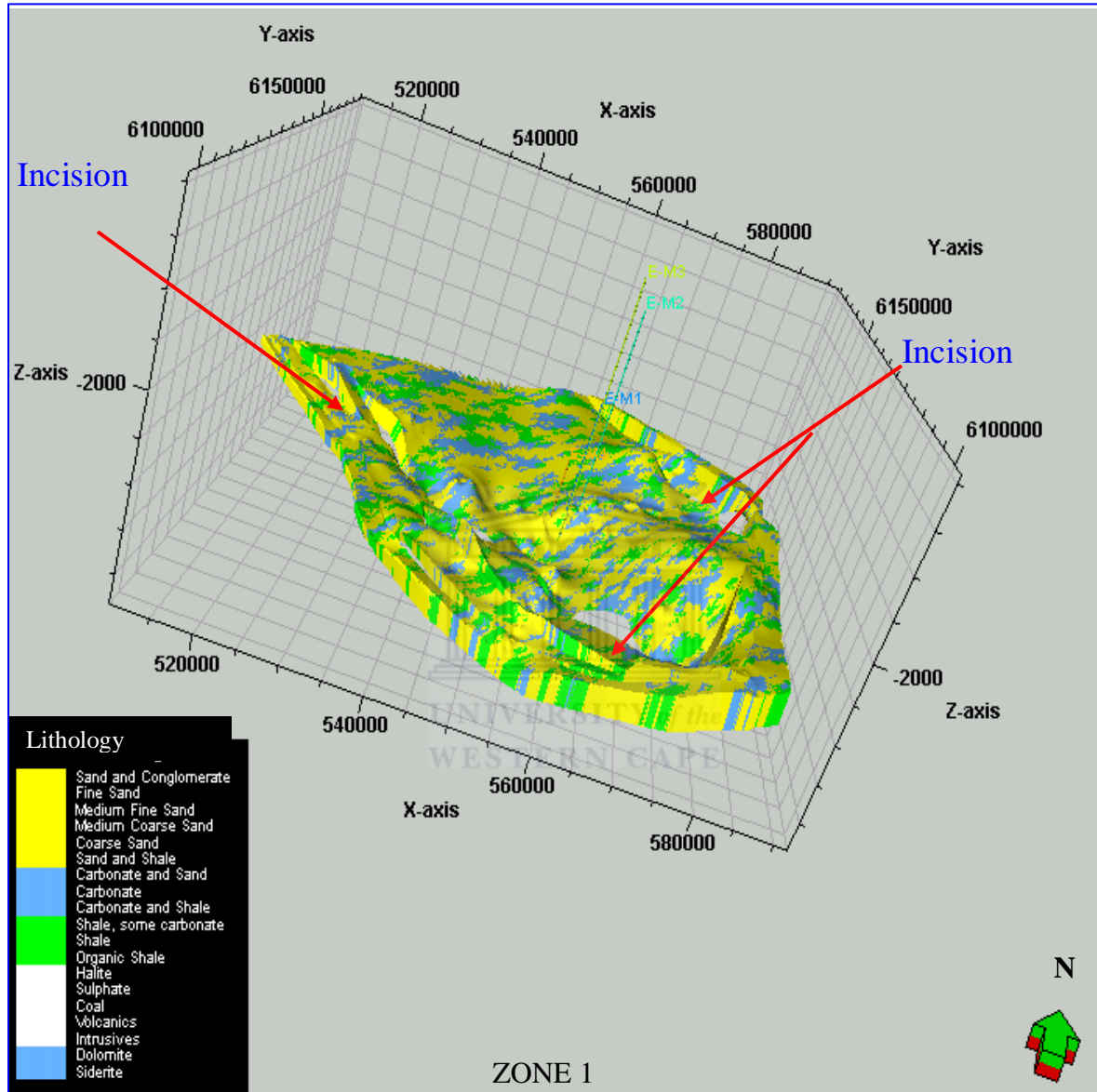
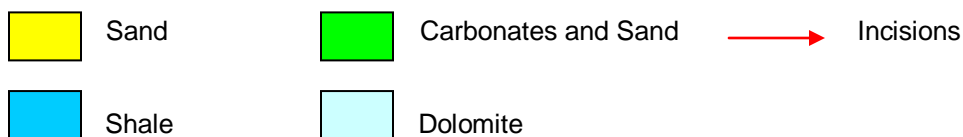


Figure 5.51: Sand rich zone 1



The affects of zone 2 can be clearly observed in figure 5.51 and as stipulated before, dividing the reservoir into two compartments. The zone acts as a seal preventing fluid flow from bottom half of the reservoir to the top half. The permeability within this zone is close to non existent as its densely compacted shales.

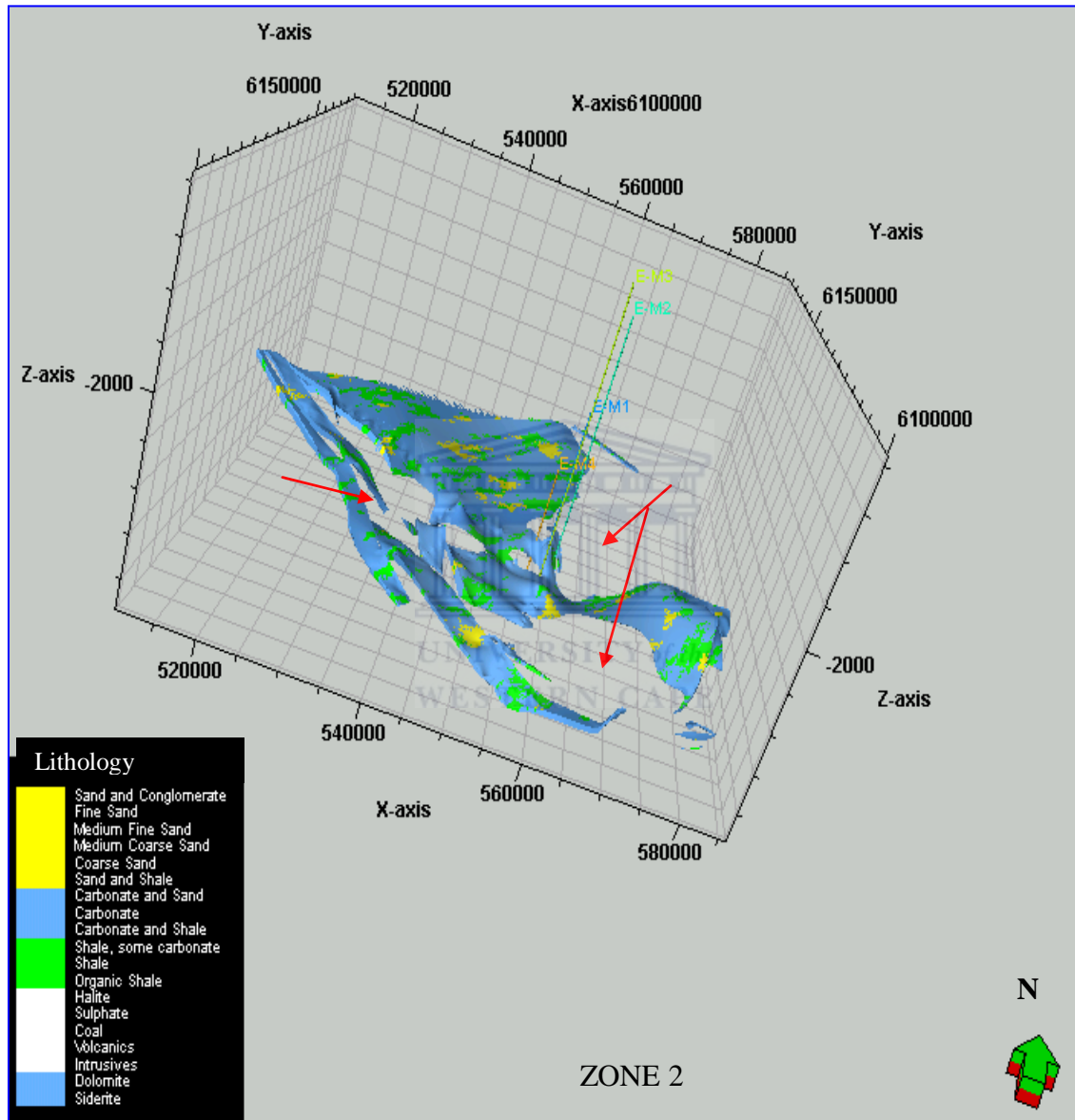
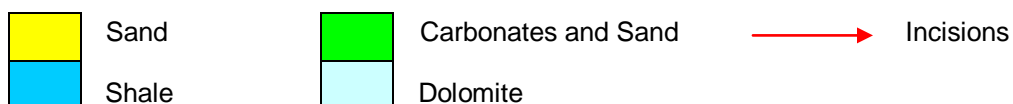


Figure 5.52: Top Zone 2, showing the distribution of the confining shale layer.



The incisions shown within the model could provide possible entry points later within the exploration/ production of this field. As noticeable the incisions if used as entry point will connect the top and the bottom half of the reservoir which would improve the production rate within this field.

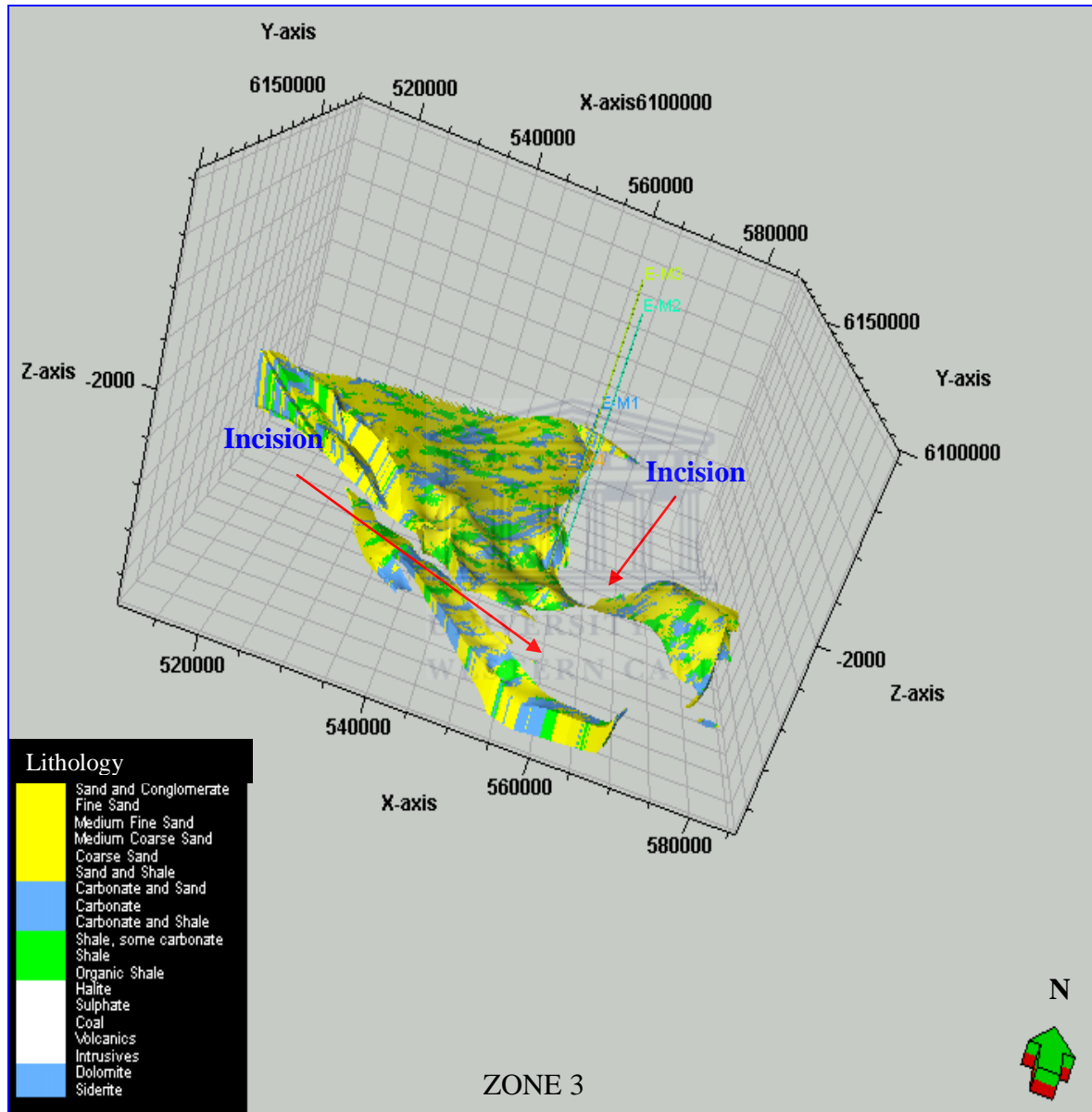
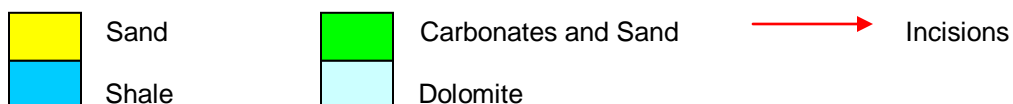


Figure 5.53: Sand rich bottom zone 3 showing possible re-entry points with incisions.



Progression of features that suggest the development of incised valley and the subsequent infill with sand rich sediment could be observed. The incised valley could have been formed by the basinward extension of fluvial system channels in that way eroding into underlying strata in reply to a relative fall in sea level while it probably got filled up throughout the following Lowstand Systems Tract (LST) and capped by Transgressive Surface (TS).

The whole package is described in the geological well completion report as stacked lobe/channel mass flow sandstones with interbedded claystone, which formed as a result of the fall in sea level in the mid-Albian resulting into material being eroded from pre-existing highstand shelf sandstones and transported into the central basin by turbidity currents from the west-southwest (Turner, *et al.*, 2000).

The lower sand is described in the geological well completion report as prograding low stand wedge comprising of stacked lobe/channel mass flow sandstones with interbedded claystone. The facies pattern of distribution and the trend of observed incision in all the zones show northwest-southeast trend of flow. They are separated in succession by interbedded shaly zone 2. Features that reflect incision and infilling are noticeable in some of the zones. The incised valleys are formed in response to the lowering of sea level.



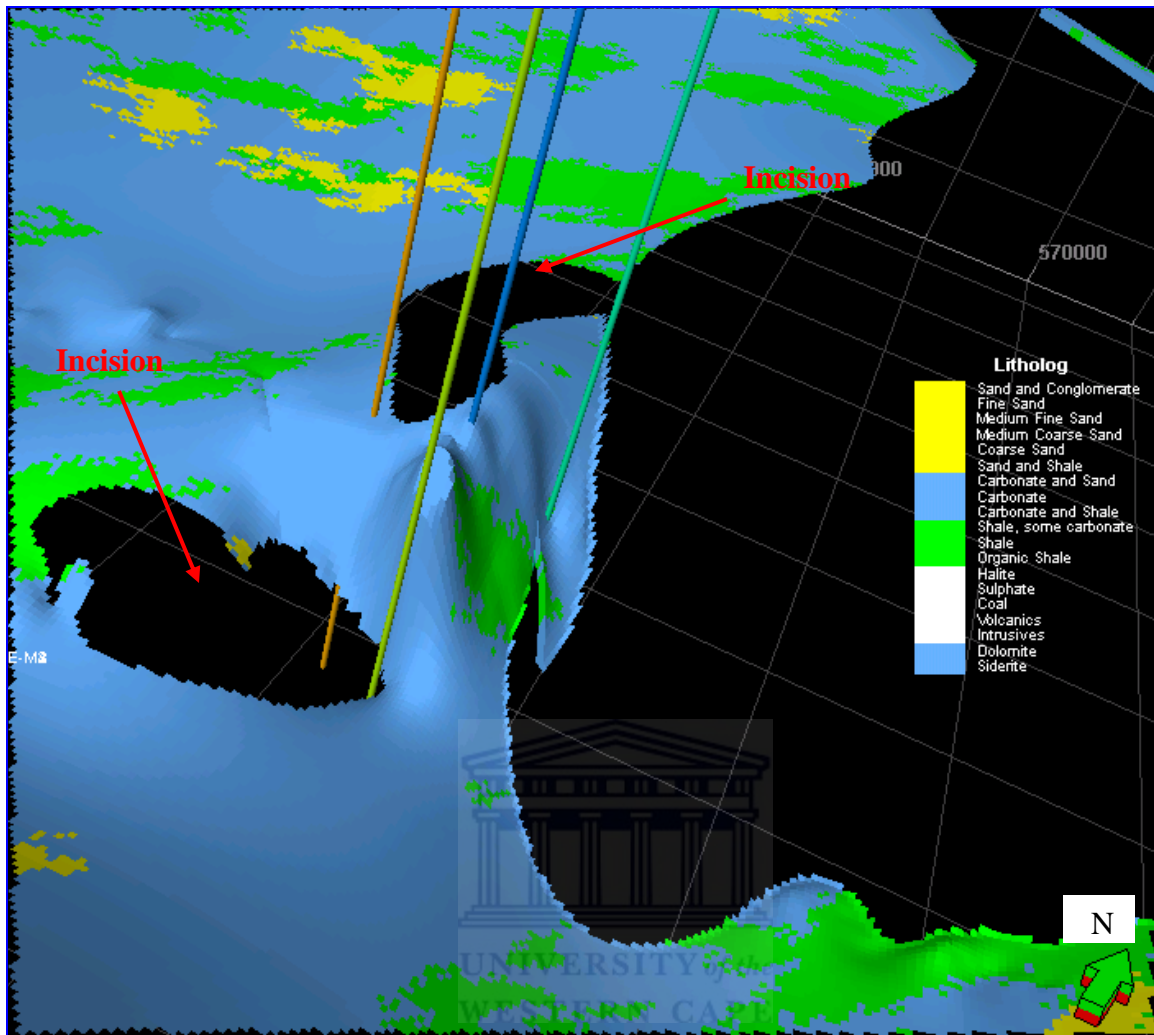
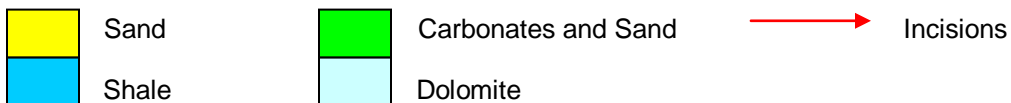


Figure 5.54: Zoomed section of zone 2, E-M 1(Yellow), E-M 2(Green), E-M 3(Blue), E-M 4 (Orange)



Currently the wells are producing from zone one just above the confining shale layer. E-M 1(Yellow) is situated within an incision that will make it more productive than the other 3 wells. The remainder of the 3 wells is situated on the 10km<sup>2</sup> domal closure and only 1 of the 4 wells is currently in contact with the upper and the lower reservoir which is E-M1.

### 5.1.10 Cross Section East -West

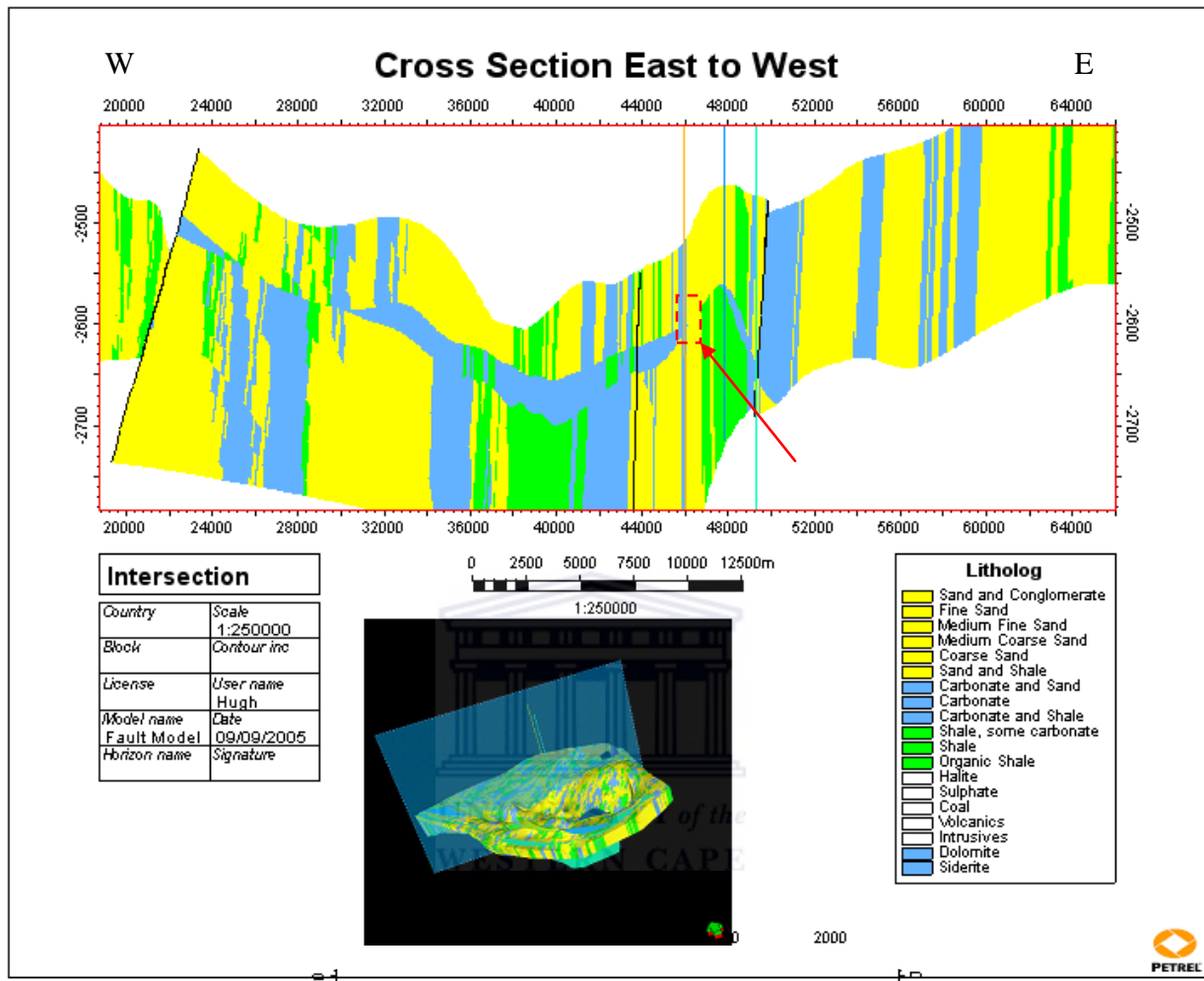


Figure 5.55: Well location within zone 1, 2, 3

Figure 5.53 illustrates the location of the wells within zones 1, 2 and 3. Due to the lack of data not all the fault systems could be modeled. The wells are cut off on the East and West by two confining faults further compartmentalizing the area. Two smaller faults are situated between E-M 2 and E-M 3 confining these two wells to their own compartments illustrated in the figure 5.55. Visible within the cross-section, E-M 1 (yellow) is the only well not restricted by the shale (light blue) layer dividing the reservoir. Indicated by the red arrows and box shown within Figure 5.55 and 5.56.

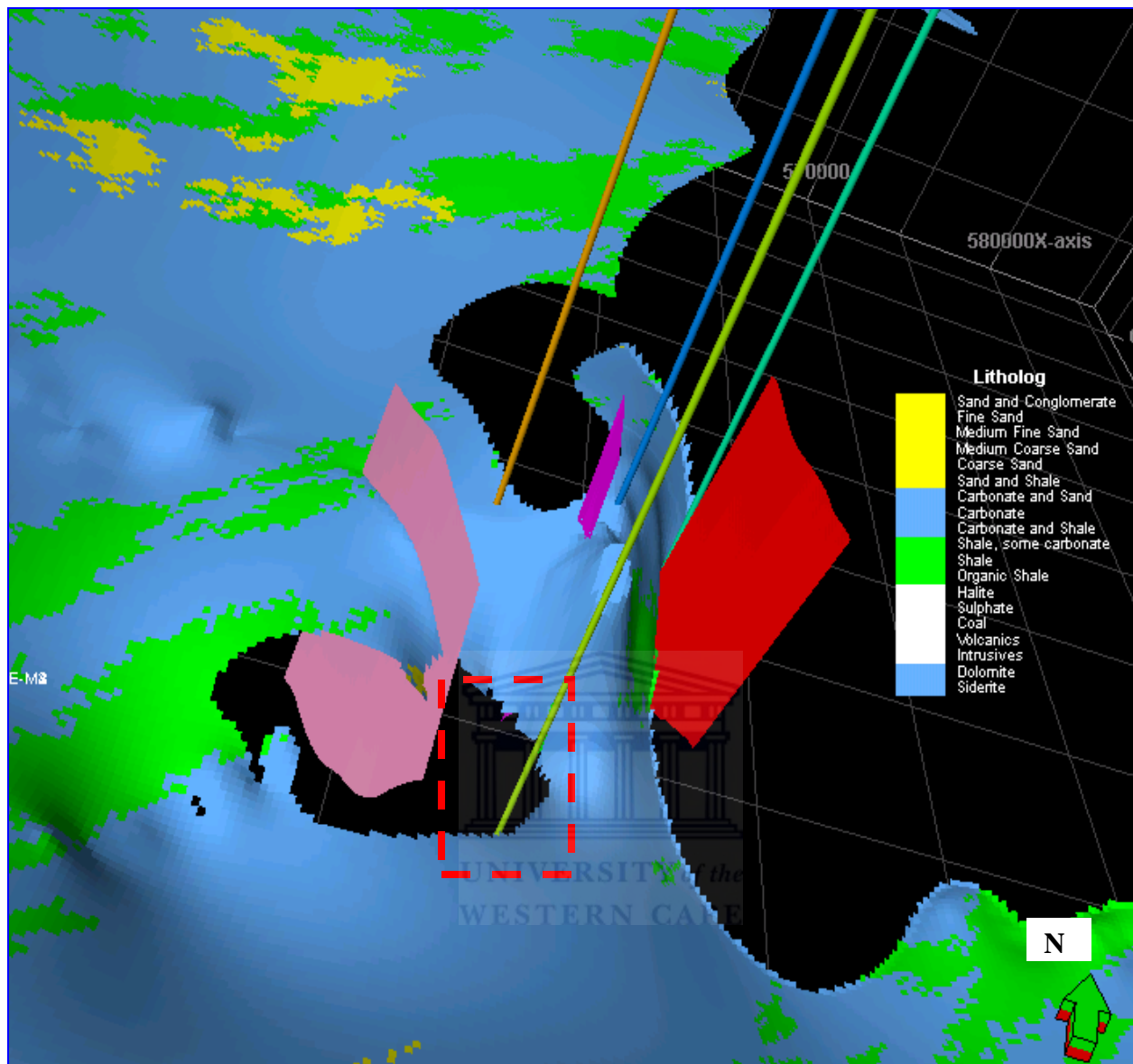
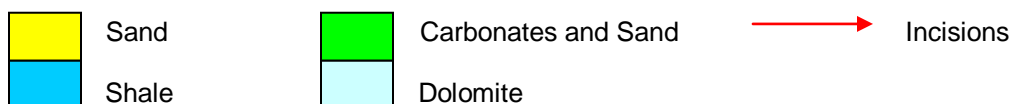


Figure 5.56: Compartmentalization by minor faults between zone 1 and 3



These faults acts as buffers as well not allowing fluid flow from one compartment to the next thus adding to the restrictions of the compartmentalizing affect of the granulation seams within zones 1 and 3 containing the reservoir sand. No fluid flow or connectivity has been reported within the geological reports as well as the fluid flow tests.

## Chapter 6

### Conclusions and Recommendations

#### Conclusion

The sandstone reservoir units encountered by the four central basin wells have been largely studied in this study within the limit of the value and quantity of available data. The Studied interval falls within the transitional rift-drift phase (6At1 – 14At1) of the development of Bredasdorp and other sub basins of Outeniqua Basin.

The available core was comprehensively analyzed determining porosity, permeability, grain sizes as well as lithology distribution over the reservoir. The reservoir is mainly dominated by sand with thin interbedded shales consisting of two main facies, a fluvial and shallow marine facies.

Porosity varies over the reservoir between 5% - 15%. Permeability has been found depleted in some areas where it has dropped to as low as 0.6mD in contrast to areas where permeability is as high as 800mD.

The permeability distribution is a direct indication of the pore connectivity within the reservoir reflecting excellent in the areas with high permeability and visa versa.

The dominant formation orientation is within southwest-northeast dip directions. These channel deposits contain packages of inclined heterolithic stratification, formed from sandstone and conglomerate, in mutually erosive sets of a few meters thickness, that are similar in many ways to fluvial point bar deposits. Paleocurrent data, taken mostly from clast imbrications in conglomerates, indicate current modes along the channel thalweg, but with secondary flow either up or down the point bar.

Succeeding accumulation of flows of the previous shelf high stand system eroded and transported sediment into the central basin during the relative sea level fall by turbidity current. The 3-dimensional models generated for these mass flow packages imitate sediment source directions which vary from southwest to northwest. At times the lower part of the turbidity currents flowing down the channels is behaving similarly to within-bank fluvial flows, with a cross-channel component of flow towards the cut bank, and return flow at the bed sweeping up the point bar. At other times this secondary circulation is reversed.

The fractures within the reservoir are very discordant and disjointed showing no dominant strike direction. The fractures is described as closed as they filled with calcite cement which in turn reflects that little or no fluid movement is possible across or through these sections, thus compartmentalizing sections of the reservoir. In addition the granulation seams contribute to the compartmentalization of the reservoir. The granulation seams was determined to be mechanically driven through gravitational pull, forming seal like fractures and diminish permeability.

The combination of sealed granulation seams as well as closed fractures is causing problems for the mobility of fluid movement horizontally through the reservoir as they create compartments which are not in fluid communication with each other.

This explains the drop in pressure in the production well, as it was drilled within one of these compartments the hydrocarbons were extracted lowering the pressure within the compartment leading to the lowered production rate of the reservoir.

The trapping mechanism observed within the area of study is essentially structural while the reservoirs are sealed by marine shales and condensed sections developed during their respective transgressive phases. The faults run through the deeper reservoir and relatively die out as they cut through the shallower reservoir.

The results presented are based largely on the amount of data available for the research. More well and seismic (preferably 3D cube) data would imply more control points and higher accuracy in the estimated figures.

## Recommendations

1. Additional wells would be required to appraise the E-M structure and determine to what extent the granulation seems has affected fluid flow as well as the degree of sedimentation that could impede fluid flow. There are areas still containing untapped resources thus the recommendation for extra wells.
2. It could be necessary to carry out an analogous outcrop base modeling in order to understand the permeability distribution and simulate flow pattern in these reservoir rocks.
3. It may well be essential to re-evaluate the granulation seem distribution and orientation. No data was available to model the distribution and orientation and this may prove to be extremely important information if captured for future study within the E-M suite as this would increase production capabilities of the reservoir.
4. It would also be feasible to look at the option of horizontal drilling as this method would penetrate or punch through more compartments and increase production as the compartments would then be in fluid communication with each other.
5. More extensive formation tests should be performed over the reservoir to determine the fluid communication over the regions of interest.

These recommendations are made on the results presented within the paper and set forward as additional options to increase the production capacity of the E-M field.

This work may well be reviewed with more data input from PetroSA (well, seismic and production data) for additional studies, predominantly with respect to reservoir modeling and flow simulation.





## Bibliography

Allen 1984. Sedimentary structures: their character and physical basis: Developments in Sedimentology, v. 30.

Antonellini and Aydin 1995. Effect of faulting on fluid flow in porous sandstones: Geometry and spatial relations, Bull. Am. Ass. Petrol. Geol. 79, pages 642-671.

Balbinsky and Masters (AEA Technology). A New Flow Based Cut off Criterion for Permeability in Dry Gas Reservoirs.

Barton and Christopher 1997. US. Geological Survey, 600 4th St., South, St. Petersburg, FL., 33701, Tel. 813-893-3100 X 3014 Spatial Distribution of Large and Small Fault Systems in Sandstone Reservoirs: An outcrop Study and Fracture Geometry and Fluid Flow.

Bathurst 1971. Carbonate Sediments and Their Diagenesis: Elsevier, New York, pp. 93-216.

Beach 1999. Fault damage zone scaling and spatial organization of granulation seams in porous sandstone. Implications for flow properties.

Beard and Weyl 1973. Influence of texture on porosity and permeability of unconsolidated sand. AAPG Bulletin, v. 57, p. 349-369.

Berkhouse 1985. Sedimentology and diagenesis of the Lower Cretaceous Kootenai Formation in the Sun River Canyon area, northwest Montana. [MS thesis]: Bloomington, Indiana University, p. 151.

Booth and DuVernay III 1990. Sequence Stratigraphic Framework, Depositional Models, and Stacking Patterns of Pondered and Slope Fan Systems in the Greater Auger Basin: Central Gulf of Mexico Slope.

Broad 2004. South Africa Activities and Opportunities. An Unpublished Power Point Presentation to PetroChina.

Broger 1997. Glauconite sandstone exploration: A case study from the Lake Newell project, Southern Alberta, in *Petroleum geology*.

Bjørlykke and Saigal 1992. Diagenetic processes in the Brent Group. Pp.263-289 in: *The Geology of the Brent Group*. Geological Society, London, Spec. Publ. 61.

Burruss 1987. Paleotemperatures from fluid inclusions: Advances in theory and technique, in Naeser, N.D. & McCulloh, T.H. (eds.): *Thermal history of sedimentary basins, methods and case histories*, AAPG Spec. Publ. 41, 121-131.

Burhannudinnur and Morley 1997. Anatomy of growthfault zones in poorly lithified sandstones and shales: implications for reservoir studies and seismic interpretations: Part 1, outcrop study: *Petroleum Geoscience*, v. 3, p. 211-224.

Clifton 1969. Beach lamination: nature and origin. *Marine Geology*, Vol, 7, p. 553-559. Climate and sea-level change, glaciation and a northward drift. *The geology of England and Wales* 469-475 Publisher: Geological Society of London.

Compensated Density Sonde (modified from Wahl *et al*, JPT, 1964)

Darby and Haszeldine 1997. Illite date's record deep fluid movements in petroleum basins. *Petroleum Geosciences*. 3, 133-140.

Davis Jr. 1994. Barrier island systems – a geologic overview, In: R.A. Davis, Jar (Ed.) Geology of Holocene Barrier Island Systems. Springer –Verlag, 1-46.

De Wit 1991. Inversion tectonics of the Cape fold belt, Karoo and Cretaceous basin of South Africa p. 33-44.

De Wit and Ransome eds. 1992. Inversion Tectonics of the Cape Fold Belt, Karoo and Cretaceous Basins of Southern Africa.

Dravis and Yurewicz 1985. Enhanced Carbonate Petrography Using Fluorescence Microscopy, J. Sed. Petrology, v. 55, p. 795-804.

Fowles and Burley 1994. Textural and permeability characteristics of faulted, high porosity sandstones, Mar. Petrol. Geology, 11, pages 608-623.

Gerlach and Bhattacharya 1999. Cost Effective Techniques for the Independent Producer to Evaluate Horizontal Drilling Candidates in Mature Areas: AAPG Hedberg Conference, International Horizontal Well Symposium: Focus on the Reservoir.

Goldstein and Reynolds 1994. Systematics of fluid inclusions in diagenetic minerals. SEPM short course 31, 199pp.

GSA Bulletin, 1992, Vol. 104, p. 106. Eocene Tectonics in the Omineca Belt, Northern British Columbia, Canada: Field,  $^{40}\text{Ar}/^{39}\text{Ar}$ , and Fission Track Data from the Horseshoe Range; senior author: H. E. Plint. File size: 21 p.

Haltenbach 1999. Faults and Fractures in Sedimentary Basins- Examples from the North Sea.

Hartley and Jolley 1995. Tectonic implications of Late Cenozoic sedimentation from the Coastal Cordillera of northern Chile (22-24°S). *Journal of the Geological Society of London*, Vol. 152, p. 51-63.

Hunter, Clifton and Phillips 1979. Depositional processes, sedimentary structures, and predicted vertical sequences in barred nearshore systems, southern Oregon coast. *Journal of Sedimentary Petrology*, Vol. 49, p. 711-726.

Houston 1986. Dynamic core-hole screening effects in the C-KVV Auger line shape of graphite

Jacobs and Fanning 2003. Late Neoproterozoic/Early Palaeozoic events in central Dronning Maud Land and significance for the southern extension of the East African Orogen into East Antarctica.

Jonk and Durant 2000. Using image analysis to quantify textural changes due to post-depositional remobilization of fine-grained sands  
Department of Geology and Petroleum Geology, University of Aberdeen, AB24 3UE, Aberdeen, UK.

Judson and Stamey 1933. Overhanging Salt On Domes of Texas and Louisiana: *Bull. Am. Assoc. Petrol. Geol.*, Vol. 17, pp. 1492-1520.

Knut Bjorlykke 1998. Fluid-Flow response to Production from reservoirs Bounded by Fault Relay Structures.

Laura 1997. Pyrak-Nolte Department of Civil Engineering & Geological.

Levorsen 1958. The mid continent; a land of geological opportunity, , *A.I. World Oil*, vol. 147, no. 4, pp. 101-104, Sciences University of Notre Dame, Notre Dame.

Locality map of onshore and offshore basins explored for oil and gas courtesy of the Petroleum agency of South Africa (PASA) PASA brochure 2004.

Milliman 1974. Marine Carbonates: Springer-Verlag, New York, pp. 153-249.

Mitchum 1991. Siliciclastic Sequence Stratigraphy in Well Logs, Cores, and Outcrops: Concepts for High-Resolution Correlation of Time and Facies.

Mitra 1988. Effects of deformation mechanisms on reservoir potential in Central Appalachian overthrust belt, Bull. Am. Ass. Petrol. Geol. 72, pages 536-554.

Matthai 1991. Quantitative Modeling of Fault-Fluid-Discharge and Fault-Dilation-Induced Fluid-Pressure Variations in the Seismogenic Zone; senior 12 p.

Optical image of a glauconitic sandstone (made at 20X magnification) showing formation of a pseudomatrix that occludes the original primary porosity (courtesy of Rob Lavinsky, Omni Laboratories, Inc).

Panda and Lake 1994. Estimation of single-phase permeability from parameters of particle-size distribution. AAPG Bulletin, v. 78, p. 1028-1039

Petroleum South African brochure 2004.

Pitman 1981. Effect of fault-related granulation on porosity and permeability of quartz sandstones, Simpson group (Ordovician), Oklahoma Am. Assoc. AAPG. Geol., Bull. ; Vol/Issue: 65:11.

Pitt 2000. Quality Management, Part One: Drainage design philosophy, effects and sources of stormwater.

Philip and Kibler 2003. A Catalog of Porosity and Permeability from Core Plugs in Siliciclastic Rocks Open-file Report 03-420;

Reading 1978. Sedimentary Environments and Facies: Elsevier, 557 p.

Reading 1996. Sedimentary Environments, Processes, Facies and Stratigraphy, Blackwell, Oxford.

Reifenstuhl 2002. Reservoir Characterization Studies in Alasca, vol. 6,no 3, by, Alaska Division of Geological and Geophysical Surveys.

Rider 1996. The Geological Interpretation of Well Logs: Caithness.

Schlumberger publications (1993) : ARI Azamuthal Resistivity Imager.

Schlumberger publications 1997: ARI Array Induction. Schlumberger publications 11994: Array Sonic Tool.

Schlumberger 2004. Petrel Online Help, Petrel 2004 Version.

Schlumberger 2005. Schlumberger Oil Field Glossary: Where the Oil Field Meets the Dictionary. URL: <http://www.glossary.oilfield.slb.com>.

Serra 1986. Advanced Interpretation of Wireline Logs Schlumberger Publication.

Sondergeld and Rai July 1993. A New Concept in Quantitative Core Characterization, The Leading Edge: 774-779.

Sondergeld and Rai 1988. Geophysical evaluation module operator's manual, Amoco Research Report T88-E-0033:



SPWLA Glossary, 1984-97

Stover and Screatton 1999. Hydrologic Characteristics of Shallow Marine Sediments of Woodlark Basin, Site 1109.

Storey and Livermore of African Earth Sciences 1999, v. 29, no. 1, p. 153-163, Reconstruction and breakout model for the Falkland islands within Gondwana.

Turner, Grobber and Sontundu 2000. Geological modelling of the Aptian and Albian sequences within Block 9, the Bredasdorp Basin, offshore South Africa: Journal of African Sciences, 31(1), 80.

Underhill and Woodcock 1987. Faulting mechanisms in high-porosity sandstones; New Red Sandstone, Arran, Scotland, in Deformation of sediments and sedimentary rocks, Jones, M. E. and Preston, R. M. F. (eds), Geol. Soc. Spec. Publ. 29, pages 91-105.

Van der Merve and Fouche 1992. Inversion tectonics in the Bredasdorp basin, offshore South Africa p, 49-58.

Van Wagoner, Mitchum, Campion, and Rahmanian 1990. Siliciclastic Sequences, Stratigraphy in Well Logs, Cores and Outcrops: Amer. Assoc. Petroleum Geology, Methods in Exploration, (7), 55.

Van Wagoner 1992. Sequence stratigraphy applications to Shelf sandstone reservoirs: Outcrop to subsurface.

Widrig and Schwartz 2001. Estuarine Tidal Deposits within a Fluvial Dominated Cretaceous Foreland Basin, Western Montana. Northeastern Section of the Geological Society of America, v. 32, p. 60.

Wood, M. [Petroleum Agency of South Africa (PASA) Pty. Ltd., Cape Town (South Africa)] 1995. Development potential seen in Bredasdorp basin off South Africa.



# Appendix 1:



UNIVERSITY *of the*  
WESTERN CAPE

## Appendix 1

### Porosity and Permeability Distribution for the E-M Suite

E-M 1	Depth (m)	Porosity (%)	Permeability (mD)
core 1	2508.64	13.7	25
	2509.27	12.7	8.8
	2510.5	14.7	17
	2511.07	15.5	25
	2511.24	15.9	116
	2512.11	15.8	103
	2513.77	15.5	55
	2515.11	18.4	169
	2516.07	16.8	2
	2517.19	17.1	246
	2517.64	17.8	694
	2517.75	17.8	575
	2519.21	15.6	10.7
	2520	17.3	106
	2520.4	16.1	8
	2520.52	17	17
	2521.79	16.3	38
	2522.86	14.2	4.7
	2524.05	16.3	538
	2524.71	13.2	6.1
	2527	14.2	9.3
	2527.97	13.4	7.3
Core 2	2528.1	13.1	17.6
	2529.1	13.8	25
	2530.07	15.1	55
	2531.1	16.9	104
	2532.25	15.4	492
	2533.48	17.1	656
	2533.48	17.7	714
	2534.42	17.5	422
	2535.51	17.7	935
	2536.52	13.5	260
	2537.55	13.3	34
	2538.62	15.7	93
	2539.42	14.9	151
	2540.32	17.4	144
	2541.42	13.9	164

	2542.46	14.4	20
	2543.49	15.1	139
	2543.65	17.6	519
	2544.98	15.5	144
	2546.07	15.9	82
Core 3	2547.07	11.1	176
	2548.16	14.4	153
	2548.16	16.5	455
	2549.19	15.1	100
	2550.15	17.1	592
	2551.46	17	251
	2551.57	13.2	10.5
	2552.66	15.8	489
	2553.59	16.7	165
	2554.79	15.7	846
	2555.87	13.4	56
	2556.93	13.8	35
	2557.89	17.5	847
	2558.03	15.3	1235
	2558.96	17.1	468
	2559.7	15	446
	2561.24	14.5	26
	2562.26	16	472
	253.31	17.3	405
	2565.2	36.3	4.8
Core 4	2566.25	8.9	4.5
	2567.23	5.8	0.18
	2568	10	1.6
	2569.63	16.4	98
	2570.78	16.1	63
	2570.9	16.1	37.3
	2571.68	13	23
	2572.94	12	2.9
	2573.91	19.1	474
	2574.84	16.1	151
	2575.95	12.4	0.97
	2576	17.6	239
	2576.77	17.6	250
	2577.25	10	94
	2578	7.6	4.2
	2579.08	9	0.5
	2580.22	12.1	5.5
	2581.81	9.9	1
	2584.3	15.1	38
Core 5	2585.44	14.6	13

	2586.55	15	12.8
	2587.66	15.3	28
	2588.68	15.1	26
	2589.69	16	35
	250.62	16.3	211
	2592.73	15.6	211
	2593.92	13.8	18
	2594.57	16	57
	2595.35	3.1	0.3
	2595.47	2.9	0.4
	2601.04	4.1	0.07
Core 6	2602.69	6.2	0.1
	2602.79	6	1
	2603.71	4	0.12
	2605.04	12.6	1.8
	2605.93	3	0.09
	2610.23	11.9	1.4
	2611.23	13.3	18
	2612.63	13.7	40
	2613.65	5.7	2.2
	2613.76	10.5	12.9
	2614.63	11.8	1.7
	2615.43	12.1	7.7
Core 7	2616.1	12.5	5.9
	2617.24	19.9	4.8
	2618.29	11.9	3
	2619.34	17.6	138
	2619.34	15.7	137
	2620.35	16.1	102
	2621.43	16.5	187
	2622.55	11.9	1.6
	2623.63	13.8	32
	2623.77	13.6	19.4
	2625.42	14.1	20
	2631.74	13.7	8
	2631.81	13.8	4.4
	2631.68	14.5	13
Core 8	2633.56	14.9	6.7
	2634.57	15.1	45
	2635.67	15.7	33.3
	2636.54	15.5	17
	2637.54	13.5	11.2
	2638.49	12.9	31
	2639	13.2	15
	2641.02	13.5	8.3



	2642.06	13.5	11.2
	2642.2	14.3	11.8
	2642.85	151	121

E-M 2	Depth (m)	Porosity (%)	Permeability (mD)
<b>Core 1</b>	<b>2605</b>	<b>13.9</b>	<b>0.6</b>
	2606.08	3.3	0.26
	2608.32	12.6	1
	2609.62	14.5	10.2
	2610.7	16.2	13.9
	2612.55	10.7	0.3
	2613.94	15.8	49
	2615.33	14.4	24
	2615.47	15.8	33
	2617	13.8	0.8
	2619.55	13.1	0.4
	2620.97	14	2.3
	2621.96	12.38	
	2623.52	8.6	0.12
<b>Core 2</b>	<b>2624.54</b>	<b>15.1</b>	<b>49</b>
	2626.13	12	0.77
	2627.76	15.2	225
	2629.04	13.7	2.4
	2631.91	13.8	81
	2633.11	15.7	0.86
	2634.17	14.7	149
	2635.31	16.7	370
	2637.84	14.3	68
	2638.94	14.6	166
	2639.88	14	166
	2641.12	14.3	311
	2641.82	10.4	34
<b>Core 3</b>	<b>2642.62</b>	<b>16.7</b>	<b>39</b>
	2644.19	15.5	218
	2646.15	15.3	289
	2647.41	17.5	295
	2649.57	13.6	78
	2650.63	15.5	75
	2651	17.8	132
	2653.09	11.3	8.7
	2654.12	15.2	126
	2655	14.5	120
	2656.69	13.9	18

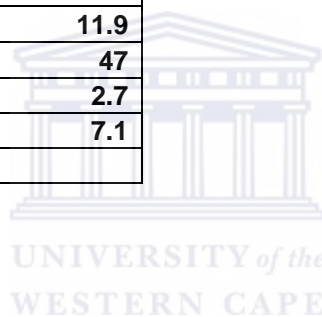
	2657	15.2	15
	2658.42	12.4	281
	2659.47	13.5	42
	2659.85	13.9	74
<b>Core 4</b>	2661.27	14.6	44
	2662.49	3.7	0.24
	2663.84	14.5	56
	2665.03	11.5	2.2
	2667.69	14.2	14
	2669.12	14.1	40
	2670.43	10.9	10

<b>E-M 3</b>	<b>Depth</b>	<b>Porosity</b>	<b>Permeability</b>
	2568.47	14.2	0.8
	2587.56	14.6	0.8
	2588.43	5.4	0.1
	2590.95	5.8	0.2
	2694.16	10.9	0.3
	2595.49	13.4	9.2
<b>Core 1</b>	2604.4	8.5	0.2
	2605.37	6.8	0.2
	2611.62	10.4	0.3
	2612.57	9.7	0.2
	2620.48	6.5	0.27
<b>Core 2</b>	2621.48	6.5	0.27
	2622.58	12.7	6.5
	2624.32	6.2	0.3
	2625.83	12.3	0.95
	2626.86	10.7	2.5
	2628.33	10.5	1.2
	2629.34	9.1	0.3
	2630.29	11	0.31
	2631.33	10.2	0.7
	2632.18	12.3	1.9
	2633.3	11.2	1.2
	2634.33	12.2	0.88
	2636	10.6	0.4
<b>Core 3</b>	2637.26	11.2	6.8
	2638.25	10	0.4
	2639.73	9.2	0.64
	2641.35	6.4	2.7
	2642.34	8.7	0.62
	2643.62	3	0.1
	2644.51	7.6	0.25

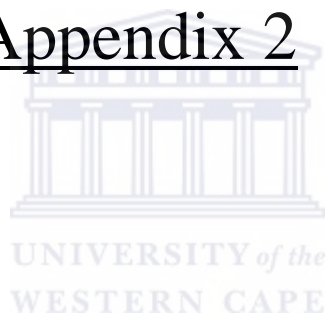
	2646.06	11.2	1.5
	2646.92	12.2	1.6
	2648.08	11.9	5.4
	2649.16	12.4	2.8
	2650.13	15.3	6.3
	2650.92	10.2	0.09
	2651.95	13.2	1.3
	2653.14	15.2	7.4
	2654.44	13.4	0.8
core 4	2655.38	12.9	2.8
	2656.39	13.6	5.8
	2657.87	14.4	10.7
	2658.84	13.6	3.6
	2660.06	12.1	0.44
	2661.7	12	5.4
	2662.63	12.9	3.6
	2663.64	12	14
	2664.92	11.2	0.29
	2665.86	11	1.3
	2667.49	13.2	10
	2669.68	12.6	4.6
	2670.96	13.4	4.6
core 5	2673	12.2	7.9
	2674.05	11.9	1.12
	2675.23	13.1	7.3
	2676.18	12.2	3.8
	2677.28	13.8	3.8
	2677.28	13.8	3.8
	2678.54	13.1	9.3
	2680.07	14.2	11.6
	2681.22	12.7	18
	2682.12	13.1	9.3

E-M 4	Depth (m)	Porosity (%)	Permeability (mD)
	2562.75	15.2	114
	2565.22	13.4	0.45
	2567.49	15	4.4
	2569.55	15	4.2
	2571.63	11.8	12.2
	2574.22	13.9	0.6
	2576.24	10.5	41
	2578.34	11.3	0.2
	2580.3	13.5	1.8
core 2	2582.83	13	3.7
	2585	15.9	4.3

	2587.08	17.5	293
	2588.96	17.4	260
	2590.57	15.1	6.5
	2592.55	16.3	71
	2594.61	16.7	169
core 3	2596.54	10.3	89
	2597.72	12.6	8.7
	2599.48	14	3.4
	2601	13.5	181
	2603.87	14.9	98
	2605.68	12.9	53
	2607.35	17.6	290
	2610.73	13.2	26
	2612.29	12.6	28
core 4	2613	16	77
	2615.97	13.2	39
	2618.9	13.4	14
	2621.01	10.7	2.6
	2632.29	11.8	0.9
	2635.27	15.6	5.7
	2638.3	13.2	11.9
	2640.44	14.9	47
	2643.1	13	2.7
	2645.84	15.7	7.1

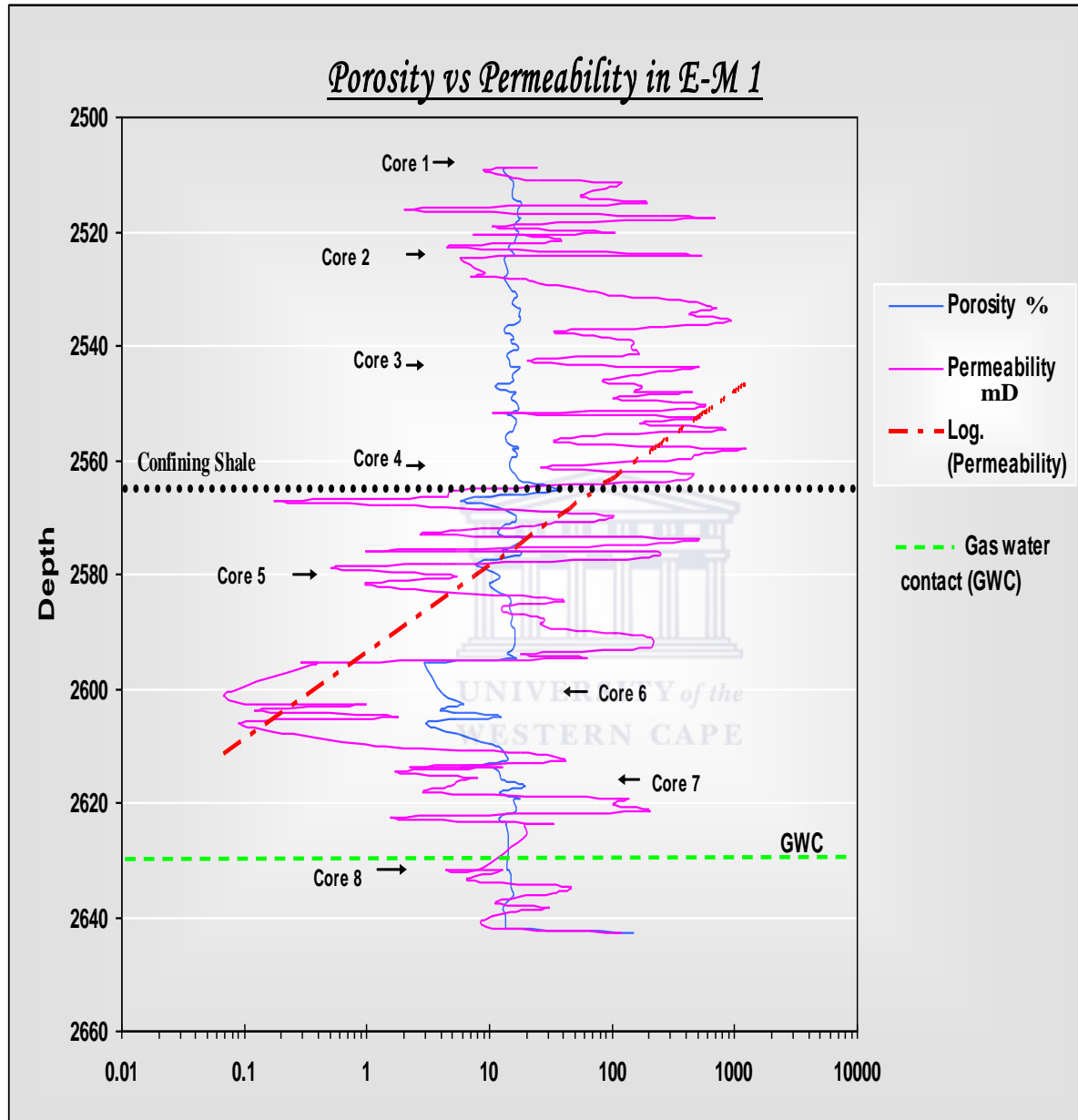


## Appendix 2



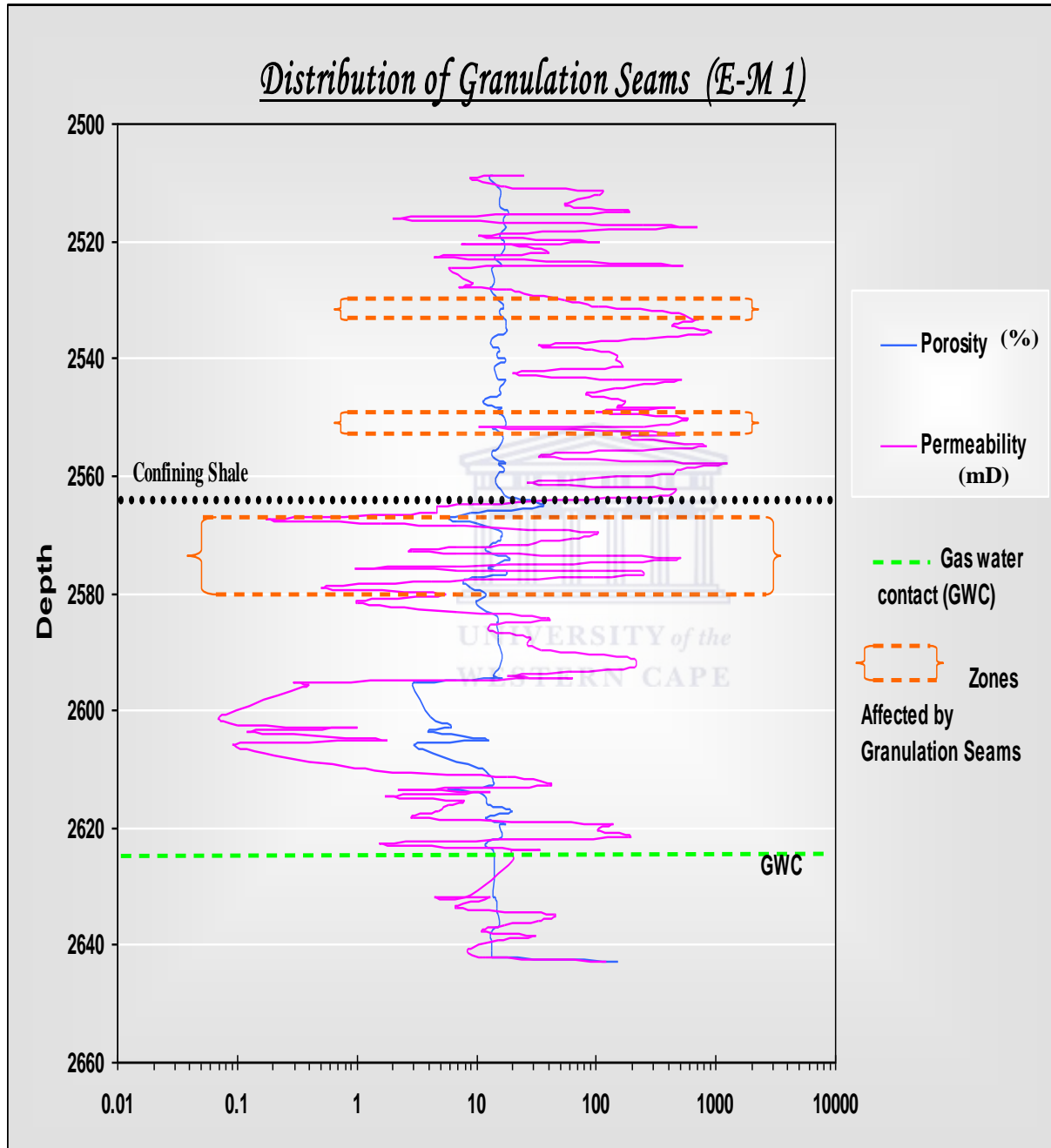
## Appendix 2a

### Porosity vs. Permeability over E-M 1



## Appendix 2b

### Distribution of the Granulation Seams (E-M 1)



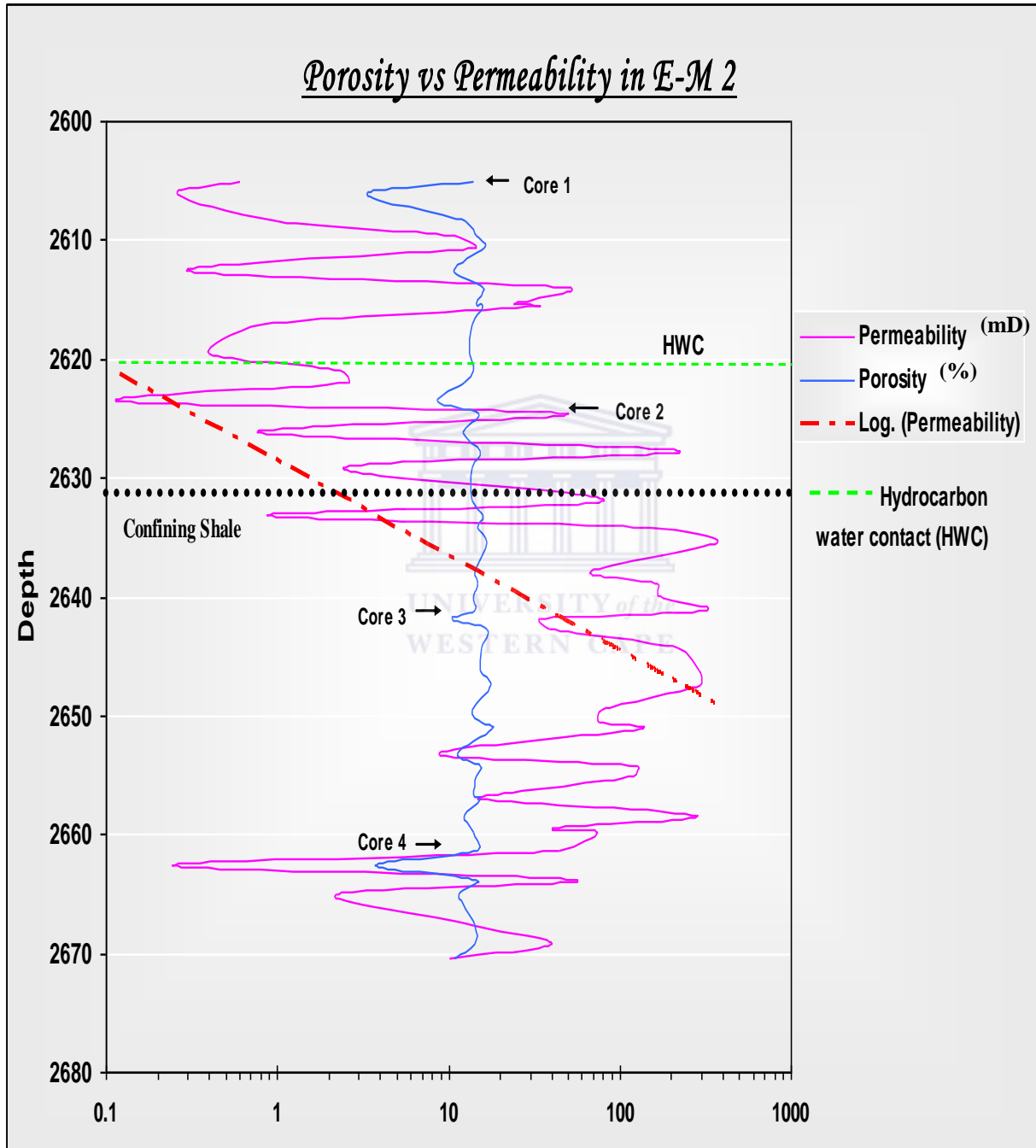


## Appendix 3



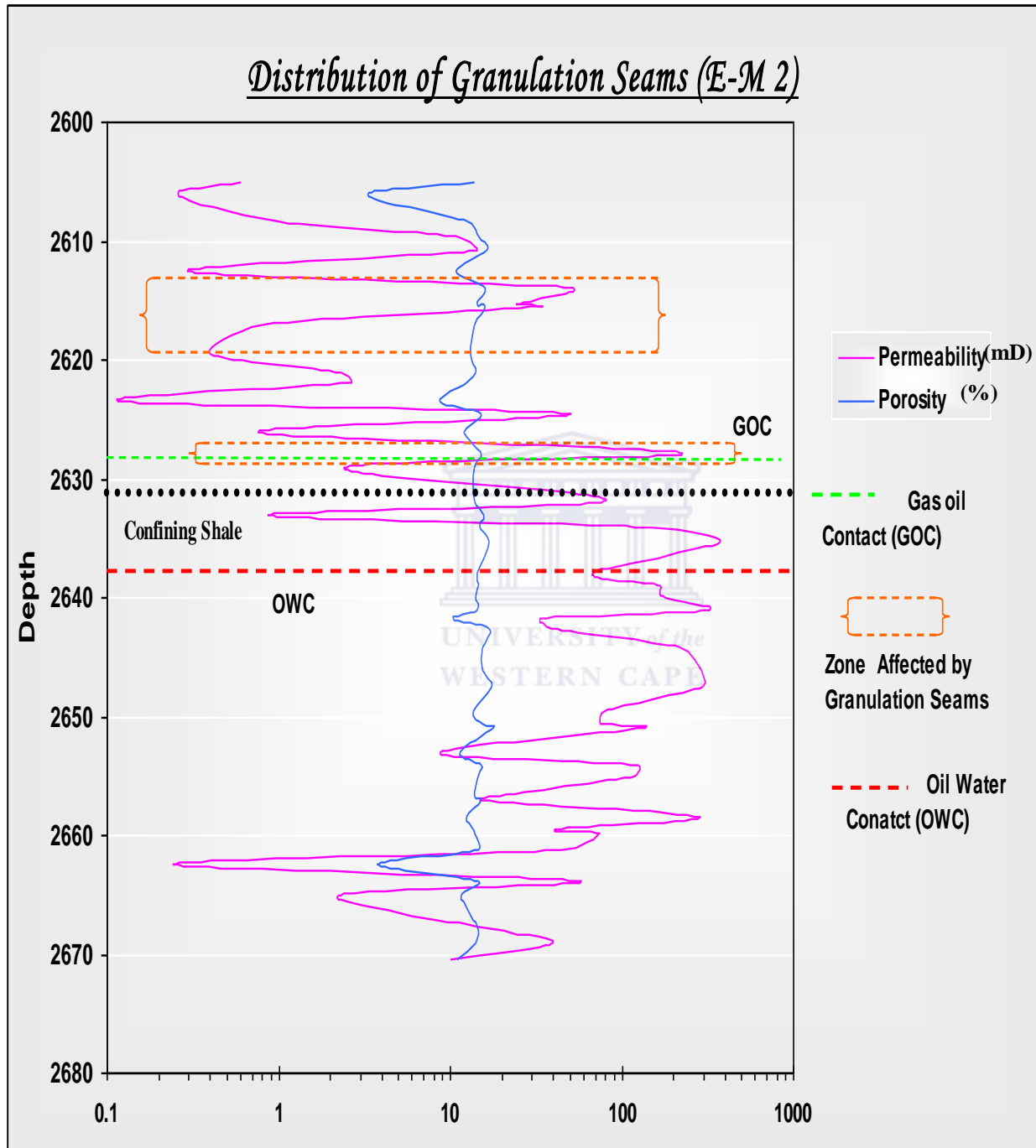
## Appendix 3a

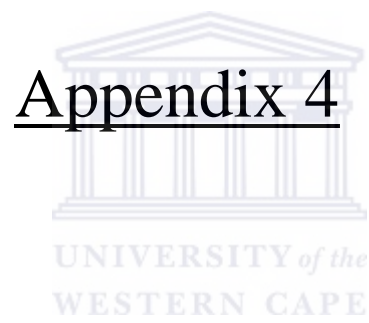
### Porosity and Permeability Distribution over E-M 2



## Appendix 3b

### Distribution of Granulation Seams

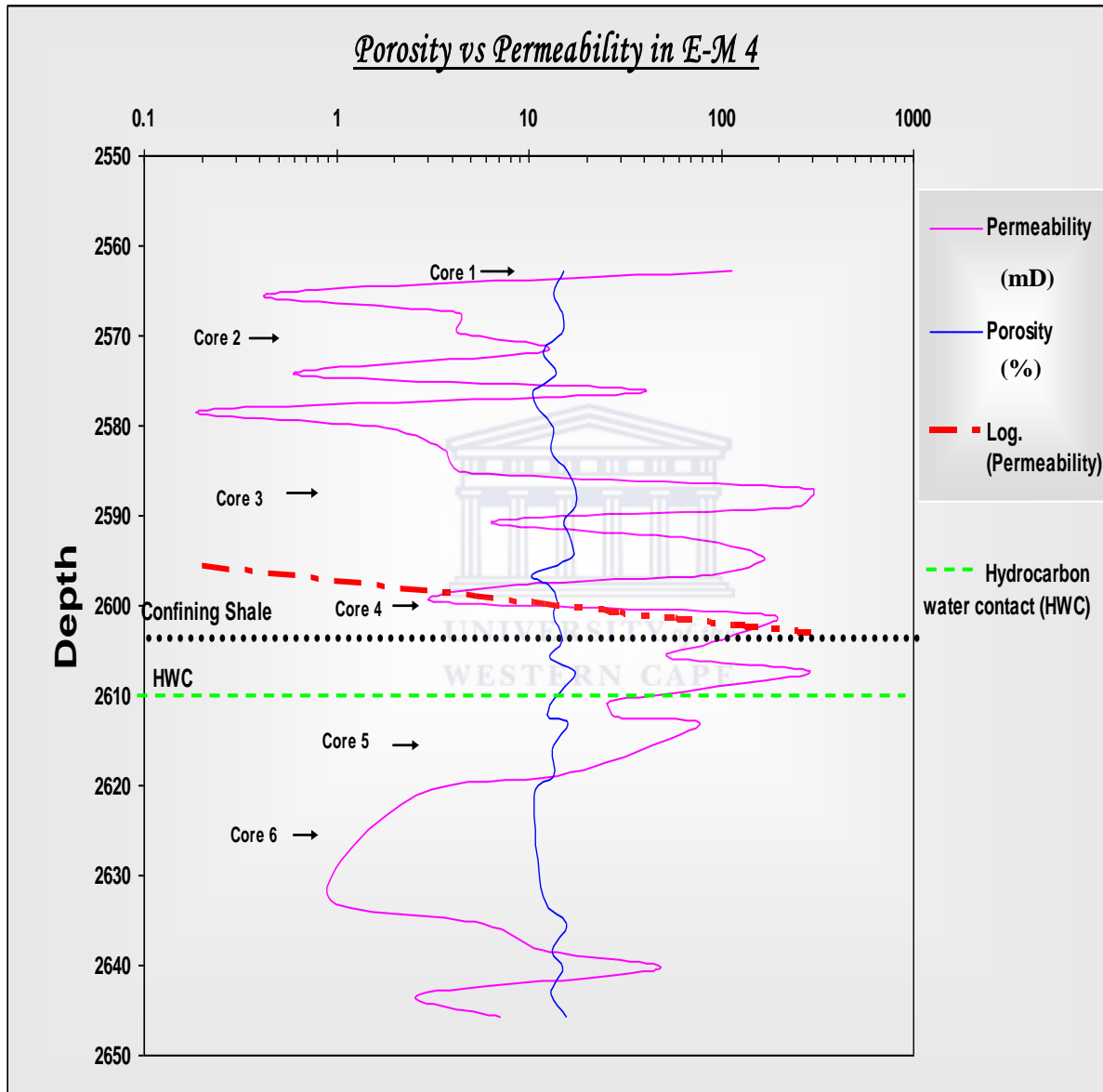




## Appendix 4

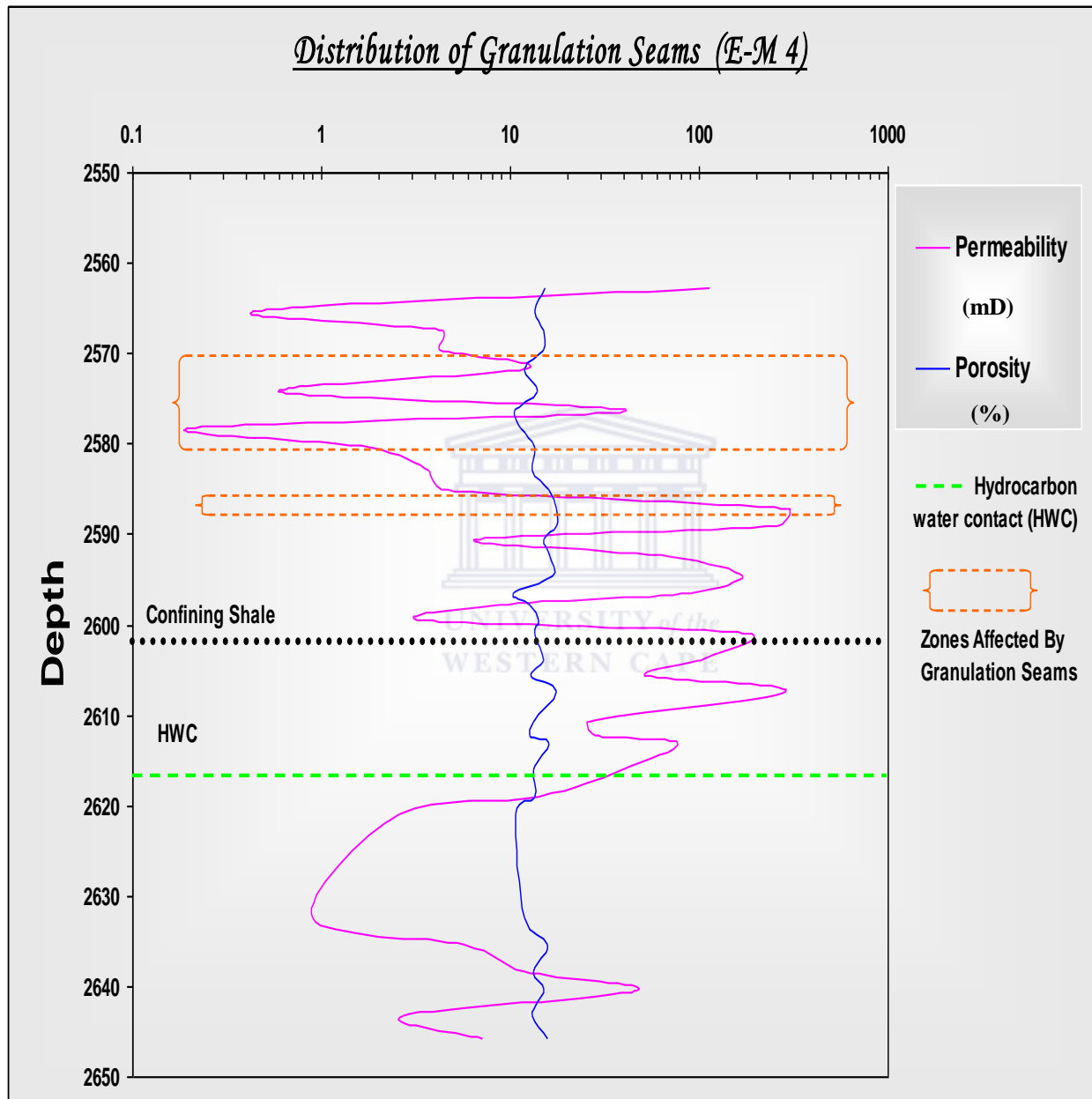
## Appendix 4a

### Porosity vs. Permeability over E-M 4

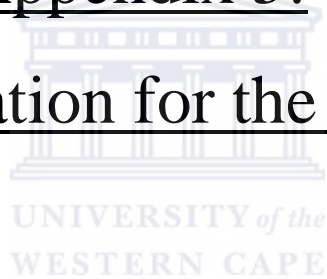


## Appendix 4b

### Distribution of Granulation Seams



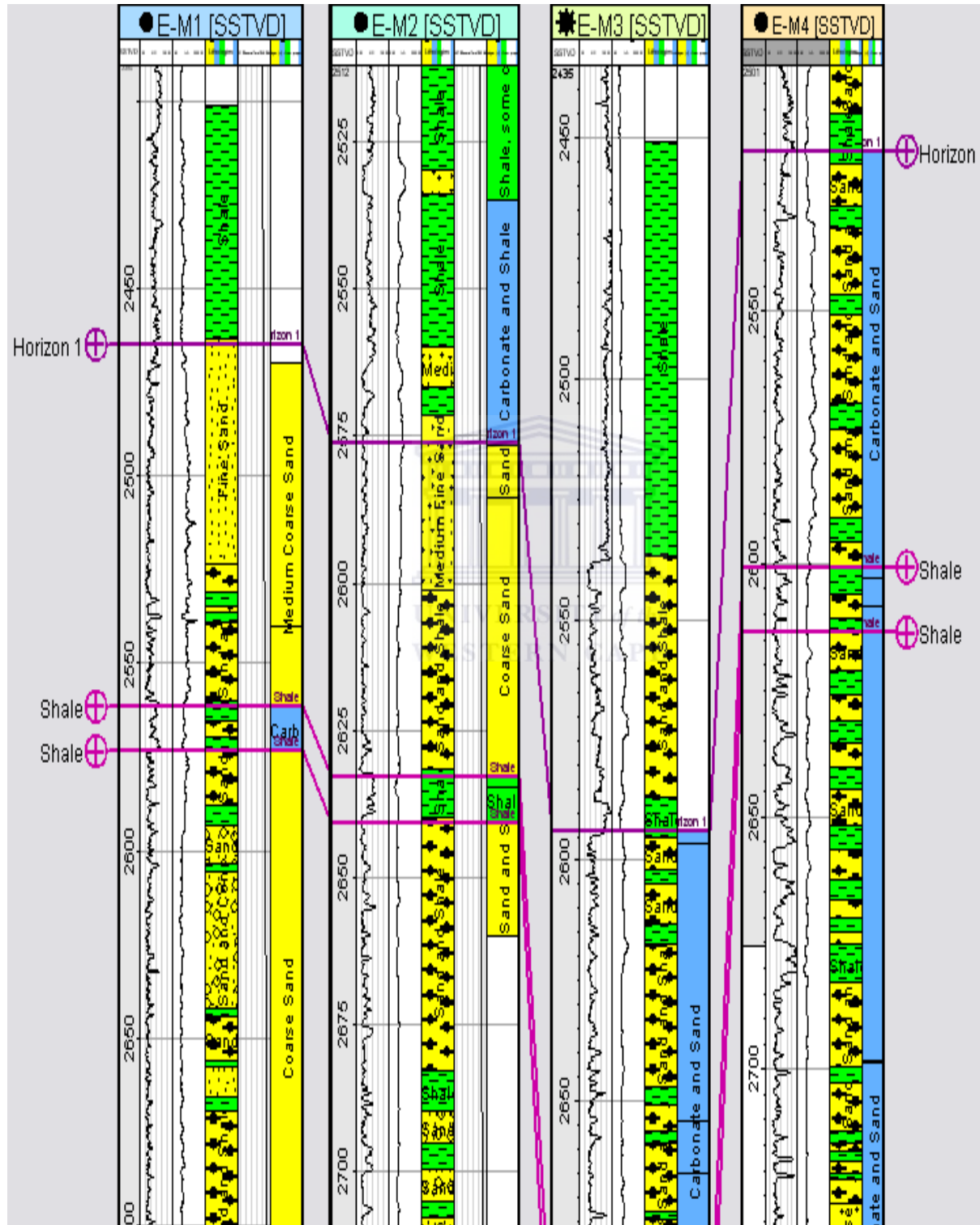
Appendix 5:  
Well Correlation for the E-M Suite





## Appendix 5A

### Well correlation for the E-M Suite



## Appendix 5B

## Well Correlation of the E-M Suite

